NASA Contractor Report 3616

Application of In Situ Fiberization for Fabrication of Improved Strain Isolation Pads and Graphite-Epoxy Composites

R. W. Rosser, R. W. Seibold,
and D. I. Basiulis

CONTRACT NAS1-16437
SEPTEMBER 1982

NASA

DISCLAIMER NOTICE

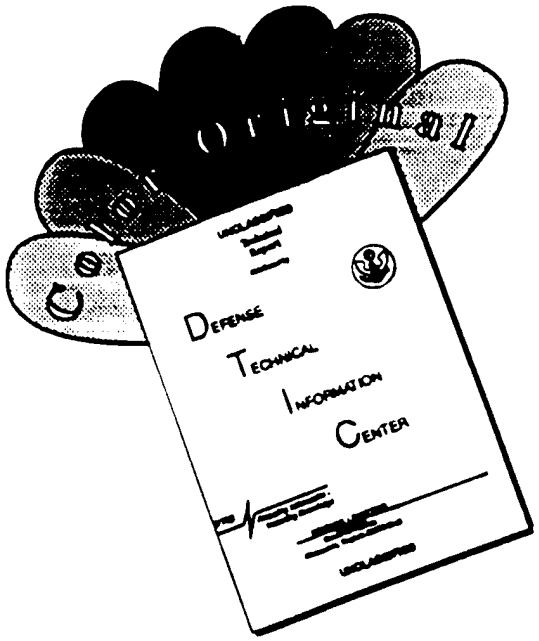

THIS DOCUMENT IS BEST QUALITY AVAILABLE. THE COPY FURNISHED TO DTIC CONTAINED A SIGNIFICANT NUMBER OF COLOR PAGES WHICH DO NOT REPRODUCE LEGIBLY ON BLACK AND WHITE MICROFICHE.

NASA Contractor Report 3616

Application of In Situ Fiberization for Fabrication of Improved Strain Isolation Pads and Graphite-Epoxy Composites

R. W. Rosser, R. W. Seibold,
and D. I. Basiulis
Hughes Aircraft Company
Culver City, California

Prepared for
Langley Research Center
under Contract NAS1-16437

National Aeronautics
and Space Administration

**Scientific and Technical
Information Branch**

1982

Use of trade names or names of manufacturers in this report does not constitute an official endorsement of such products or manufacturers, either expressed or implied, by the National Aeronautics and Space Administration.

FOREWORD

The Program Manager and principal investigator of the program at Hughes was Robin W. Rosser. The literature search required for the Strain Isolation Pad (SIP) portion of the program was conducted by Danute I. Basiulis, who also performed and directed extensive SIP experimentation. T. Kirk Dougherty and David J. Mueller were responsible for many of the agitation experiments, and Bette J. Kehoe assisted in several areas of effort. Assistance in the candidate polymer selection and procurement process was provided by Norman Bilow.

In the graphite/epoxy (GR/EP) effort, William H. Fossey was largely responsible for the initial planning of the test matrix and for preliminary specimen fabrication and testing. J. Daniel Frantz conducted all the In Situ Fiberizations of the graphite fiber arrays. The fabrication of the arrays, as well as the impregnation and testing of all specimens, was directed by Robert W. Seibold with valuable assistance and contributions from Bruce W. Buller and Manual B. Valle. Testing of the GR/EP specimens was performed at the University of Wyoming in Laramie, under the direction of David E. Walrath and Donald F. Adams.

Finally, valuable technical consultation was provided by Charles H. Sherwood, Raymond E. Kelchner, Brent G. Shaffer, Arthur B. Naselow, L. Brian Keller, and Arnold J. Tuckerman.

CONTENTS

CONTENTS (Concluded)

LIST OF ILLUSTRATIONS

LIST OF ILLUSTRATIONS (Continued)

LIST OF ILLUSTRATIONS (Continued)

LIST OF ILLUSTRATIONS (Concluded)

LIST OF TABLES

1.0 SUMMARY

An accelerated study has been performed to determine the feasibility of applying Hughes Aircraft Company's patented In Situ Fiberization (ISF) process to the fabrication of: (1) improved Strain Isolation Pads (SIPs) for the Space Shuttle, and (2) improved graphite/epoxy (GR/EP) composites. The ISF process involves the formation of interconnected polymer fiber networks by agitation of dilute polymer solutions under controlled conditions. Most previous work was performed using aliphatic hydrocarbon polymers which have limited high temperature capabilities.

In Task 1 of the program, attempts were made to advance ISF technology by fiberization of high temperature polymers which would be suitable for SIP use. Progress was made toward that objective with the successful fiberization of polychlorotrifluoroethylene, a relatively high melting polymer. Attempts to In Situ Fiberize polymers with even greater thermal stability were not successful. The latter difficulty is presumed to derive from poor solubility, low molecular weight, and/or high chain stiffness, all caused by the presence of aromaticity in the backbone of such materials.

During Task 2, two-dimensional arrays of graphite fiber were interconnected with polypropylene In Situ Fibers. Following epoxy resin impregnation and lamination of the arrays into panels, mechanical property tests were performed to gauge the effectiveness of the In Situ Fibers for improvement in intralaminar and interlaminar shear strength, and hence fracture toughness. Test results were generally, though not universally, unpromising. Poor performance is believed to reflect incomplete In Situ fiber/resin wetting, poor graphite fiber packing, and perhaps low In Situ Fiber moduli.

In all, the results of both portions of the program showed promise for eventual In Situ Fiberization use, but did not demonstrate feasibility. Additional development is therefore indicated.

2.0 INTRODUCTION

The primary thermal insulation for the Space Shuttle currently consists of lightweight ceramic tiles that cover much of the surface of the vehicle. Each tile is bonded to an intermediate SIP, which in turn is bonded to the airframe. The adhesive used is a silicone rubber and the SIP is a Nomex fiber felt. As its name implies, the SIP serves to isolate the fragile tile from strains that occur in the aluminum skin of the vehicle.

During preflight testing of the above Thermal Protection System, failures were observed at many tile/SIP interfaces. It was determined that these failures arose because of stress concentrations caused by inextensible fibers, or "stakes," present in the Nomex felt. These stakes are bundles of fibers which are needled through the thickness of the felt at regular intervals in order to compress the material and to increase its transverse (through the thickness) tensile strength. Figure 2-1 is a cross-sectional view of a piece of SIP, and shows the stakes.

In general, the majority of fibers in any felt are oriented within the plane of the material. Consequently, mechanical properties are anisotropic. The staking procedure is a technique used to provide additional fibers in the direction through the thickness, thereby providing more isotropic strength and stiffness. Unfortunately, the stakes are strain-incompatible with the bulk felt. They are comparatively inextensible and therefore accept the major part of transverse tensile loading. In application, this gives rise to the observed stress concentrations at the SIP/tile interface and concomitant failure of the tile. In addition, it results in transverse stress-strain behavior which is unpredictable and unreproducible; the act of deforming the material during test changes its structure and its subsequent properties.

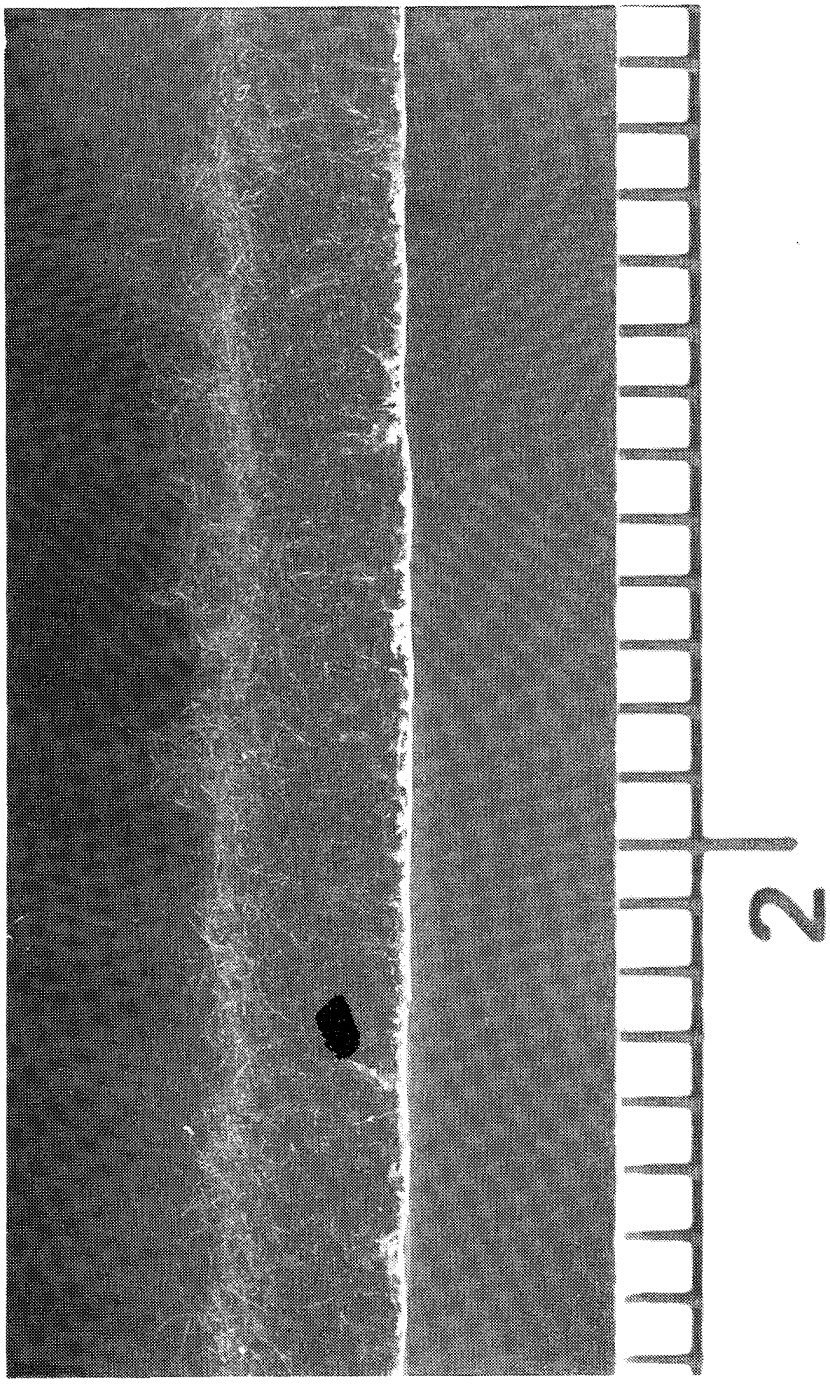

Figure 2-1. Nomex felt SIP. Ruler divisions are 0.16 cm (1/16 inch).

The short term solution to this problem involved extensive proof-testing and densification of the inner mold line of the tile so that stress concentrations at the interface would not be harmful. On the other hand, a possible long term solution is to produce an isotropic SIP which has acceptable and predictable stress-strain behavior, does not give rise to stress concentrations, and which is resistant to the high temperatures expected during and immediately after shuttle reentry 533-644 K (500-700°F). One potential technique for producing such a SIP involves the use of Hughes Aircraft Company's patented In Situ Fiberization (ISF) process.[1,2] Invented and developed by Hughes, this unique process allows for the fabrication of isotropic fibrous materials from polymer solutions. However, prior to the current program fibrous masses had been achieved only by use of highly crystalline aliphatic polymers which have relatively low upper-limit use temperatures. It was therefore proposed to investigate the feasibility of extending ISF technology to higher temperature polymers for SIP fabrication. The first task of the work discussed in this report was performed with that objective.

Another valuable area of potential application for the In Situ Fiberization process is fracture toughness enhancement of graphite/epoxy (GR/EP) composites. GR/EP is now in use as secondary structure in civilian and military aircraft, and extensive use as primary structure is impending. Space applications for GR/EP are now common: e.g., antennas, solar cell substrates, satellite equipment shelves, and thrust cones and tubes. The importance of these composites to many NASA and DoD programs is clear. However, one of the factors limiting their usefulness is inefficient intralaminar and interlaminar stress transfer from fiber to fiber through the epoxy matrix, resulting in insufficient fracture toughness. One potential technique to eliminate this deficiency is to interconnect the graphite fibers with In Situ Fibers. Preliminary experiments conducted at Hughes have demonstrated that interconnected networks of the latter can be grown directly on graphite fiber arrays. It was therefore proposed to investigate the feasibility of preparing GR/EP/ISF composites with improved fracture toughness relative to ordinary GR/EP. This was the objective of the second portion of the program.

In sum, the program described in the following sections was a short term, accelerated effort, and was devised to determine the feasibility of utilizing the ISF process for two important NASA applications.

3.0 IN SITU FIBERIZATION

3.1 HISTORY

Several years ago, the Technology Support Division of Hughes Aircraft Company began a research effort to develop a technique for growing polymer fiber networks from solution. Motivated by a need for high strength encapsulants for high voltage applications, Hughes proposed to permeate the complex spaces of electronic packages with a dilute polymer solution and then to induce the polymer to precipitate into a fiber network. The fiberized package would subsequently be impregnated with a low viscosity resin, and after curing of the latter, would thus be contained in a uniformly fiber reinforced encapsulant. The difficulty, of course, was to find a way to induce fiber network precipitation; the process developed involved flow-induced crystallization.

Flow-induced crystallization of polymers from solution is a well known effect and has been extensively studied during recent years.[3,4,5,6] It has been observed by use of many different techniques, all of which revolve around a single natural phenomenon. When supercooled solutions of certain highly crystalline polymers are subjected to appropriate flow fields, the molecules are deformed and precipitate into crystals with high degrees of preferred molecular orientation. However, all of the studies reported in the literature, though they involved a variety of flow geometries, resulted only in the formation of isolated fibers or two-dimensional fiber mats. Three-dimensional fiber networks were not reported.

Then Hughes made a novel discovery; under conditions of low amplitude solution agitation, polymers can be induced to crystallize into three-dimensional, interconnected networks. The first variation of this In Situ

Fiberization process involves the agitation of bulk, dilute solutions of polymers and their containers. By this technique, fiber masses are obtained which duplicate the shape of the container and which occupy the space filled by the original solution. Figure 3-1 shows a polypropylene fiber mass formed in a test tube; other configurations can be achieved by use of appropriately shaped containers. The second ISF variation involves the agitation of an object or device immersed in the polymer solution. As illustrated in Figure 3-2, an interconnected fiber network is grown in and around the object.

Continued research resulted in fiberizations with several aliphatic backbone, highly crystalline, hydrocarbon polymers: polyethylene, polypropylene, poly-1-butene, poly-4-methyl-1-pentene, and isotactic polystyrene. Although noticeably less distinct with polypropylene, the characteristic "shish kebab" fiber structure reported in other flow-induced crystallization work[3,4,5,6] was observed with all five polymers. This morphology is believed to result in very high fiber strength and modulus.[4] Work with nonhydrocarbon polymers led to flow-induced crystallization of polyvinylidene fluoride, but the product was not fibrous. Finally, some fiberizations were achieved with noncrystalline polymers by use of a seeding technique involving coprecipitation with one of the polymers noted above. However, interconnected fiber networks were not achieved in the absence of a hydrocarbon, aliphatic backbone, crystallizable polymer.

3.2 THEORY

The molecular processes involved in In Situ Fiberization are not completely understood, as the interaction of thermodynamic, hydrodynamic, and kinetic variables is complex indeed. Nevertheless, certain generalizations can be made about the conditions necessary for fiber formation. At the risk of oversimplifying this very complicated process, or worse yet of implying a greater understanding than is actually possessed, a simple free energy diagram of the ISF process is shown in Figure 3-3. This diagram is similar to those used by chemists to describe the energetics of a chemical reaction, and to show the effects of heat, catalysts, etc.

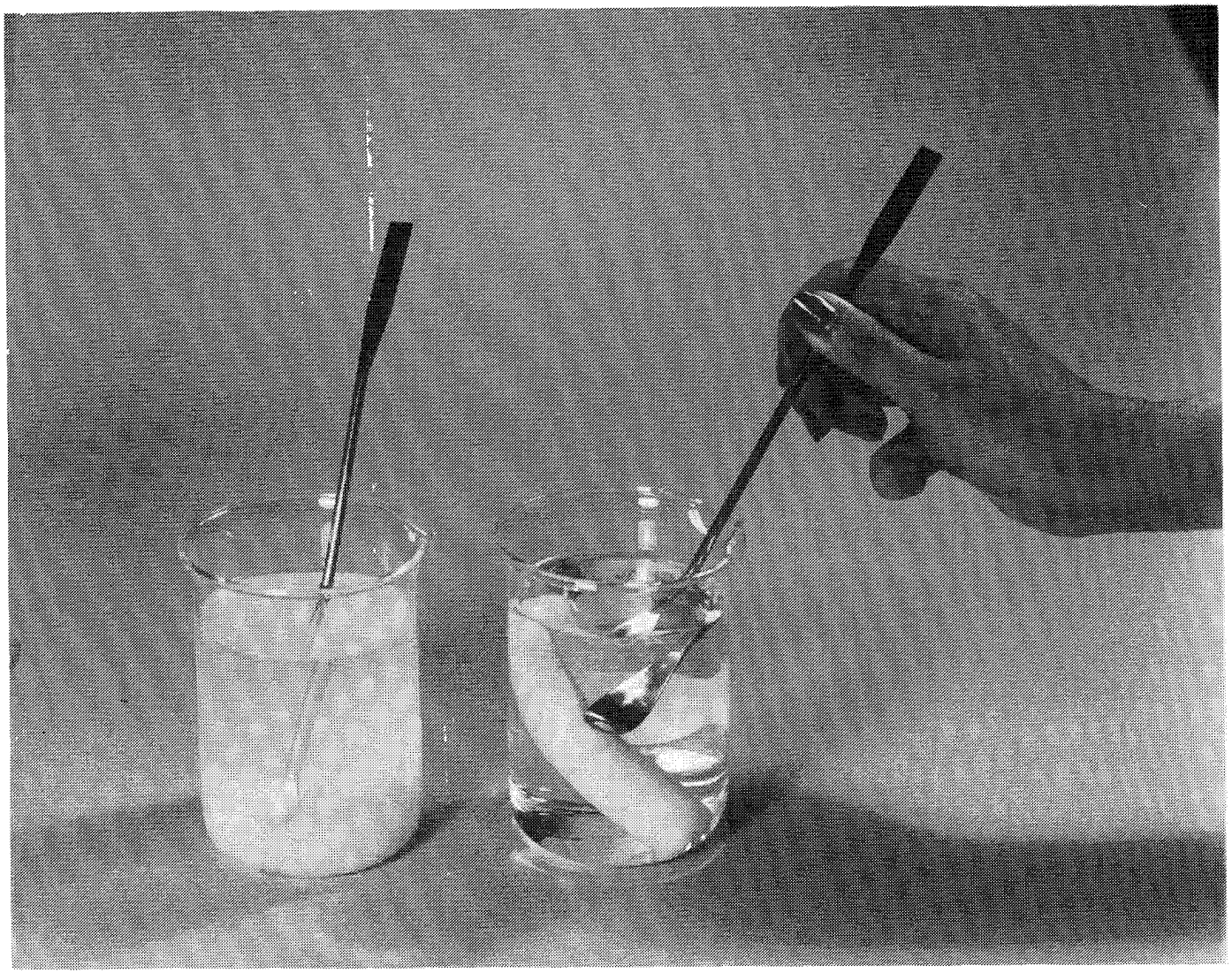

Figure 3-1. Fiber mass formed by agitation of a solution of isotactic polypropylene in a test tube, compared to quiescently crystallized material.

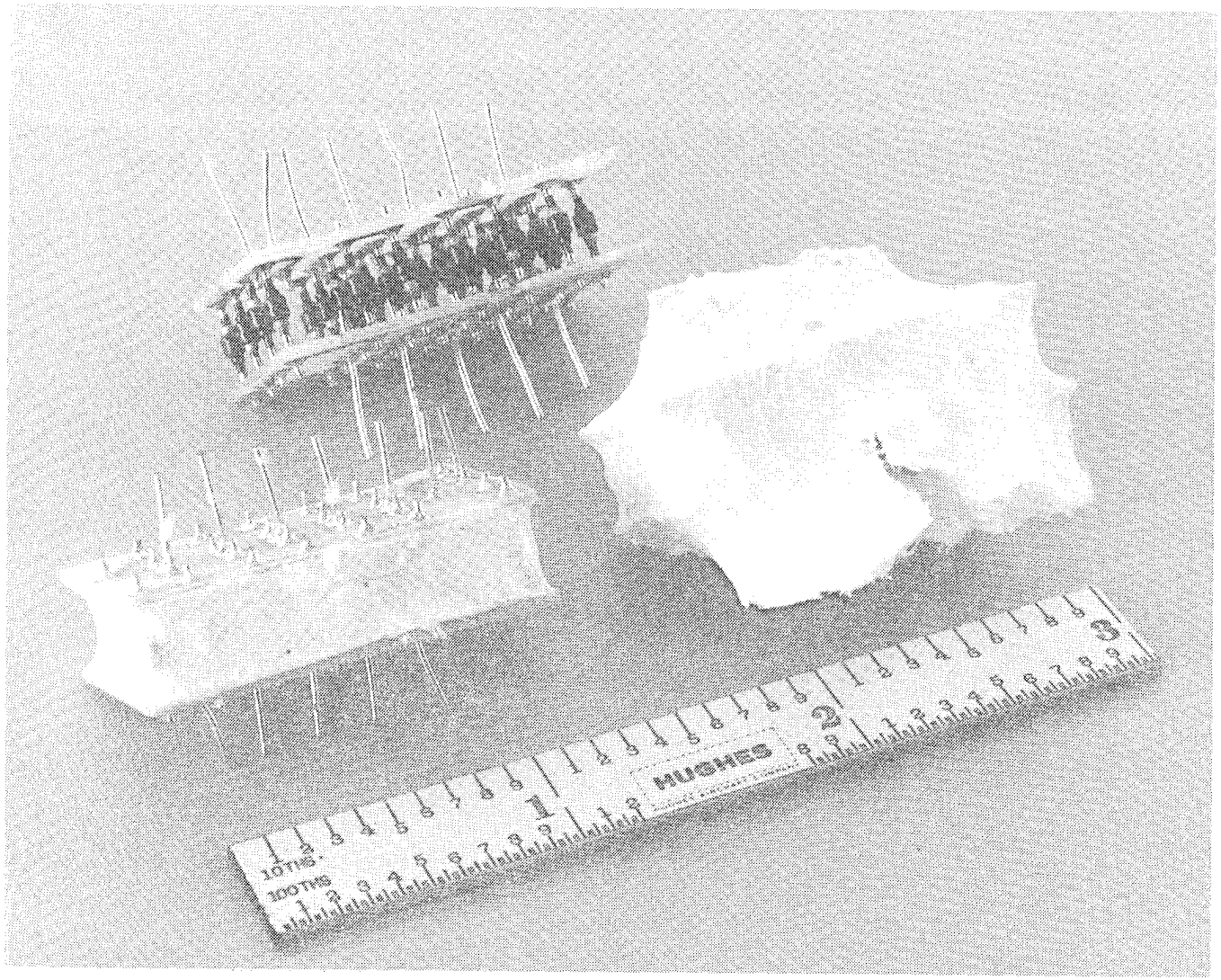

Figure 3-2. Electronic components shown unfiberized, fiberized with isotactic polypropylene, and fiberized and trimmed.

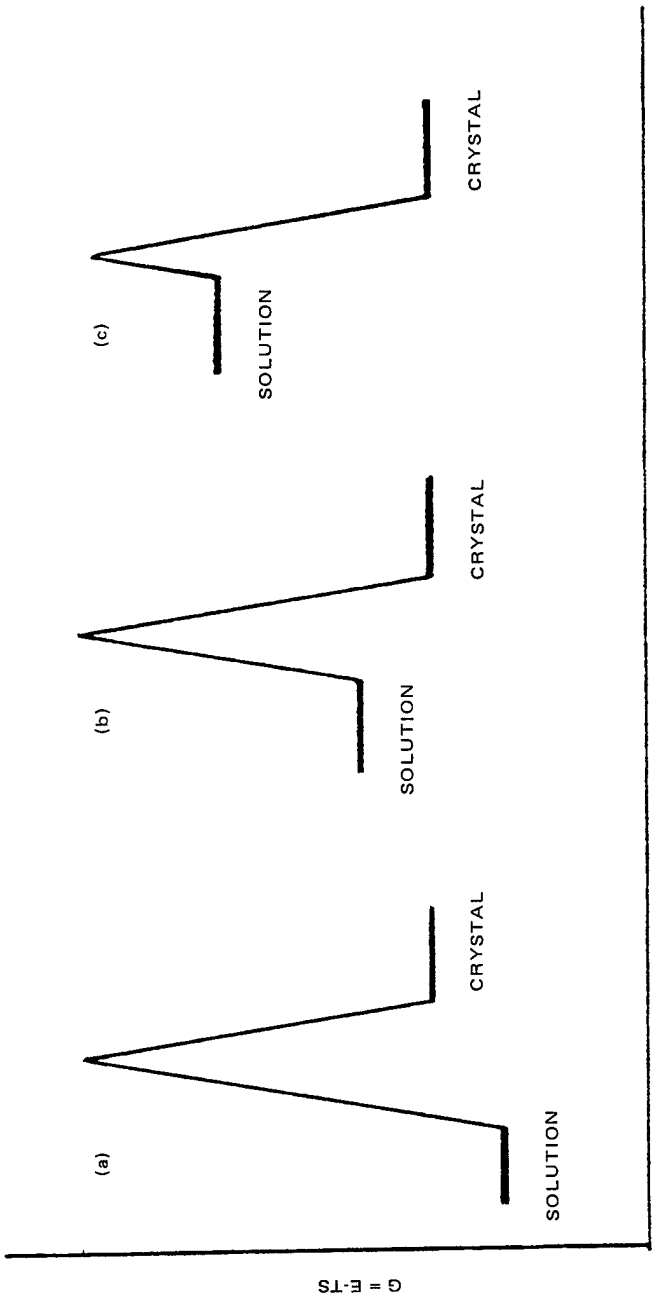

Figure 3-3. Simple free energy diagram of a solution of a crystallizable polymer: (a) hot, (b) supercooled, (c) supercooled and flowing.

In Figure 3-3(a), the solution temperature, T, is above the supercooling point. Hence, for the polymer molecules, the solution state is thermodynamically favored over the crystalline state. Although the energy, E, of the latter state is lower, nevertheless the free energy, G=E-TS, is lower in the solution state because of its greater entropy, S.

As T is lowered, the entropy term becomes less dominant, until finally the supercooled region is achieved, Figure 3-3(b). Now, the crystalline state is thermodynamically favored, but crystallization still does not occur, because of the kinetic barrier. This barrier is thought to reflect the fact that the long polymer chains cannot readily move cooperatively into configurations which allow crystal nucleation and growth. Hence the polymer remains in solution.

As flow is added, the free energy of the solution is raised further and the kinetic barrier is lowered because the entropy of the solution decreases when the distribution of polymer molecule configurations is moved away from equilibrium (maximum randomness). This is shown in Figure 3-3(c). The kinetic barrier may be lowered even further as increased alignment of molecular chain segments in the flowfield facilitates interactions conducive to crystallization. Now, the barrier is low enough and flow-induced crystallization can occur.

The above model leads to four criteria which should be met if In Situ Fiberization is to occur.

1. There should be sufficient attraction between polymer molecules in solution to thermodynamically favor the crystalline state.
2. The velocity gradients of the flow field should be large enough to move the distribution of chain configurations away from equilibrium.
3. The applied velocity gradients should be of sufficient duration to move the distribution of chain configurations away from equilibrium. This is clearly a corollary to (2).
4. The period of flow must be long enough, or conversely the kinetics of crystallization fast enough, to allow crystal nucleation and growth to occur while the molecules are in nonequilibrium configurations.

Roughly, requirement (1) is thermodynamic in nature, (2) and (3) are hydrodynamic, and (4) is primarily kinetic (though partially hydrodynamic). Each is discussed in more detail below.

Sufficient Thermodynamic Attraction

This is a requirement on the polymer, and to some extent on the solvent. For polymers which have been successfully fiberized in the past, it is clearly met. If fiberizable solutions of the latter are cooled sufficiently, then polymer crystallization will occur without agitation. This fact suggests that a useful test for determining whether a polymer solution meets the first requirement for ISF may be to quiescently cool it and watch for the appearance of crystalline material.

Sufficient Velocity Gradients

This requirement should be met if the velocity gradients are at least as large as the reciprocal of the longest relaxation time, τ , of the polymer molecules in solution. If the velocity gradients do not meet this criterion, then the molecules will be able to relax faster than they are perturbed. Hence, they will maintain their equilibrium configurations during flow, entropy will not be decreased, and the solution will behave as if there were no agitation.

From basic molecular theory[7] of dilute polymer solutions,

$$\tau \approx 1/2\ (\eta-\eta_s)M/cRT$$

Here, η and η_s are the solution and solvent viscosities, respectively, M is the polymer molecular weight, c is the polymer concentration, R is the gas constant, and T is the absolute temperature. For typical past fiberizations, rough estimates of these parameters might be: $(\eta-\eta_s) \approx 1$ centipoise (g/cm sec); $M \approx 3 \times 10^5$ g/mole (though there is a wide distribution of molecular weights in any sample); $c \approx 0.01$ g/cm^3; $R \approx 8.3 \times 10^7$ g cm^4 sec^2/K mole; and $T \approx 375$ K. Therefore $\tau \approx 5 \times 10^{-4}$ second. Analysis of the dynamics in typical ISF experiments, though difficult to perform precisely

because of the complexity of the flow fields, indicate that velocity gradients of magnitude substantially greater than $1/\tau$, 2000 sec^{-1}, have been achieved. Details of the calculations are given in Appendix A. Therefore, if the same techniques are used with new polymer/solvent combinations, then sufficient flow will exist as long as molecular relaxation times are not substantially shorter than about 5×10^{-4} second. If, however, relaxation times of new materials are too short, then more violent agitation may be necessary in order to increase velocity gradients.

Sufficient Flow Duration for Molecular Deformation

To satisfy this requirement, flow duration must be long compared to τ. Otherwise, the molecules won't have time to respond to the flow, and therefore it should have no effect on the crystallization process. In past experiments, the frequency of agitation was typically 50 Hz, which provided flow duration very long compared to τ. There should be no difficulty in continuing to satisfy this requirement for any reasonably comparable polymer solution.

Sufficient Kinetics

This is the most difficult requirement to analyze. However, it is reasonable to expect that this requirement may be harder to meet for new polymers than for those previously fiberized since the latter are relatively fast crystallizers. If so, then it may be necessary to lower agitation frequencies. This however, would require an increase in agitation amplitude in order to maintain sufficiently large velocity gradients. Since this may not be experimentally feasible, a potential reason exists for nonfiberization of polymers which crystallize slowly.

4.0 FEASIBILITY STUDY – IN SITU FIBER STRAIN ISOLATION PADS

When it was first proposed to investigate the feasibility of using ISF techniques to fabricate an improved SIP, two approaches were considered. One involved first making a SIP from a polymer, such as polypropylene (PP), which was known to fiberize readily. Then, after a PP SIP had been fabricated and shown to have suitable properties at relatively low temperatures, efforts would be expended to convert to a higher temperature polymer. The other approach was to take the opposite tack. Feasibility of In Situ Fiberization with a high temperature polymer would be demonstrated first, and then SIP fabrication would be undertaken. Though both approaches are reasonable, the second was chosen for this program. The decision was based on the hypothesis that techniques learned for PP SIP fabrication might not be useful when it came time to fabricate SIP from different polymer types. Though only supposition, this hypothesis was deemed sufficient to tip the scales toward the second approach.

In order to demonstrate ISF applicability to high temperature polymers, a three-phase effort was devised. Phase I involved the selection of promising polymer/solvent systems for study. Phase II involved determination of critical solubility temperatures. (The idea was to find out at what temperature the polymers would quiescently crystallize from solution in order to locate the supercooled regions.) Phase III then involved fiberization experiments. As originally planned, a fourth phase would have been devoted to SIP fabrication and testing, but this was not achieved. Details of Phase I - III efforts are described below.

4.1 PHASE I - DETERMINATION OF POTENTIAL POLYMER/SOLVENT SYSTEMS

Initially, a literature search was conducted in order to identify candidate polymers. To compile such a list, polymers were sought which possessed three characteristics: solubility in at least one solvent; crystallinity; and an upper limit use temperature above 533 K (500°F). The first two requirements are, of course, processing requirements while the third is an application requirement. However, during compilation it was quickly learned that very few materials possess all three required characteristics. Therefore, for screening purposes, materials possessing only two of the three requirements were considered. For example, polymers were included even though the only known solvents for them were of questionable processability – hot anhydrous sulfuric acid, for example. Also, some non-crystalline materials were included on the chance that techniques could be developed which would cause amorphous precipitation during flow. If such could be achieved, perhaps flow would still induce fiber formation and yield an amorphous fiber such as the current SIP material, Nomex. In addition, some polymers were included in the compilation despite inadequate thermal stability. These were primarily materials which have relatively low temperature capability but for which post-ISF-processing (such as imidization of a fiberized polyamic acid) might yield a suitable high temperature product. Finally, some relatively low temperature polymers were included in the study because it was expected that they would be somewhat easier to fiberize than other candidates, and because any successful fiberization of a nonaliphatic, hydrocarbon material would be a significant step forward as it would probably yield insights into proper processing techniques for other materials.

The list of initially considered polymers is shown in Table 4-1. Several potentially useful polymers - poly-4, 4'-thiophenylene oxide, poly-2, 5-distyrylpyrazine, and Nylon 4T - were excluded due to lack of availability, a prime consideration due to the short duration of the program.

TABLE 4-1. POLYMERS CONSIDERED FOR ISF/SIP APPLICATION

	Polymer	Crystallinity	Upper Limit Use Temp. (K)
1	Poly p-phenylene terepthalamide	yes	775
2	Polyphenylene sulfide (PPS)	yes	550
3	Polytetrafluoroethylene (PTFE)	yes	600
4	Poly-1,4-phenyleneethylene	yes	680
5	Polymonochloro-p-xylylene	yes	580
6	Polydichloro-p-xylylene	yes	625
7	Polyphenylene oxide (PPO)	yes	525
8	Polyacrylonitrile (PAN)	yes	590
9	Polyamic acid	no	
10	Polybenzimidazole (PBI)		575
11	Polybenzothiazole		
12	Poly (p-oxybenzoate)	yes	625
13	Polyetheretherketone	yes	610
14	Poly (p-phenylene)	yes	high
15	Poly m-phenylene oxide (polyarylether)		
16	Poly m-phenylene isophthalamide	no	645
17	Polyimide	no	
18	Polyethylene terephthalate	yes	515
19	Polybutylene terephthalate	yes	500
20	Carborane siloxane	yes	515
21	Polyhexamethylene terephthalamide	no	645
22	Polyether sulfone (PES)	no	
23	Polysulfone (PS)	no	
24	Polychlorotrifluoroethylene (PCTFE)	yes	495

4.2 PHASE II - SOLUBILITY TEMPERATURE DETERMINATIONS

As soon as samples of the selected polymers were obtained, solubility experiments were initiated. Though sulfuric acid and methanesulfonic acid were known to be solvents for several of the aromatic backbone polymers, emphasis was placed on finding organic solvents. In general, polymers which are not degraded by the acid solvents are protonated by those solvents. As a result, the polymer chains repel, rather than attract one another. Hence, the required thermodynamic drive toward crystallization does not exist in such solutions, even when cooled.

During the search for useful solvents, solubility experiments were performed with a wide variety of solvents - from aliphatic hexane, to aromatic xylenes, to more polar dimethylsulfoxide, etc. Experiments were performed at both room and elevated temperatures. Throughout the search, emphasis was placed on finding solvents in which a polymer would dissolve on heating and precipitate on cooling. This was based on two pieces of previous ISF experience. First, as discussed in Section 3-2, precipitation from solution on quiescent cooling is good evidence of the existence of favorable thermodynamic attraction among polymer chains. Second, in previous work with polyacrylonitrile (PAN) dissolved in several solvents and solvent mixtures, cooling did not result in precipitation, and agitation did not result in the formation of fiber networks. During the quest for appropriate systems, non-solvents were often mixed if the latter alone would not allow polymer precipitation. However, this seemingly promising technique did not prove to be particularly effective.

For some of the polymers in Table 4-1, no solvents were found. Despite literature reports of limited polytetrafluoroethylene (PTFE) solubility in perfluorinated kerosene, experiments to prepare such a solution were not successful. Solvent (B.P. 358 K) and PTFE powder (2 percent by weight) were placed in a sealed glass tube and heated to 473 K ($392^{\circ}F$), and then 573 K ($604^{\circ}F$), but no evidence of swelling or dissolution was evident visually. Therefore experiments were ceased, and PTFE was judged impractical for In Situ Fiberization. Poly(p-phenylene) was found to be

insoluble in all solvents tried, and poly(p-oxybenzoate) could not be dissolved in anything except concentrated H_2SO_4. Furthermore, it could not be recovered from the latter on cooling even with the addition of water. Presumably, it had been degraded by the acid rather than dissolved. Attempts to dissolve it in refluxing (596 K) benzylbenzoate resulted in blackening of the solvent but little if any solubility. Therefore, further efforts with this material were also abandoned.

As additional experiments were performed, polymers began to fall into one of four classes: (I) those, as above, for which no solvent could be found; (II) those soluble only in concentrated sulfuric or methanesulfonic acid but which would not precipitate on cooling; (III) those soluble in at least one organic solvent but which would not precipitate on cooling; and (IV) those that would dissolve in at least one organic solvent on heating and then precipitate on cooling. Clearly those in class (I) were of no further interest while those of class (IV) were most promising from a processing viewpoint. However, those in class (II) and to a lesser extent those in class (III), offered the highest maximum use temperatures. Results of all solubility experiments are summarized in Table 4-2. Two polymers listed in Table 4-1, poly-1,4-phenyleneethylene, and polydichloro-p-xylene, were eliminated because of procurement difficulties.

4.3 PHASE III - FIBERIZATION EXPERIMENTS

Polyamic Acids and other Class III Polymers

The first fiberization experiments were conducted with a LARC furnished polyamic acid (No. 8 in Table 4-2). At first, agitation experiments were performed in diglyme/alcohol (as received). In this solvent mixture, the polymer undergoes a transition, originally presumed to be liquid crystallization, upon moderate heating. It was hoped that such tendency to aggregate would provide sufficient thermodynamic attraction between molecular chains to initiate fiberization upon agitation. Accordingly, many agitation experiments were conducted: several concentrations and temperatures were used. Though some gel was collected on wire meshes agitated in solution,

TABLE 4-2. CANDIDATE POLYMERS AND SOLVENTS

(See text)	Polymer	Source	Solvents
I	(1) PTFE	E.I. Dupont De Nemours and Company Wilmington, DE	None
	(2) poly(p-phenylene)	Polysciences, Inc. Warrington, PA	None
	(3) poly(p-oxybenzoate)	Carborundum Company Niagara Falls, NY	None
II	(4) poly p-phenylene terephthalamide	E.I. Dupont De Nemours and Company Wilmington, DE	H_2SO_4
	(5) polyetherether ketone (PEEK)	ICI Americas, Inc. Wilmington, DE	H_2SO_4
	(6) polybenzothiazole	AFWAL/ML Wright Patterson AFB, Dayton, OH	H_2SO_4
III	(7) polyacrylonitrile (PAN)	Aldrich Chemical Company, Inc. Milwaukee, WI	DMF, DMSO, DMA, γ-BL
	(8) polyamic acid	LARC[1]	diglyme, DMSO
	(9) polybenzimidazole	Celanese Research Company Chatham, NJ	DMSO, H_2SO_4
	(10) poly m-phenylene isophthalamide	E.I. Dupont De Nemours and Company Wilmington, DE	H_2SO_4, 5% LiCl in DMA
	(11) polyethylene terephthalate (PET)	Aldrich Chemical Company, Inc. Milwaukee, WI	DMSO, TCE/phenol (1:1)
	(12) polybutylene terephthalate	Scientific Polymer Products Ontario, NY	TCE
	(13) polyhexamethylene terephthalamide	Scientific Polymer Products Ontario, NY	H_2SO_4, DMA
	(14) polyethersulfone (PES)	ICI Americas, Inc. Wilmington, DE	DMF, CH_2Cl_2
	(15) polysulfone (PS)	Aldrich Chemical Company, Inc. Milwaukee, WI	CH_2Cl_2, DMF, $CHCl_3$
	(16) polyimide	Ciba-Geigy, Xu 218 Ciba-Geigy Corporation Ardsley, NY	Several
	(17) Carborane siloxane	Dexsil Chemical Corporation Hamden, CT	Several
IV	(18) polychlorotrifluoro-ethylene (PCTFE)	3-M Company St. Paul, MN	2,4-dichlorobenzotrifluoride
	(19) poly(dimethylphenylene oxide) PPO	Chem Service Westchester, PA	Xylenes, α-pinene
	(20) polyphenylene sulfide (PPS)	Polysciences, Inc. Warrington, PA	biphenyl
	(21) polymonochloro-p-xylene	Union Carbide Corporation New York, NY	α-chloronaphthalene

Note: DMF = dimethyl formamide
DMA = dimethyl acetamide
DMSO = dimethyl sulfoxide
γ-BL = γ-butyrolactone
TCE = tetrachloroethane

[1] LARC-2, prepared by reacting 3,3[1],4,4[1]-benzophenone tetracarboxylic acid dianhydride with 3,3[1]-diaminobenzophenone

no fibers were obtained. Concurrently, it was discovered from other NASA sponsored work that the presumed liquid crystallization was only phase separation.[8]

Additional experiments with this material were then performed in other solvents, primarily dimethylacetamide (DMA). It was found that refluxing such solutions causes the polymer to imidize and precipitate. Thus it was hoped that agitation during reflux would provide an appropriate combination of hydrodynamic ordering and thermodynamic attraction to produce fibers. Indeed, when a brass screen was agitated in a refluxing solution and then washed and dried, a few small fibers were discovered on the screen. A scanning electron micrograph (SEM) of these is shown in Figure 4-1. Unfortunately, additional experimentation was unable to produce any better yield. Another polyamic acid, Dupont's Pyralin PI-250 was then tried under similar conditions but failed to fiberize. Further imidization/fiberization experiments were then suspended.

Agitation experiments were conducted with three other Class III polymers: poly m-phenylene isophthalamide, polyacrylonitrile (PAN), and polysulfone (PS). Since none of these could be induced to precipitate solely by manipulation of temperature, a new approach was taken. Nonsolvent was added slowly during stirring of room temperature solutions. In all cases, however, only globular, nonfibrous precipitates were formed.

Based on the above results, it was decided to abandon Class III materials and to concentrate further efforts on Class II and Class IV polymers. It was felt that the Class II materials would offer better thermal stability than those of Class III with essentially the same processing difficulties. Class IV materials, on the other hand, offered more promising thermodynamic attraction between molecules in solution, though at some loss in final temperature resistance relative to those in Class II.

Class IV and Class II Polymers

The next polymer to be agitated in solution was polychlorotrifluoroethylene (PCTFE). The results were very impressive. When a metal screen was agitated in a 2,4-dichlorobenzotrifluoride solution of PCTFE at approximately 50 Hz with a peak-to-peak displacement of about 1/2 cm (1/4 inch),

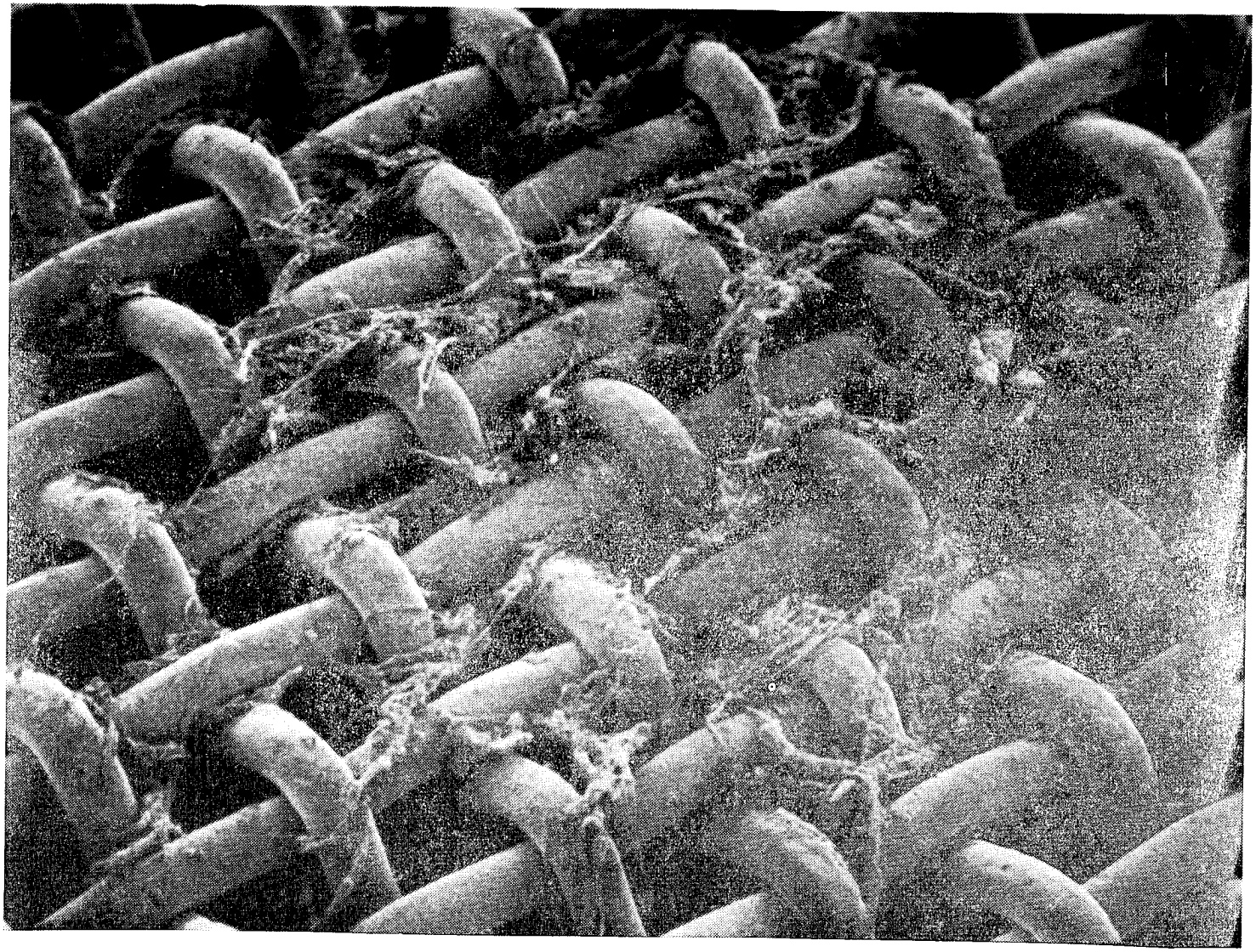

Figure 4-1. SEM of polyamic acid fibers formed on a brass screen agitated in a refluxing DMA solution. Magnification ≈ 25 X.

copious fibers were produced on the screen. Micrographs are shown in Figures 4-2 through 4-6. This was the first time that the In Situ Fiberization process had been used to generate an interconnected fibrous network without use of a hydrocarbon polymer. The experiment was successfully repeated to insure that it was reproducible.

After successful fiberization of PCTFE, plans for further work were reviewed, and since new information from NASA indicated that the 533 K (500°F) requirement for SIP use might be low and that 643 K (700°F) might actually be required in application. Two possible approaches were considered. The first was to concentrate all subsequent effort on the very high temperature resistant polymers. The second was to first expand efforts on two Class IV polymers despite their lower temperature resistance — polyphenylene oxide (PPO) at 533 K (500°F), and polyphenylene sulfide at 533 K (535°F) — before proceeding to Class II materials.

The advantage to the first approach was clear. The number of experiments with polymers suitable for SIP use would be maximized. However, the disadvantages were also clear. Both the thermodynamics and the hydrodynamics of solution agitation with the high temperature polymers are completely different than encountered in the past with aliphatic materials. The thermodynamics are different, as evidenced by the fact that no solvents were found in which the polymers can be dissolved by heating and then precipitated by cooling. The hydrodynamics are also undoubtedly different because of the high chain stiffness of the high temperature aromatic polymers. Therefore, the disadvantage of trying to advance the technology by experimentation with these materials is the difficulty of determining when one set of processing conditions (thermodynamic or hydrodynamic) is improved, since improper manipulation of either set will preclude successful fiberization. In other words, this approach would make it hard to separate variables.

On the other hand, the second approach would decrease the number of experiments performed with polymers for final SIP application, but it would allow better separation of hydrodynamic and thermodynamic variables. Both PPO and PPS have molecular chain stiffnesses comparable to those of the very high temperature polymers since both have aromatic backbones.

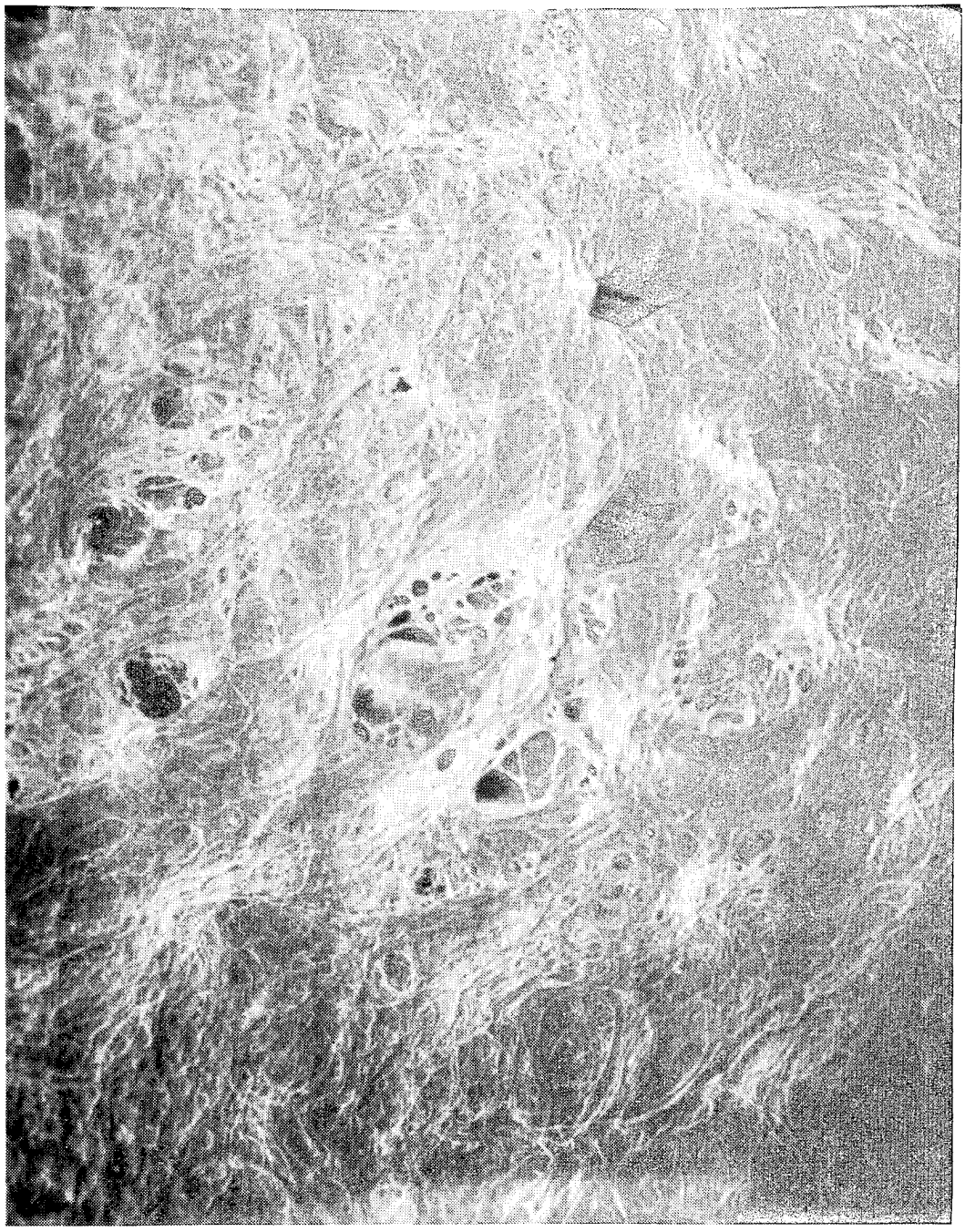

Figure 4-2. SEM of PCTFE fibers produced by In Situ Fiberization. Magnification ≈25X.

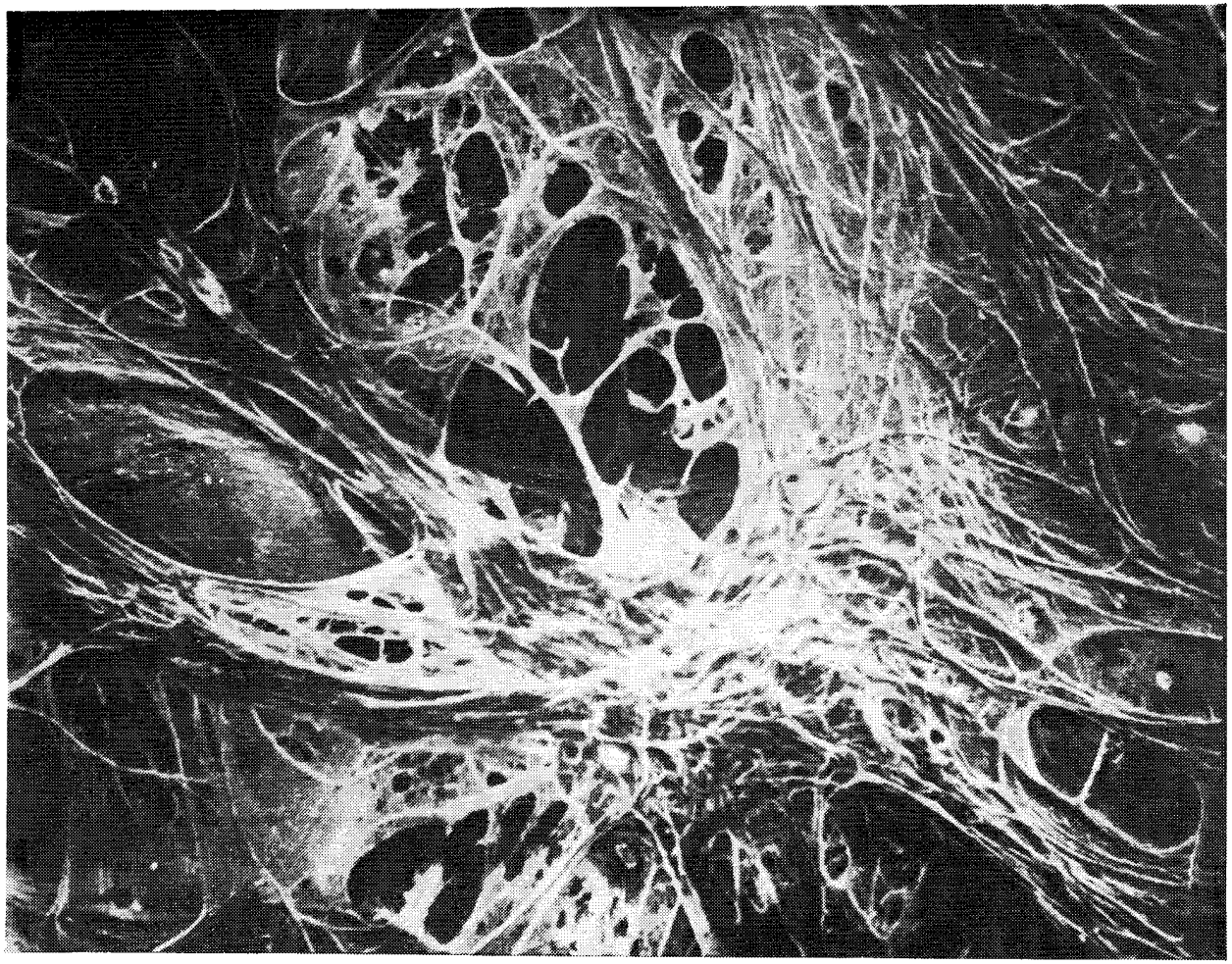

Figure 4-3. SEM of PCTFE fibers produced by In Situ Fiberization. Magnification ≈120X.

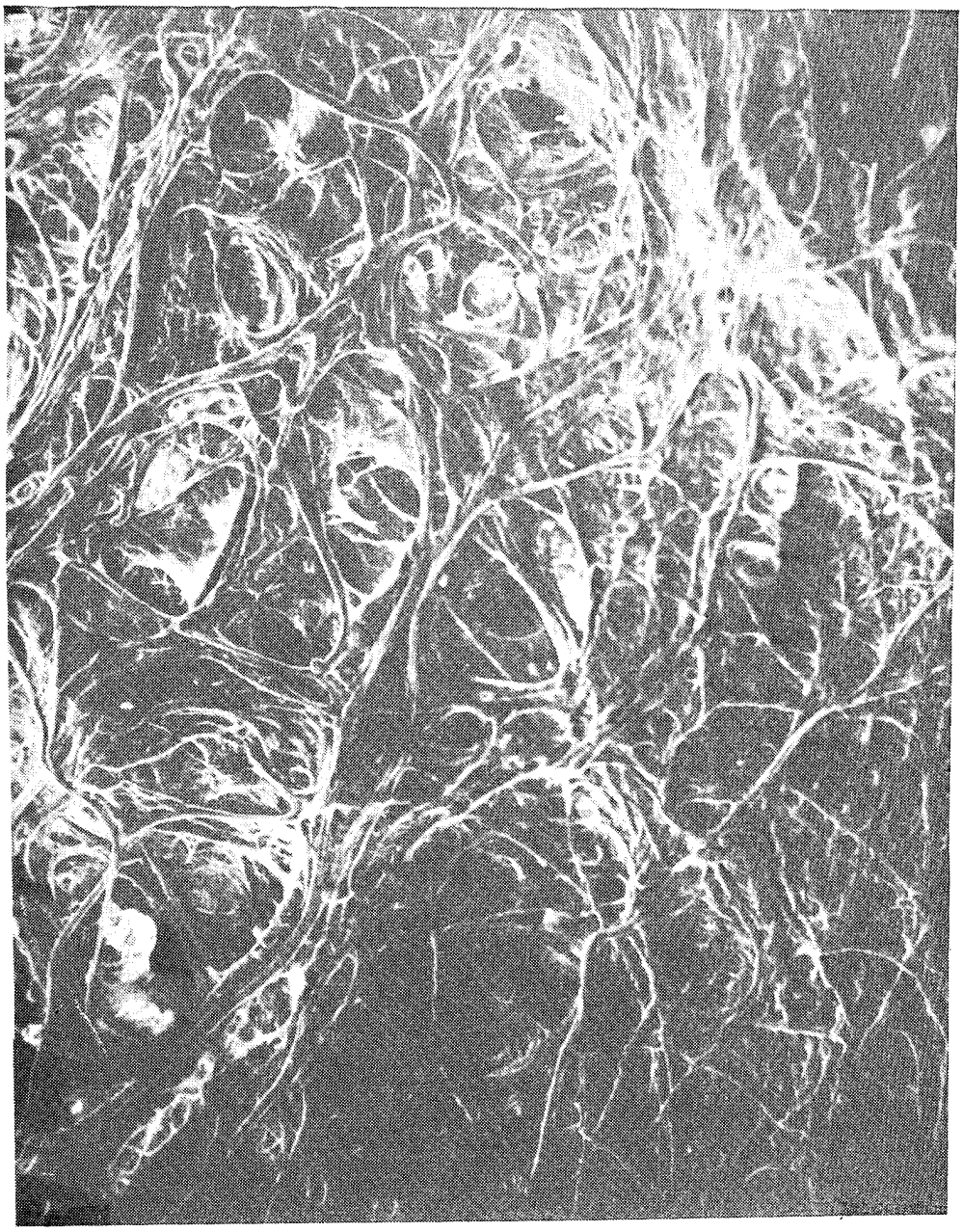

Figure 4-4. SEM of PCTFE fibers produced by In Situ Fiberization. Magnification ≈ 120X.

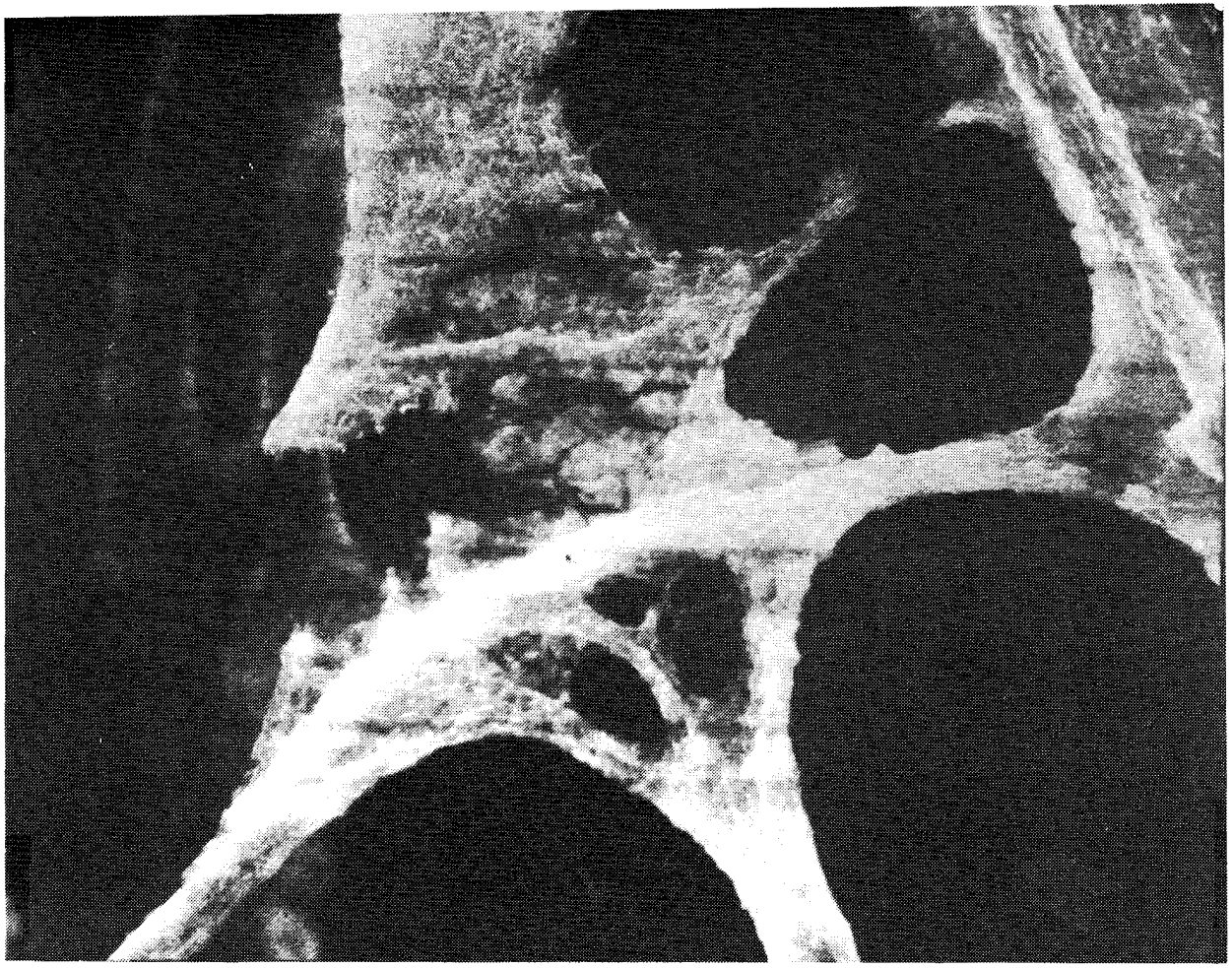

Figure 4-5. SEM of PCTFE fibers produced by In Situ Fiberization. Magnification ≈1200X.

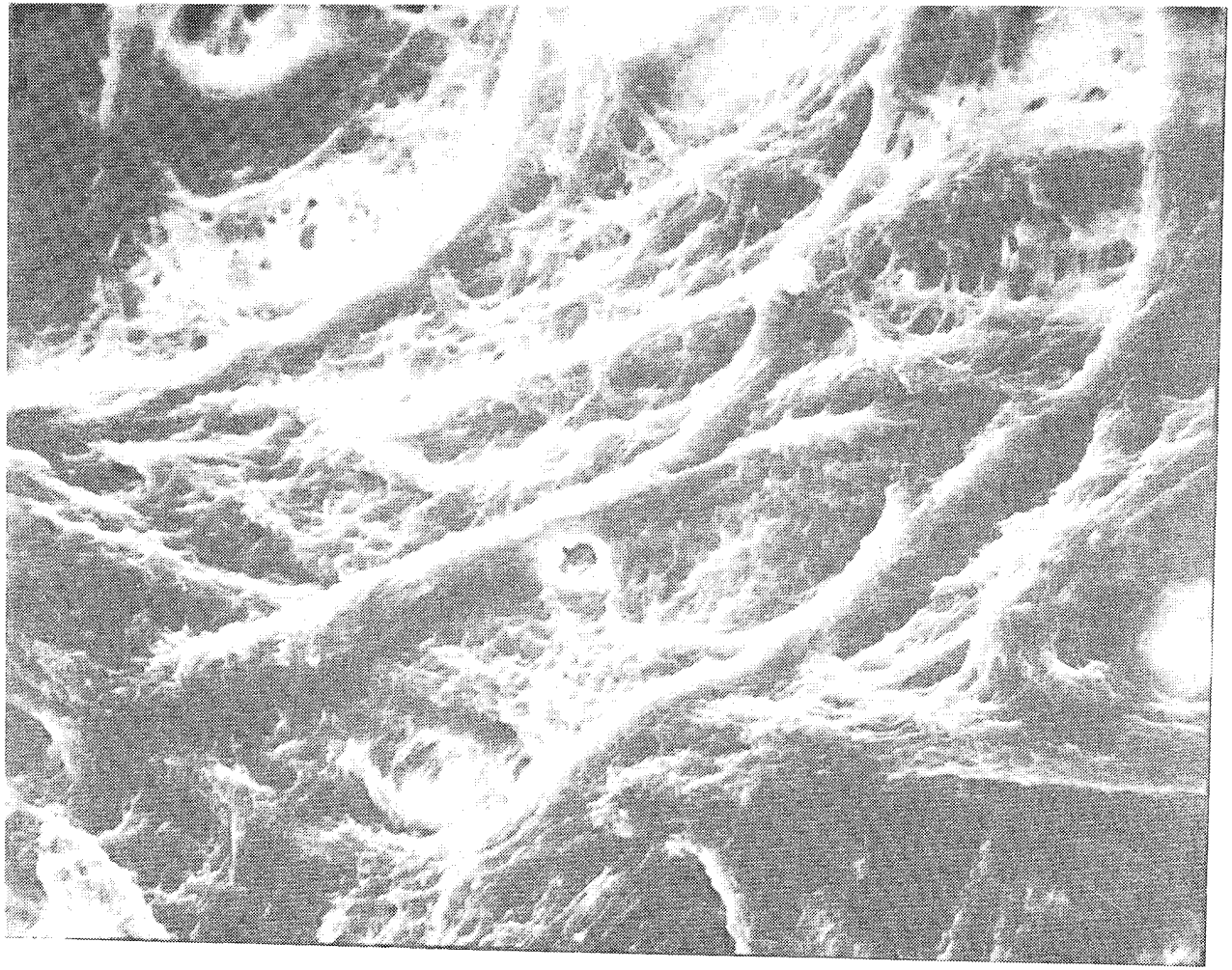

Figure 4-6. SEM of PCTFE fibers produced by In Situ Fiberization. Magnification ≈ 1200X.

However, both PPO and PPS are soluble in organic solvents and can be precipitated by cooling. Hence, at least qualitatively, only the hydrodynamics and not the thermodynamics of processing would differ from conventional ISF requirements. Presumably, experiments with these materials could be used to determine optimum hydrodynamic process conditions for stiff chain molecules in general, and subsequent experiments with Class II materials could concentrate on determining proper thermodynamic conditions for fiberization.

Based on the above logic, it was decided to continue work with PPO and PPS in an attempt to improve understanding of the hydrodynamic requirements for fiberization of stiff chain, aromatic backbone polymers. Concurrently, experiments were initiated with poly p-phenylene terephthalamide. This material was believed to be the most promising of the very high temperature polymers because of its crystallinity and availability, and because its molecular structure allows for relatively high chain flexibility (for an aromatic backbone polymer). The results of the experiments are described below in the order PPO, PPS, poly p-phenylene terephthalamide.

From a thermodynamic standpoint, the PPO which was available (actually poly-2,6-dimethylphenylene oxide) was a most promising polymer. It was found to dissolve in α-pinene at ~418 K (293°F) and to reprecipitate at ~368 K (203°F). In mixed xylenes, it dissolved at ~318 K (113°F) and recrystallized at room temperature. Mixtures of the two solvents yielded intermediate behavior. Hence, the necessary thermodynamic attraction between molecules appeared to exist. However, In Situ Fiberization was not accomplished. Experiments were performed by 20-54 Hz agitation of fine mesh metal screens and other objects in supercooled solutions containing 2-4 percent (weight to volume) polymer. Such conditions would have yielded copious fibers with polypropylene, polyethylene, or even PCTFE, but did not with PPO. In some experiments, crystallization of PPO occurred during agitation, as evidenced by the appearance of cloudiness in solution. Simultaneously, polymer precipitated onto the agitating objects. However, the precipitates were not fibrous.

Because PPO appeared to have sufficient thermodynamic drive to crystallization, the lack of In Situ Fiberization was ascribed to slow kinetics of crystallization, and/or insufficient hydrodynamics. The latter seemed particularly reasonable in view of the relatively low molecular weight of the polymer. The PPO sample used for experimentation had been obtained from Chem Services but was believed to be the same as the General Electric material used in the fabrication of Norex. If so, its number average molecular weight, Mn, would have been around 15-20,000, and its weight average molecular weight, Mw, about 50,000. This is substantially less than that for polypropylene used in typical fiberizations (Mn ~50,000 and Mw ~300,000). Since In Situ Fiberization is known to involve preferential precipitation of high molecular weight molecules, it seemed reasonable to suspect low molecular weight as the reason for the lack of fiberization. Shorter chains will "entangle" less in solution, and thus, it can be argued that an applied flow field will provide less perturbation of molecular configuration, and hence, a decreased tendency to fiberize.

In order to test this hypothesis, two higher molecular weight PPO samples were obtained from General Electric. These samples were reported to have intrinsic viscosities of 0.48 and 0.82 $\frac{dl}{g}$, from which viscosity average molecular weights, Mv ($\approx$Mw), were estimated to be 55,000 and 120,000, respectively.[9] Agitation experiments were then performed, but once again, In Situ Fiberization was not achieved. Interestingly, it did appear that agitation may have increased the rate of polymer precipitation, but this was only a qualitative observation, and was unsupported by concrete data. Overall, it was concluded that either the PPO molecular weight was still too low, or the kinetics of crystallization were just too slow to allow fiberization under experimentally attainable conditions, or both. The latter hypothesis might reflect the bulky, stiff nature of the aromatic backbone when compared with aliphatic polymers. In any case, since there was no immediately available way to solve either deficiency, further experimentation with PPO was abandoned.

Concurrent with the above experiments, efforts were also expended to fiberize the other Class IV aromatic backbone polymer, PPS. This material was found to be soluble in biphenyl at 513 K (465°F) and to precipitate from solution near 463 K (375°F). A limited number of agitation experiments were performed, but these were complicated by the fact that biphenyl, a solid at room temperature, evaporated on heating and then solidified on experimental equipment. As with PPO, fiberizations were not achieved. In view of the chemical similarities between PPO and PPS, it seems logical to presume that the same factors which preclude the former from fiberizing also inhibited the latter.

As discussed previously, while experiments with PPO and PPS were being performed, efforts to fiberize poly p-phenylene terephthalamide from sulfuric acid, H_2SO_4, were also conducted. During these efforts, the first necessity was to devise a technique for counteracting the unsatisfactory thermodynamic character of the solution. In a poly p-phenylene terephthalamide/H_2SO_4 solution, the polymer molecules are protonated and repel one another, regardless of flow conditions. Hence, to promote a polymer-polymer attraction, it was reasoned that a stronger base than the polymer would have to be added.

Therefore, the approach taken was to add water, in one form or another, to solutions during agitation. Essentially, the water would take the place of supercooling in conventional In Situ Fiberization by promoting polymer/polymer interaction at the expense of polymer/solvent interaction. Of course, the fundamental difficulty of such an approach was that the water had to be added to the solution in a slow, controlled fashion. Rapid addition would result in uncontrolled polymer precipitation, not to mention the safety hazards associated with addition of water to concentrated acid. Several techniques for accomplishing slow water release were devised. These were: (1) dropwise addition of pure water, (2) dropwise addition of diluted H_2SO_4, (3) exposure of solutions to water vapor, (4) dropwise addition of organic alcohols which presumably would be dehydrated to yield water, and (5) addition of hydrated inorganic salts - notably $CaCl_2 \cdot 2H_2O$, $MgCl_2 \cdot 6H_2O$, $MgSO_4 \cdot 7H_2O$, and $Na_3PO_4 \cdot 12H_2O$ - which would be dehydrated and also perhaps act as seeding agents for polymer precipitation.

All of these techniques were tried but none resulted in fiber growth. Nevertheless, some interesting results were achieved. It was found that dropwise addition of 50/50 H_2O/H_2SO_4 until the first appearance of cloudiness, followed by agitation of the solution with a metal screen, resulted in the precipitation of polymer onto the screen. Micrographs of the precipitate are shown in Figures 4-7 and 4-8. Furthermore, control experiments performed by letting an identical screen sit quiescently in an identically prepared solution resulted in markedly less precipitation on the screen. Hence, there was qualitative evidence that agitation accelerated the crystallization process even if it did not result in fiber growth.

On this tantalizing note, efforts on the SIP portion of the program were halted.

Figure 4-7. SEM of precipitate on a metal screen agitated in a poly p-phenylene terephthalamide/H_2SO_4 solution. Magnification ≈ 60X.

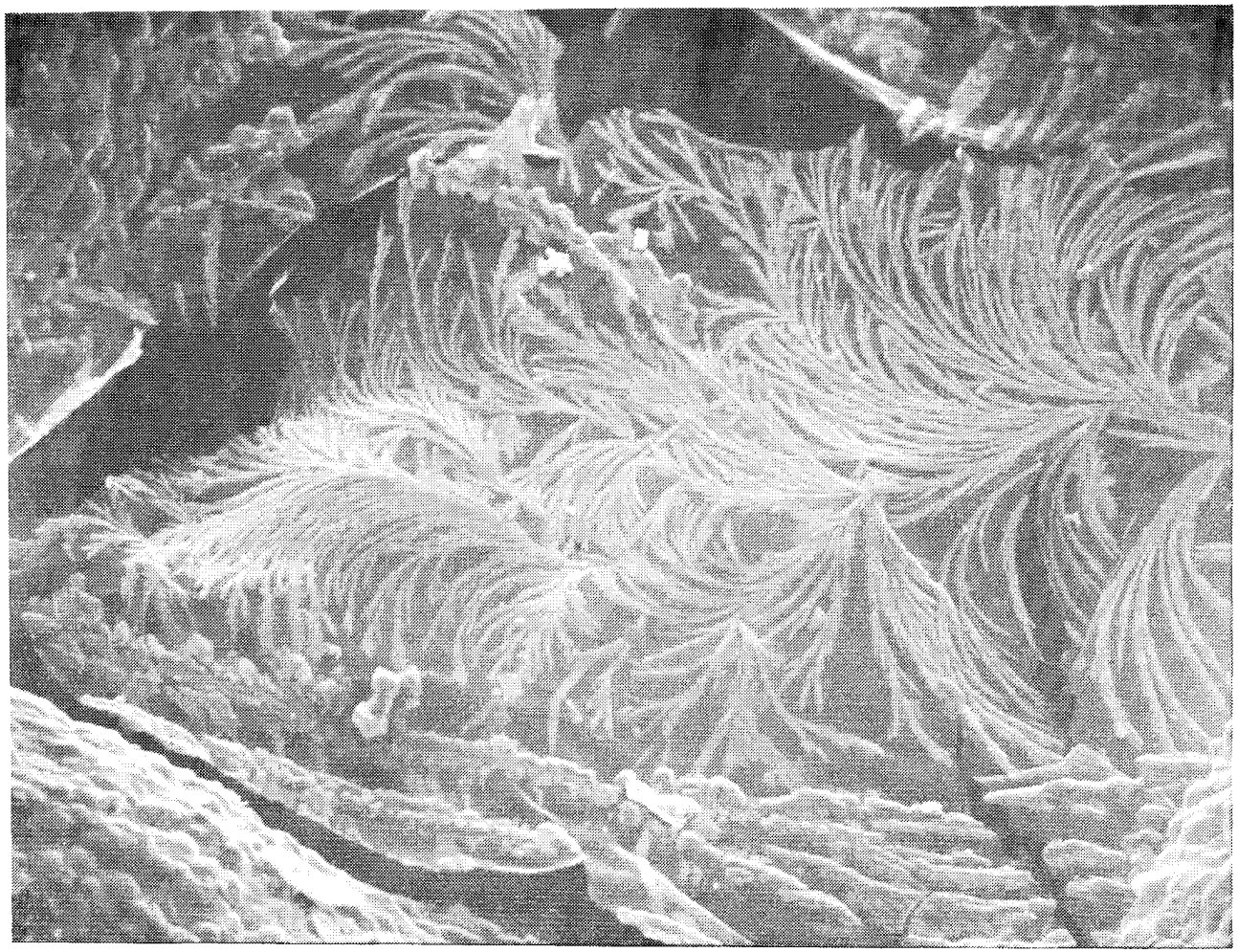

Figure 4-8. SEM of precipitate on a metal screen agitated in poly p-phenylene terephthalamide/H_2SO_4 solution. Magnification ≈ 250X.

5.0 FEASIBILITY STUDY - IN SITU FIBER/GRAPHITE/ EPOXY COMPOSITES

Prior to the initiation of this program, Hughes had demonstrated the feasibility of interconnecting two-dimensional arrays of unidirectional graphite fibers with In Situ Fiberized polypropylene. Several small specimens, up to approximately 8 cm (3 inches) by 5 cm (2 inches), had been prepared. Scanning Electron Micrographs of one specimen are shown in Figures 5-1 through 5-5. It was conceived that such graphite/ISF fiber arrays, when impregnated with epoxy resin and laminated into composite sheets, would have better mechanical properties than normal graphite/epoxy (GR/EP) composites. It was hoped that ISF fibers oriented transverse to the unidirectional graphite fibers would improve intralaminar and interlaminar stress transfer through the resin, and would thereby increase fracture toughness. Based on this hypothesis, the second task of the current program was initiated. The objective was to fabricate and test sufficient numbers of GR/EP/ISF samples and suitable GR/EP controls to determine the feasibility of the concept. As initially proposed, the test matrix consisted of three ambient temperature and two elevated temperature tests, as shown in Table 5-1.

The task was divided into four phases. Phase I involved the fabrication of relatively large graphite fiber arrays and their subsequent In Situ Fiberization. In addition, several small, previously fiberized arrays were used to evaluate impregnation and testing techniques, as well as to provide a modicum of preliminary data. During Phase II, larger fiberized arrays, as well as unfiberized controls, were laminated and impregnated with epoxy resin. The specimens were then evaluated in Phase III. Concurrent with the above efforts, Phase IV fabrication of specimens for NASA evaluation was conducted.

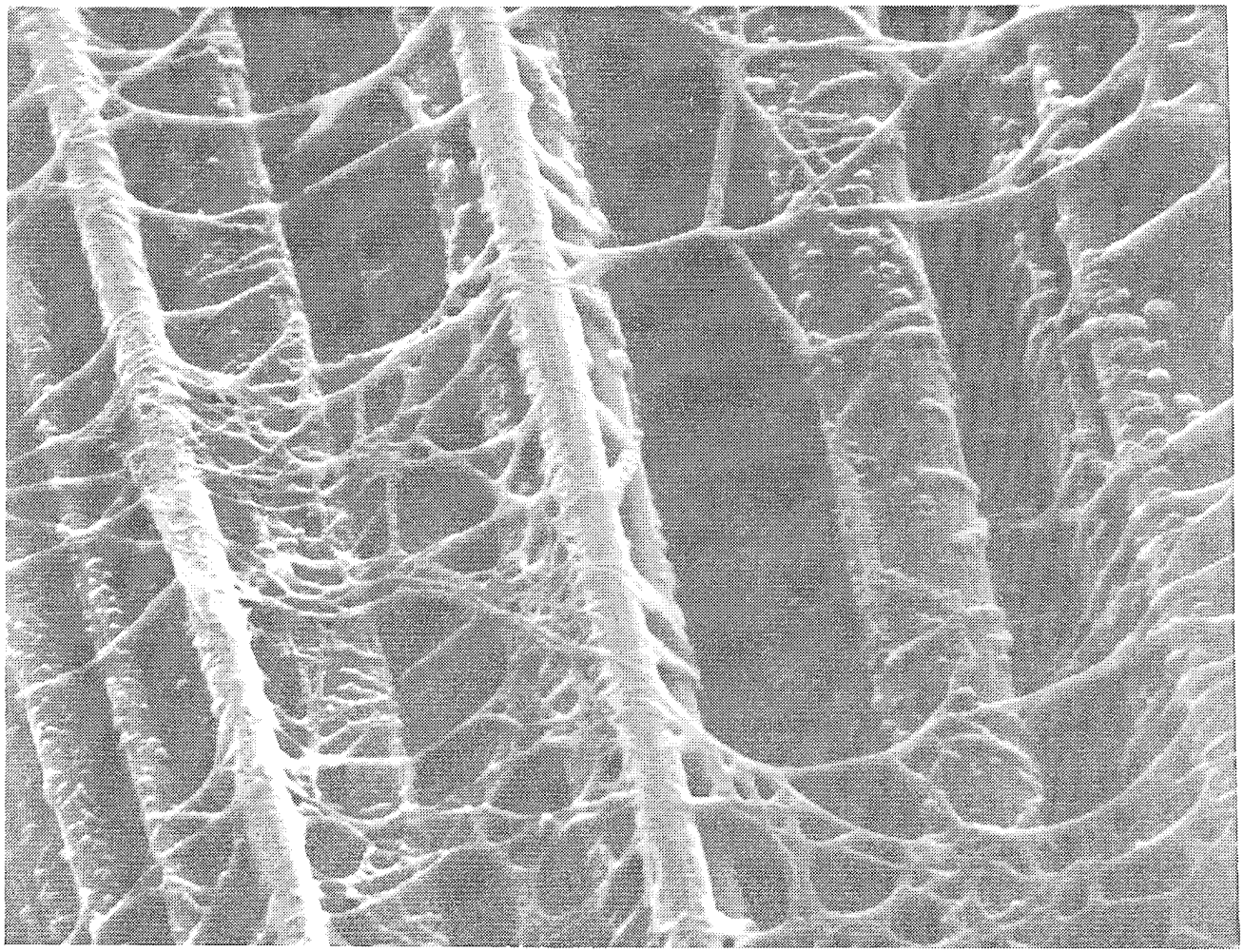

Figur5-1. SEM of unidirectionally oriented graphite fibers interconnected by In Situ Fiberized polypropylene. Magnification ≈1200X.

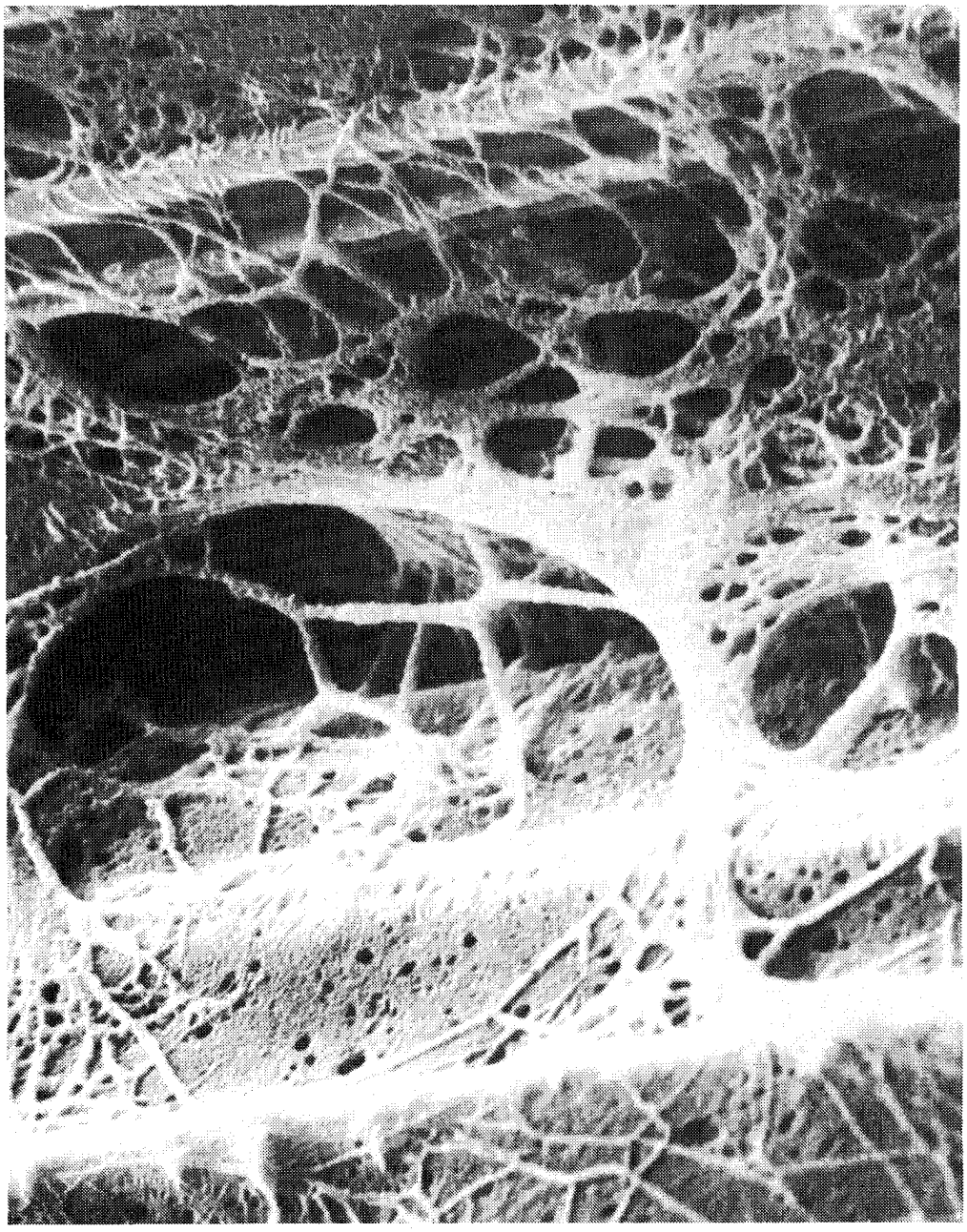

Figure 5-2. SEM of unidirectionally oriented graphite fibers interconnected by In Situ Fiberized polypropylene. Magnification ≈1200X.

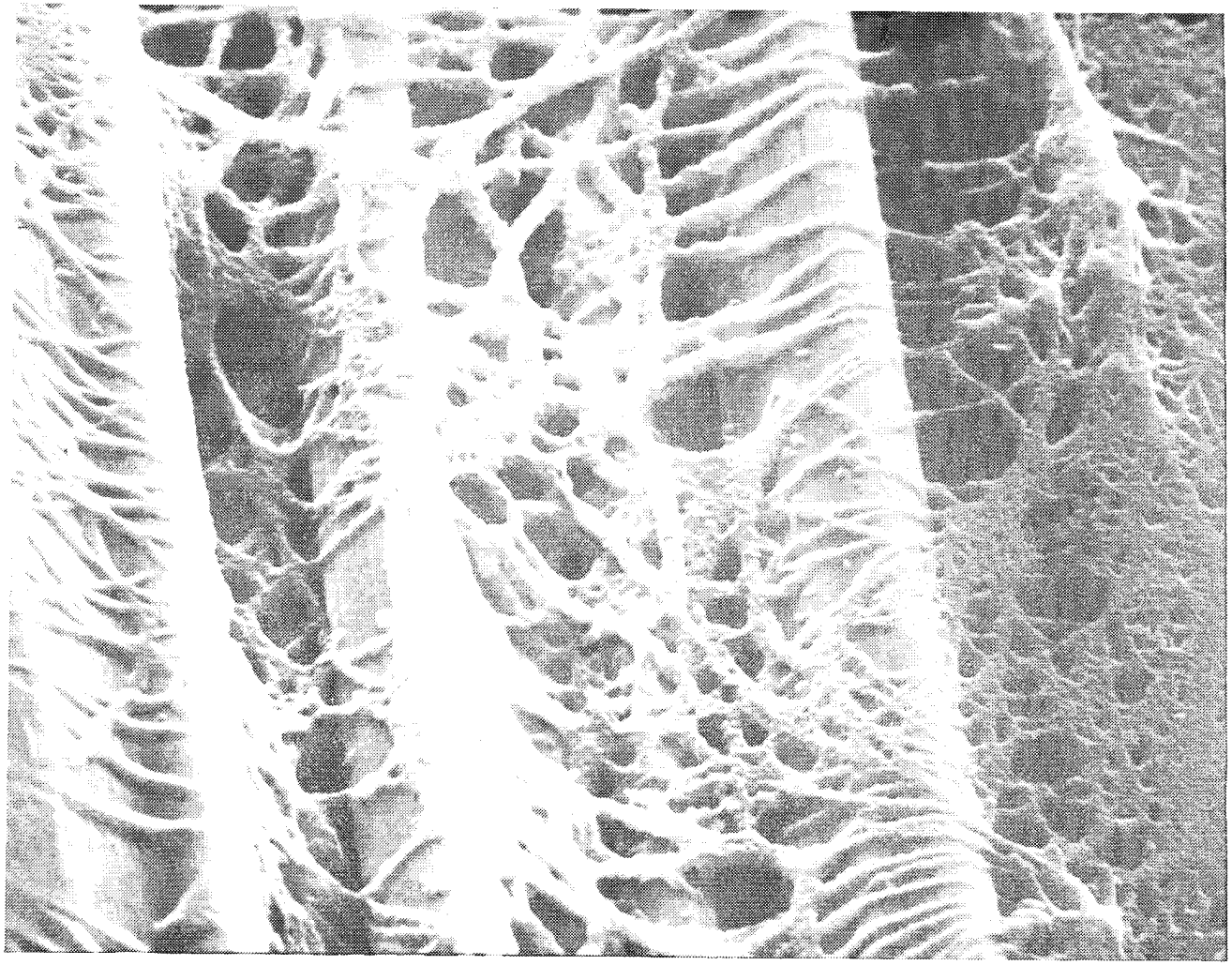

Figure 5-3. SEM of unidirectionally oriented graphite fibers interconnected by In Situ Fiberized polypropylene. Magnification ≈1200X.

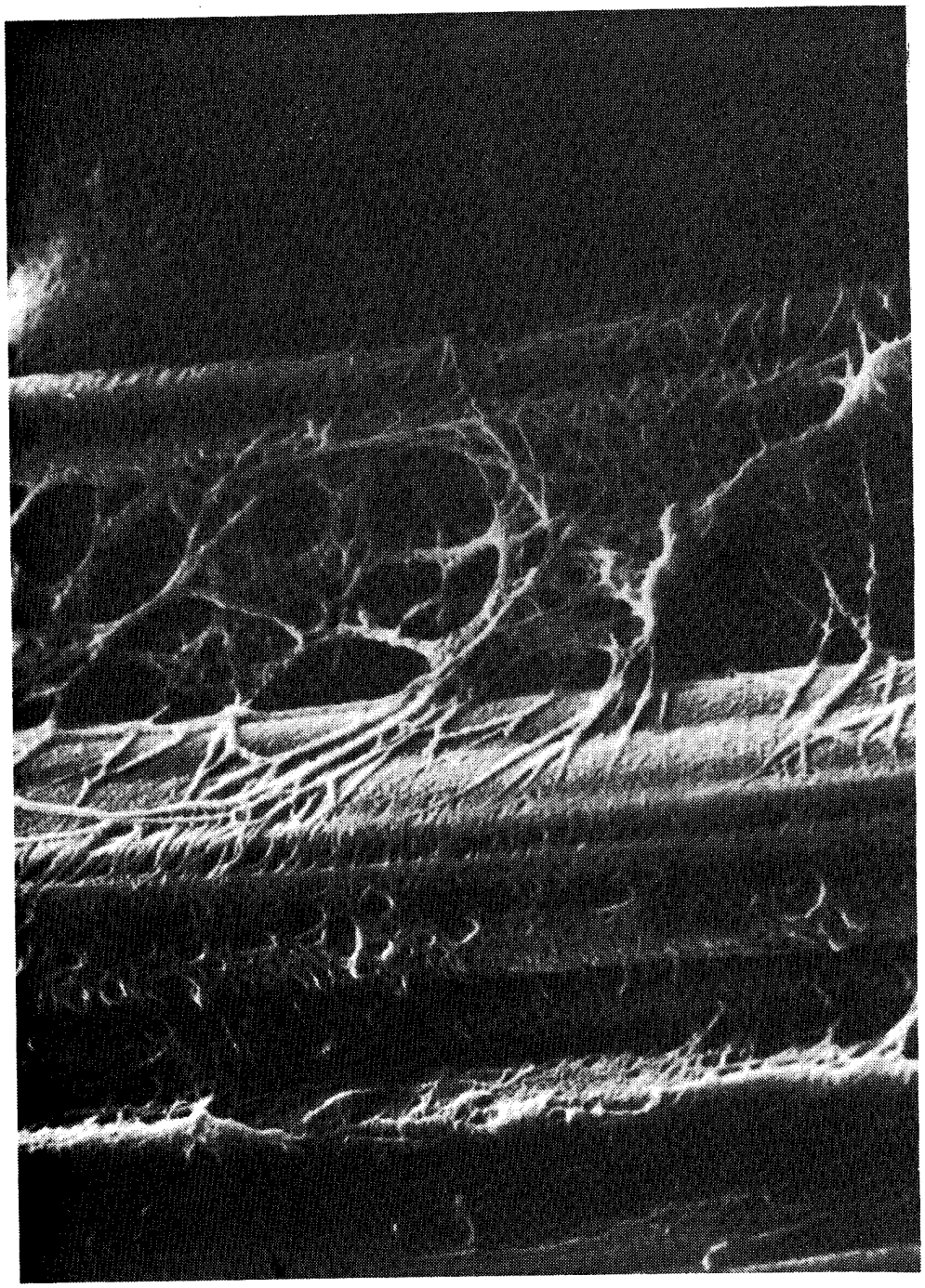

Figure 5-4. SEM of unidirectionally oriented graphite fibers interconnected by In Situ Fiberized polypropylene. Magnification≈2500X.

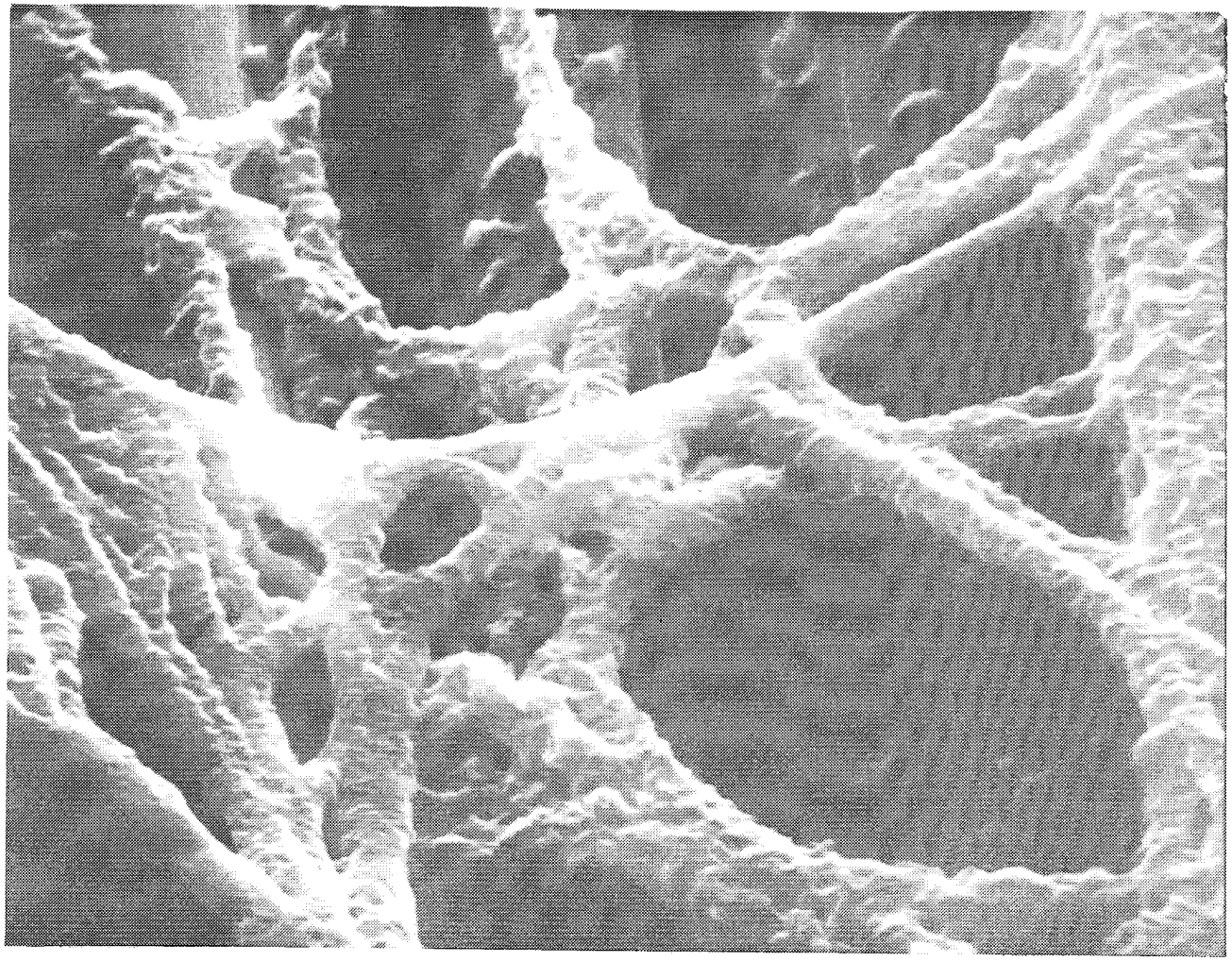

Figure 5-5. SEM of unidirectionally oriented graphite fibers interconnected by In Situ Fiberized polypropylene. Magnification≈6000X.

TABLE 5-1. ORIGINALLY PLANNED TEST MATRIX FOR GR/EP/ISF SPECIMENS AND GR/EP CONTROLS

Test	Test Temperature	No. of Replicates
(1) 45° Tension (ASTM D-3518)	RT	10
(2) 45° Tension (ASTM D-3518)	366 K (200°F)	
(3) Single Edge-Notch Fracture Toughness 0° (Advanced Composite Design Guide, Ref. Wu)	RT	20
(4) Flexure 0° (ASTM D-790)	RT	5
(5) Flexure 0° (ASTM D-790)	366 K (200°F)	5

5.1 PRELIMINARY EXPERIMENTS

As noted earlier, several small arrays of graphite fiber had been constructed and fiberized with isotactic polypropylene prior to program initiation. Figure 5-6 schematically illustrates how two "sheets" of unidirectional graphite fiber were held for simultaneous processing. Photographs of unfiberized and fiberized arrays are shown in Figures 5-7 through 5-10. After ISF processing, the bilayer specimens were extracted with acetone to remove residual xylene solvent, impregnated with epoxy, and then laminated. The resin system used was Epon 828/HV. HV is a multicomponent curing agent developed by Hughes for potting applications. One component is low boiling, and consequently the resin system has been found to be unsuitable for conventional vacuum bag laminating techniques. Nevertheless, it was

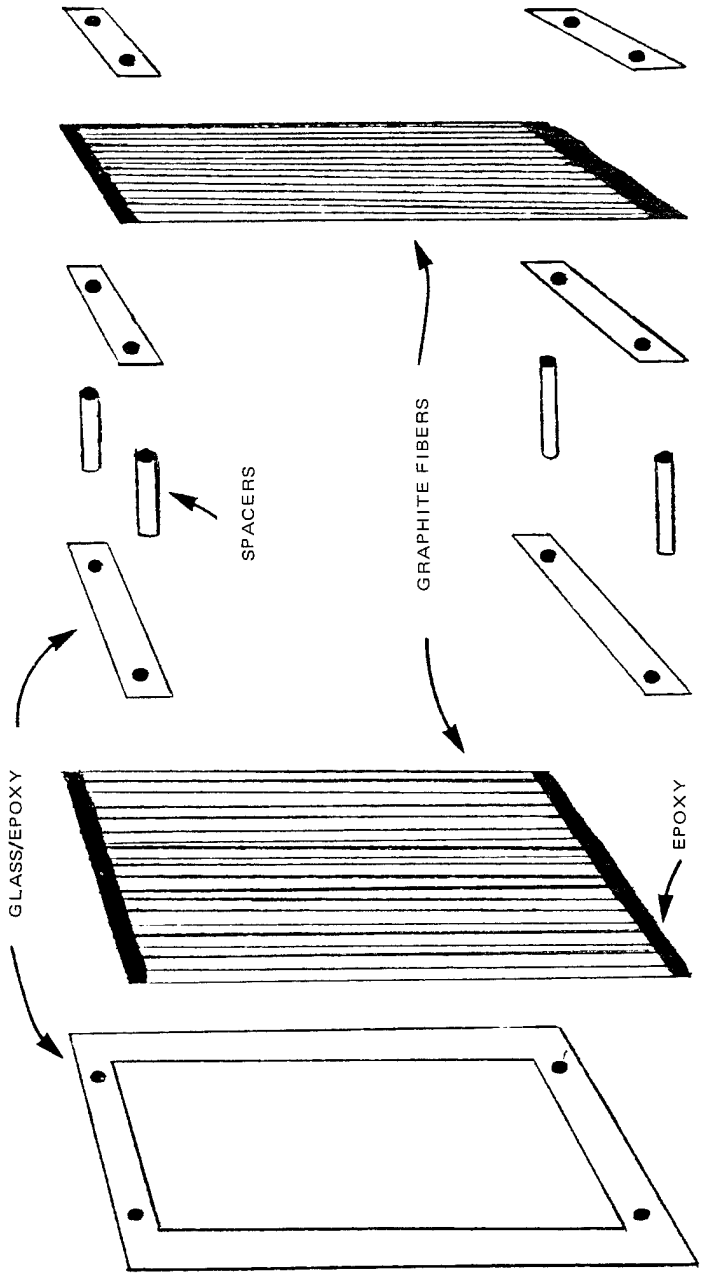

Figure 5-6. Schematic representation of experimental setup for simultaneous fiberization of two graphite fiber sheets.

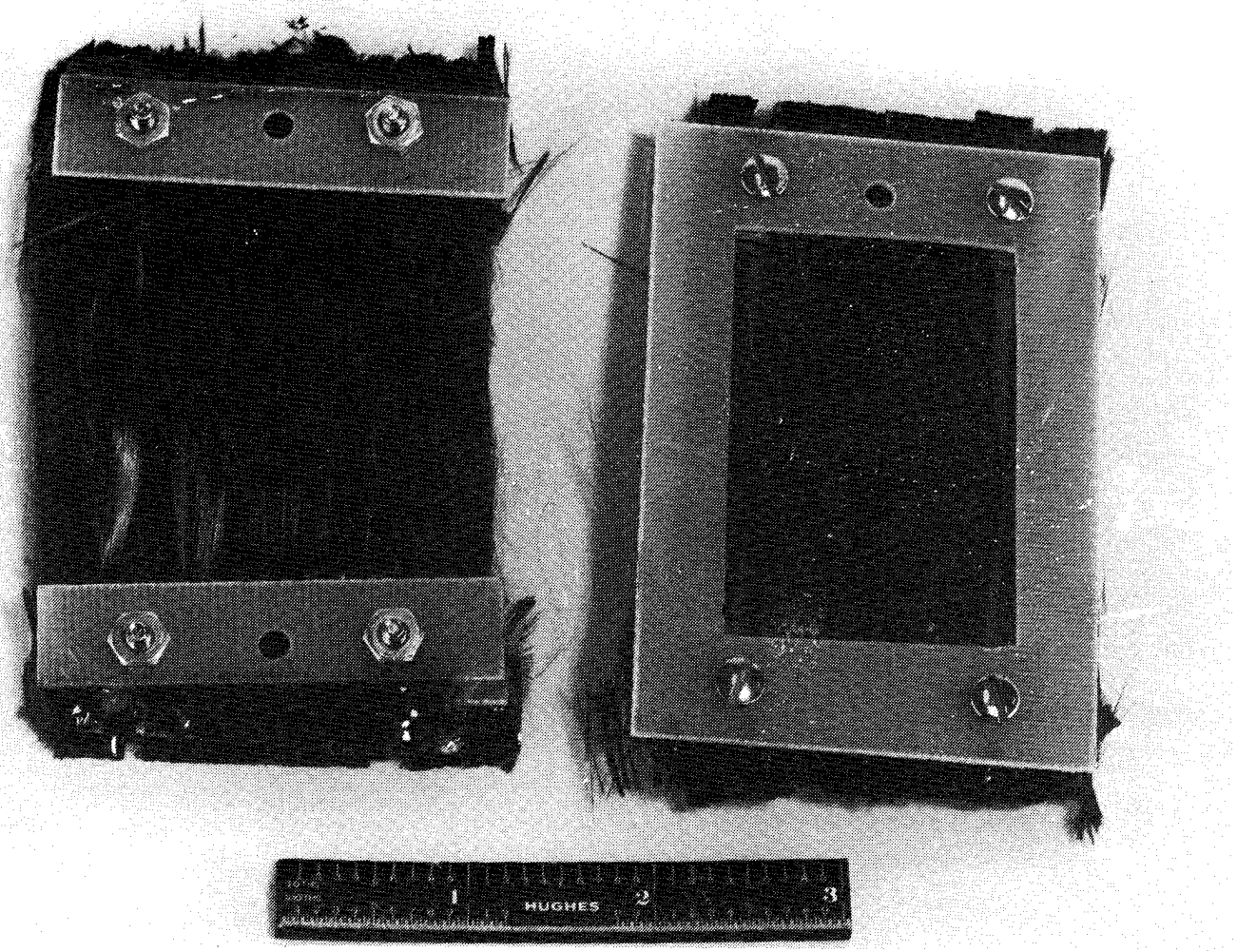

Figure 5-7. Graphite fibers arrays, constructed as in Figure 5-6.

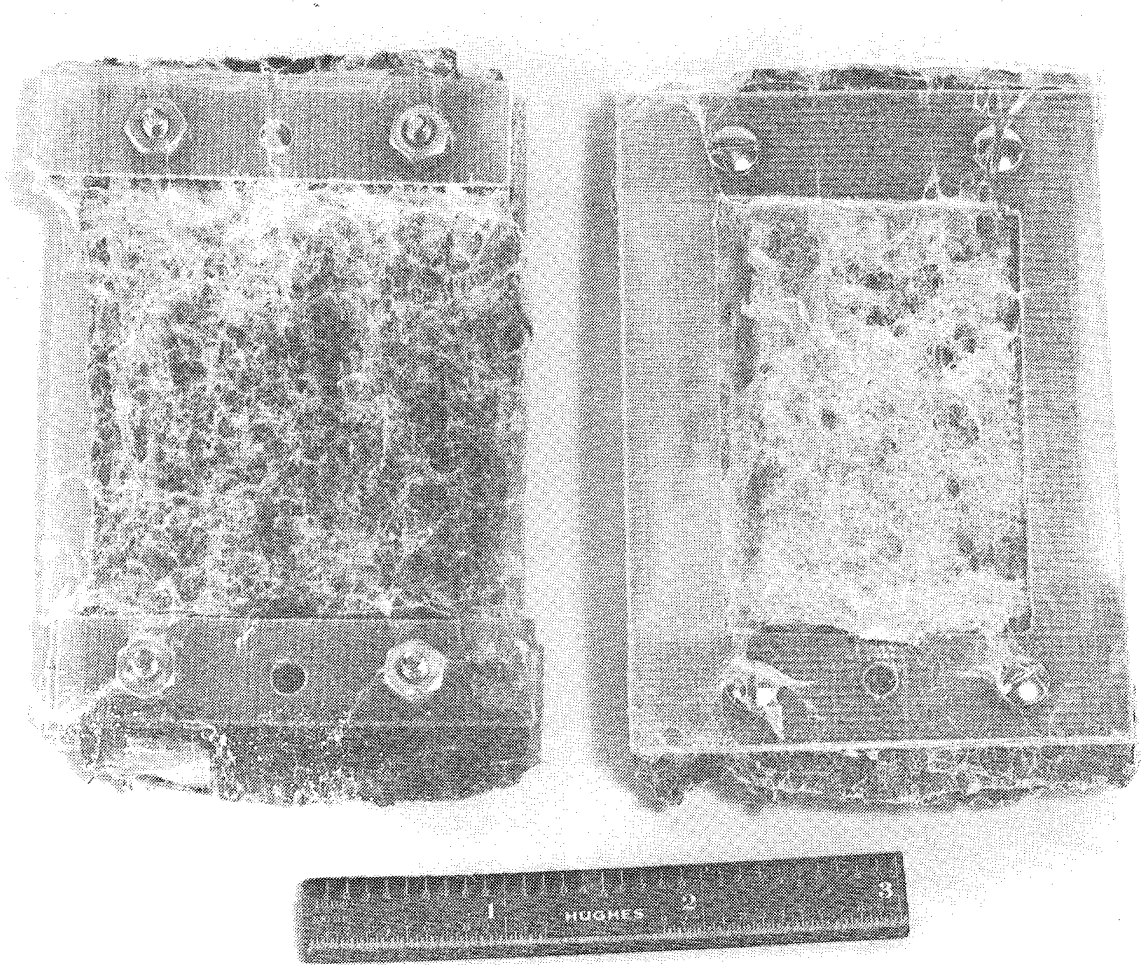

Figure 5-8. In Situ Fiberized graphite fiber arrays.

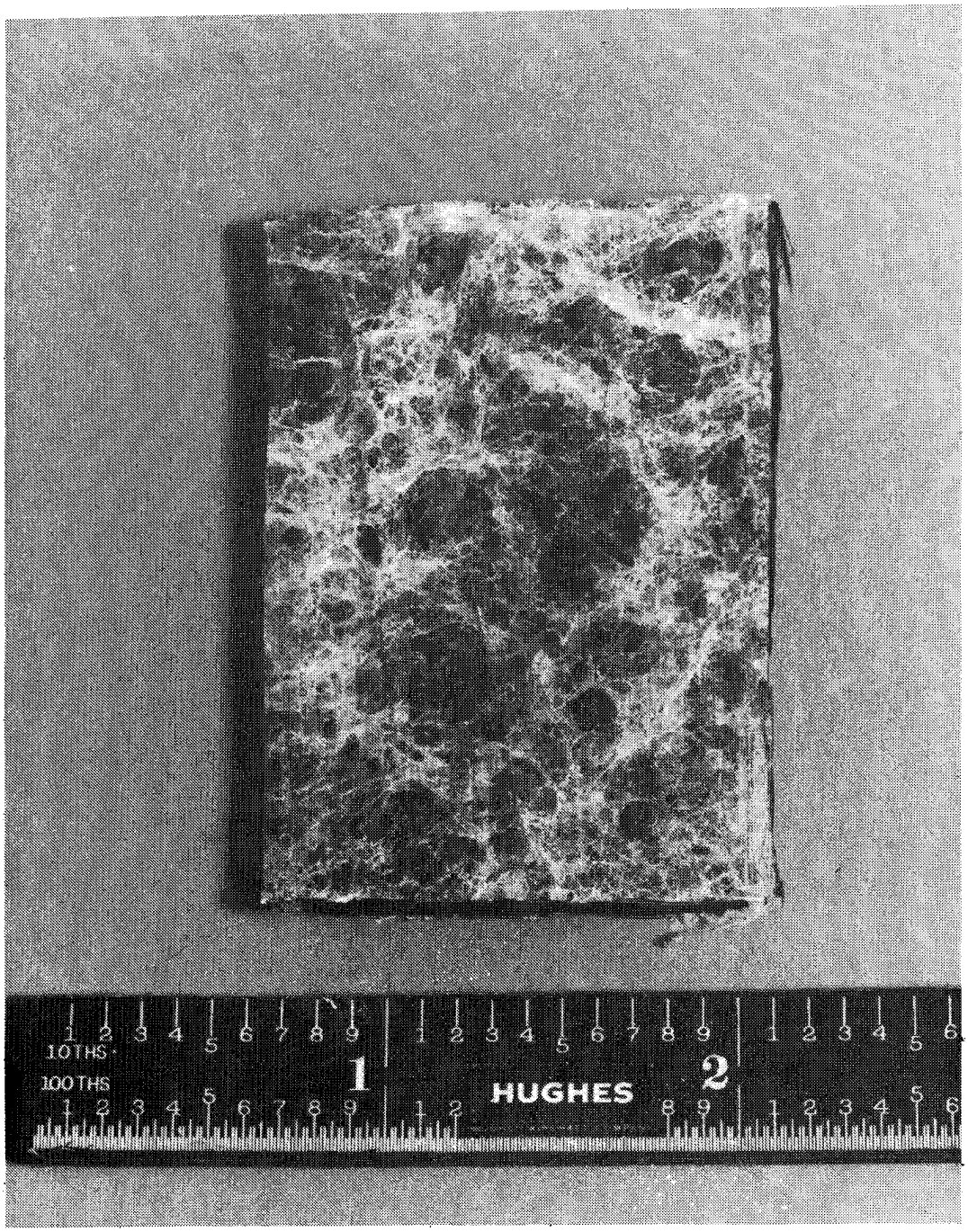

Figure 5-9. In Situ Fiberized graphite fiber array after removal from frame used for agitation.

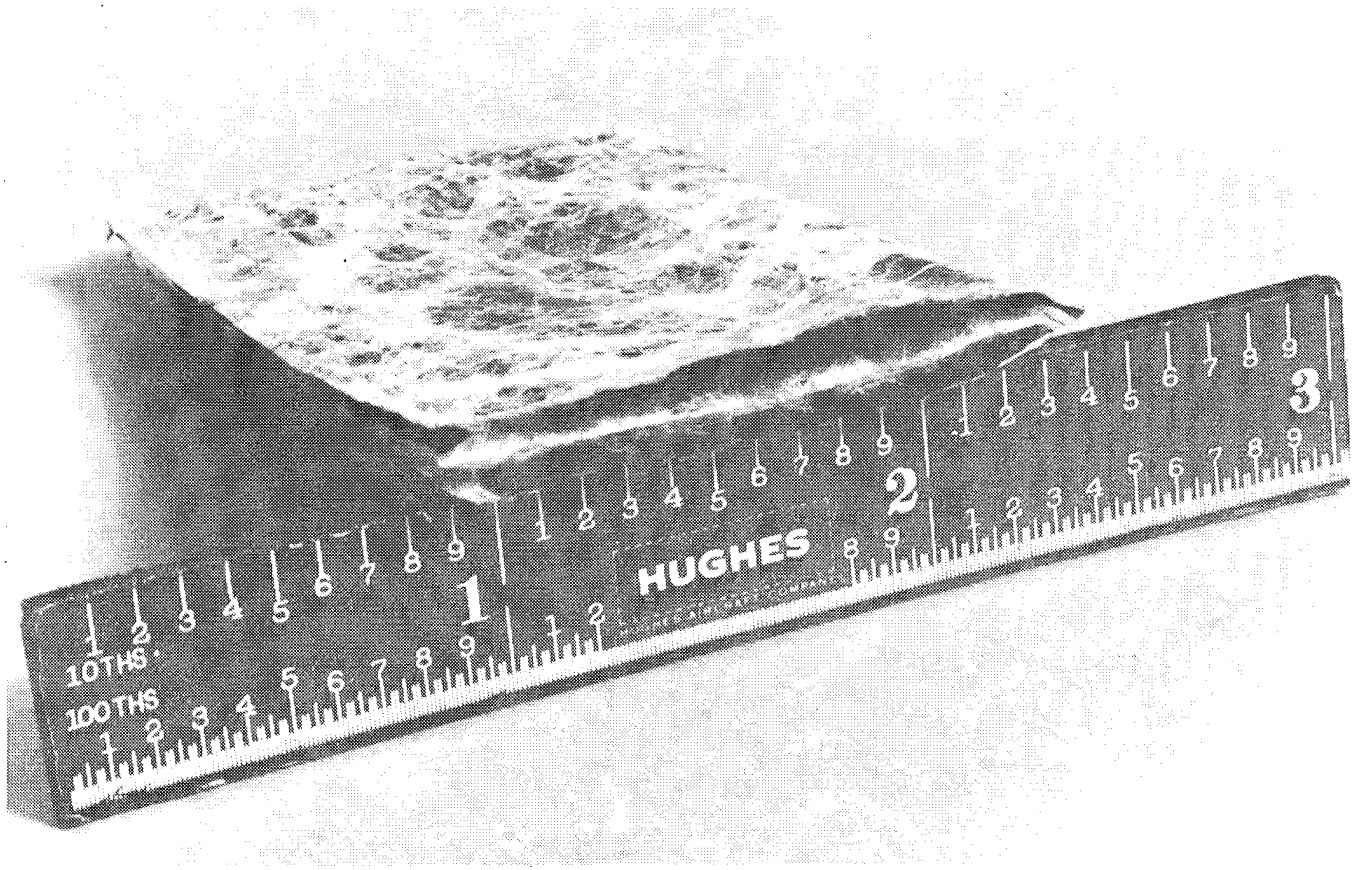

Figure 5-10. In Situ Fiberized graphite fiber array after removal from frame used for agitation.

decided to use HV for initial specimen fabrication because of previous Hughes experience working with it in conjunction with polypropylene In Situ Fibers. Specimens for test were prepared by compression molding. The composition of one such sample was subsequently determined by acid digestion (to remove resin) followed by burnout (to remove polypropylene). Details of the procedures are discussed in Appendix B. Analysis results, shown in Table 5-2, indicated that graphite fiber content was relatively low, only 41 percent, while PP and void volume percentages were 10 percent and 3 percent respectively.

Three GR/EP/ISF single edge-notch tensile fracture toughness test specimens were prepared from these preliminary laminated panels. Four GR/EP controls were also prepared. Test results, obtained by use of an Instron Mechanical Tester, were inconclusive. Instead of propagating horizontally across the graphite fibers as desired, failures propagated vertically between the fibers. The occurrence of this undesired failure mode rendered quantitative comparison of samples impossible. Nevertheless, one promising qualitative observation was made; in the fiberized specimens, cracks developed about one-quarter inch offset from the primary crack at the notch end. This phenomenon, not observed in the controls, seemed to suggest that lateral stress transfer was indeed better in the GR/EP/ISF samples than in the controls.

TABLE 5-2. COMPOSITION OF AN INITIAL SMALL GR/EP/ISF PANEL

Constituent	Weight (g)	Weight %	Assumed Sp. Gr.	Volume %
Celion-3000 Fibers*	0.836	52	1.77	41
Epoxy Resin	0.668	41	1.25	46
Polypropylene Fibers	0.116	7	0.95	10
Voids	0	0	0	3
Overall Panel	1.62	100	1.39**	100

*Celanese Corp., Chatham, NJ.

**Bulk density, g/cc

5.2 PHASE I - FIBERIZATION

Process Scale-Up

The first task was to design and construct an ISF system capable of processing graphite fiber arrays of relatively large size in relatively large quantity. In the design of the apparatus, the goal was to be able to fiberize specimens as large as possible without overloading the available agitation equipment. The apparatus constructed is shown in Figure 5-11. It consists of a driver, or shaker head, mounted on a metal frame and suspended over a container of solution held in a constant temperature oil bath. The shaker head is powered by a frequency generator/amplifier combination. Samples to be fiberized are attached to the bottom of the driver by a metal bar and then agitated in the solution below. This system allows for simultaneous agitation of two graphite fiber arrays 25 cm (10 inches) by 12 cm (5 inches) each.

As soon as the above apparatus was constructed, experiments were initiated to determine appropriate conditions for fiberizations. Preliminary specimens were fabricated from woven graphite cloth, as opposed to unidirectionally strung tow, because the former is much easier to handle. As shown in Figure 5-12, a sample of cloth was mounted in a glass/epoxy frame, which was in turn bolted to a metal rod for attachment to the shaker assembly.

Agitation experiments were conducted under a range of conditions known from previous work to be viable for ISF processing. A typical fiberized specimen is shown in Figure 5-13. After agitation of graphite cloth at 373 to 383 K (212° to 230°F) in xylene solutions containing 1 to 2 percent by weight polypropylene, SEMs of the resultant In Situ Fiberizations were obtained. Typical examples are shown in Figures 5-14 through 5-16. Qualitative observations were similar to those of previous work. Excessive lowering of the temperature or raising of the polymer concentration causes rapid fiberization. Unfortunately, it tends to be accompanied by the formation of less fibrous, presumably undesirable, precipitate. On the other hand,

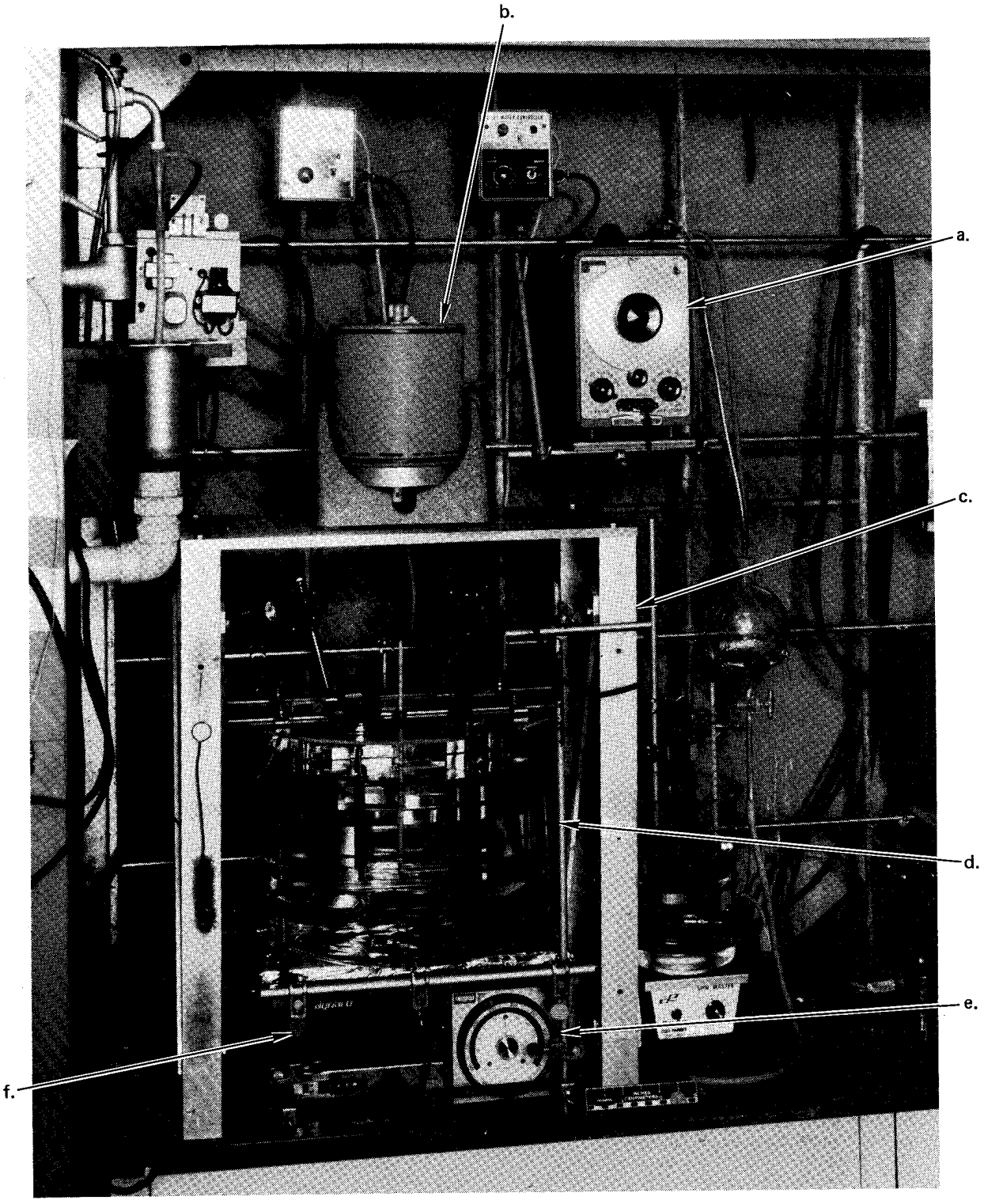

Figure 5-11. Apparatus constructed for agitation of 25 cm x 12 cm (10" x 5") graphite fiber arrays: a) signal generator; b) shaker head; c) support frame; d) oil bath assembly; e) temperature controller; f) amplifier.

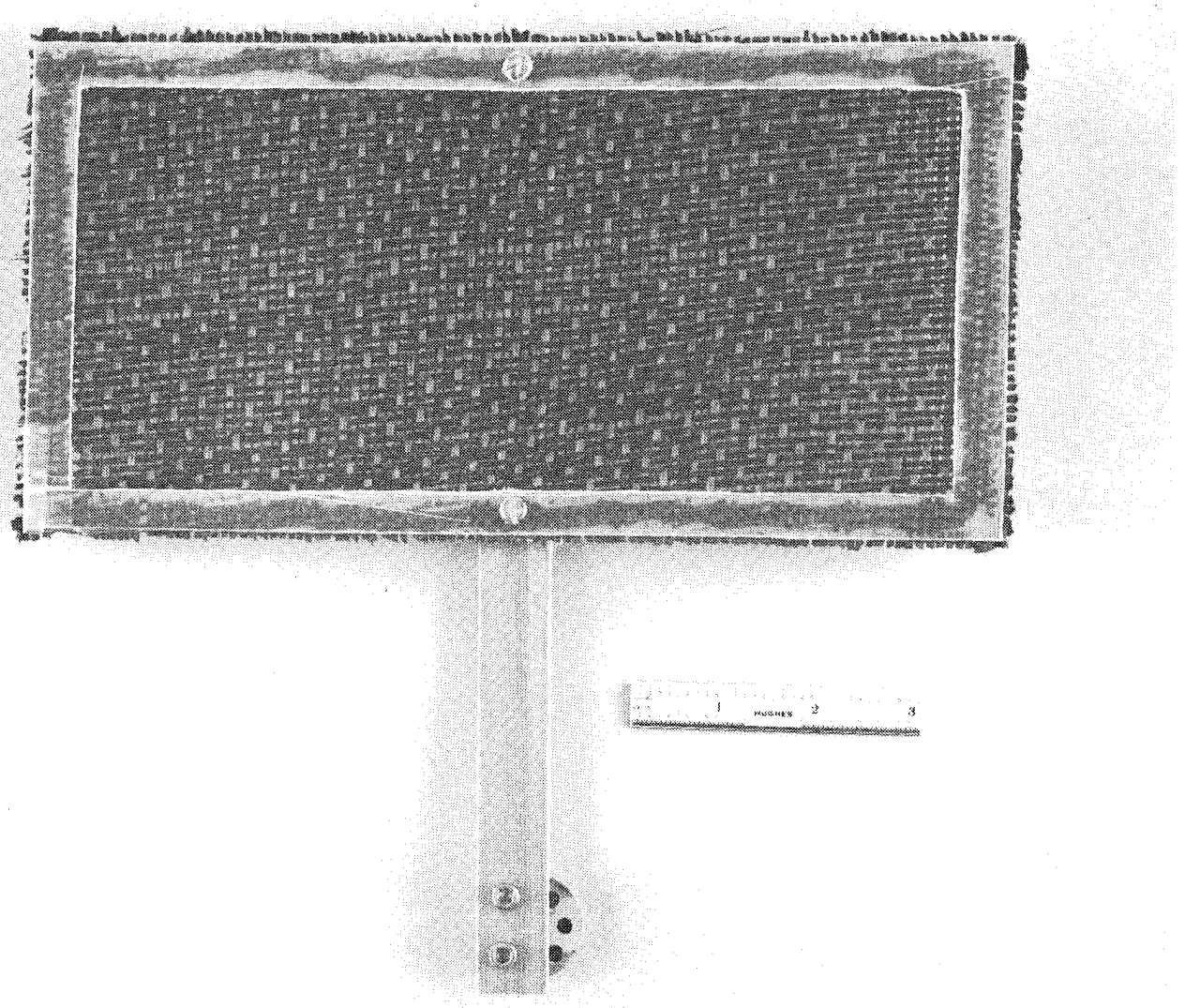

Figure 5-12. Graphite fiber cloth specimen used in process scale-up efforts.

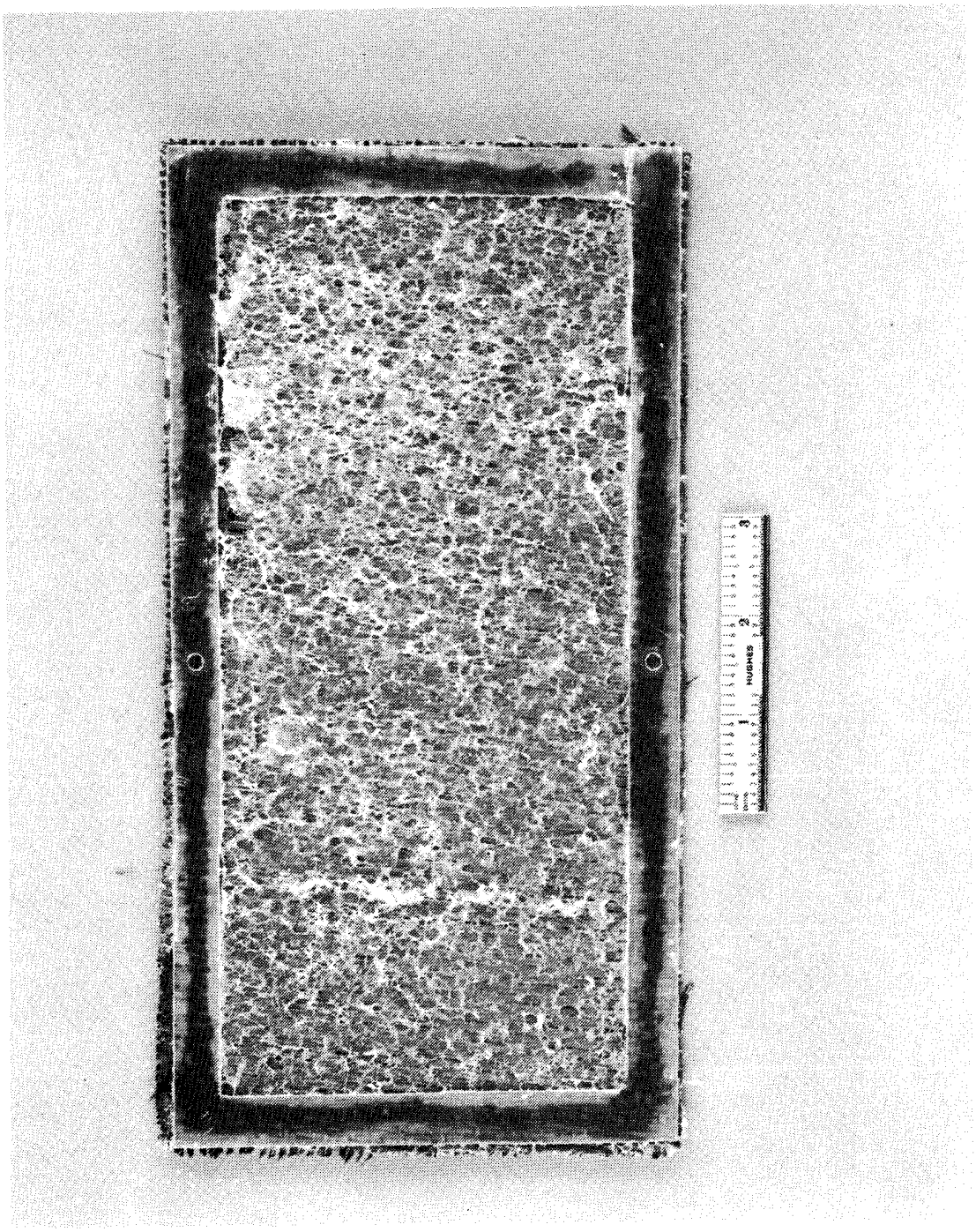

Figure 5-13. In Situ Fiberized graphite cloth specimen.

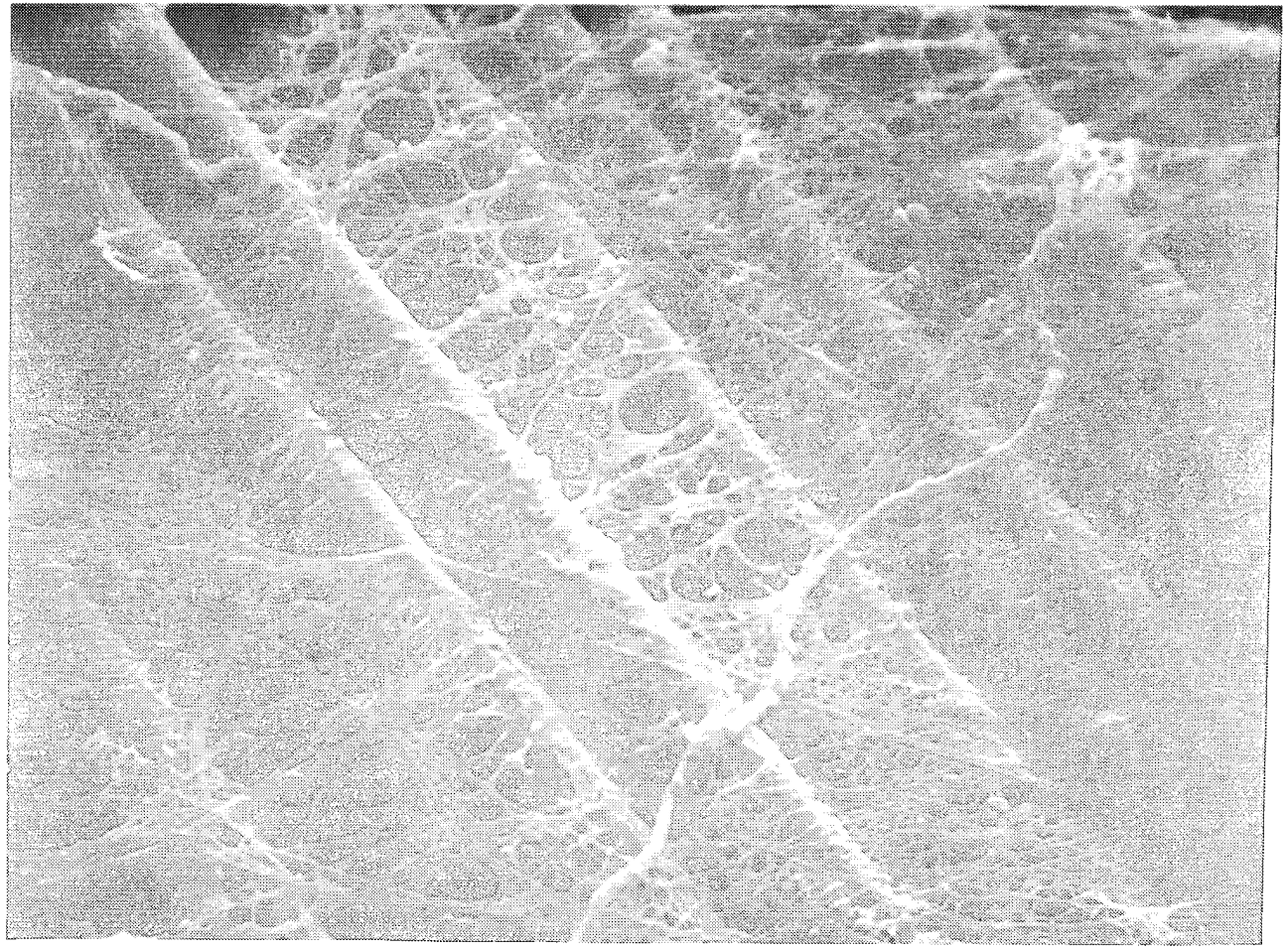

Figure 5-14. SEM of polypropylene In Situ Fibers deposited on graphite cloth from a 1.5 percent solution at 380 K (225°F). Magnification ≈1500X.

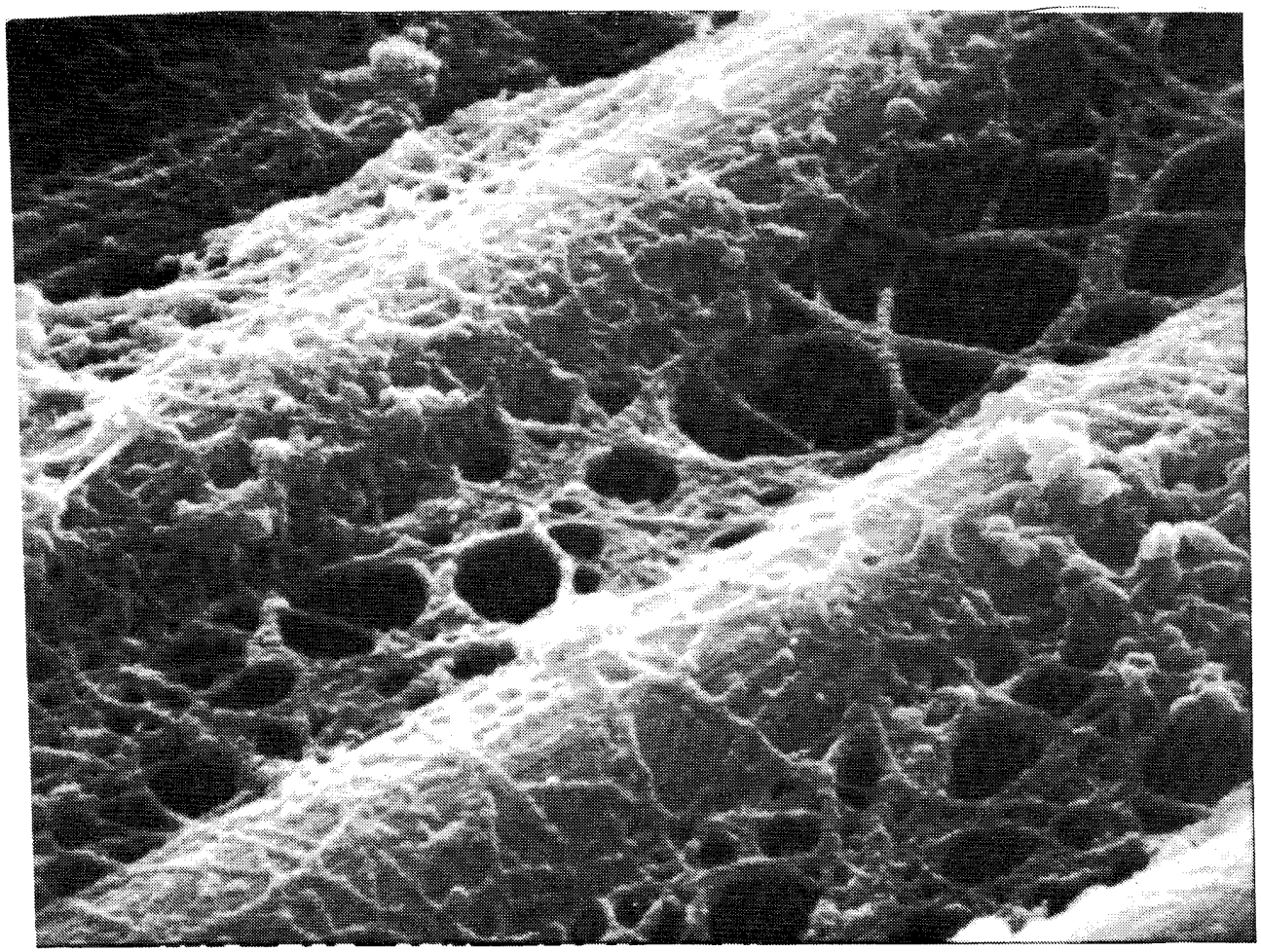

Figure 5-15. SEM of polypropylene In Situ Fibers deposited on graphite cloth from a 1.5 percent solution at 380 K (225°F). Magnification ≈6000X.

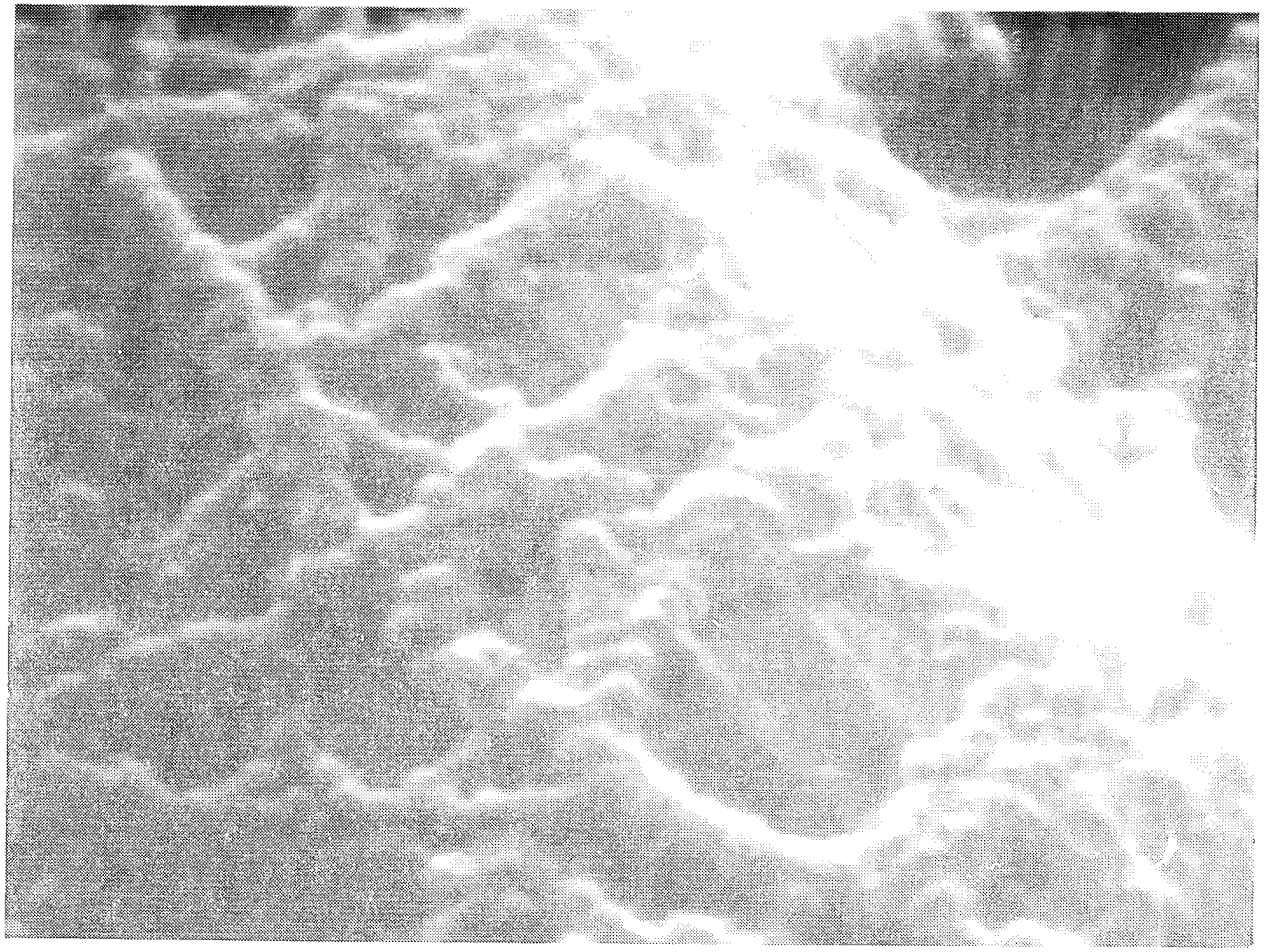

Figure 5-16. SEM of polypropylene In Situ Fibers deposited on graphite cloth from a 1.5 percent solution at 380 K (225°F). Magnification ≈30,000X.

raising the temperature or decreasing the polymer concentration lowers the rate and extent of fiberization. Based on these results, the following process was selected:

(1) Arrays were fiberized in a 1.5 percent (weight to volume) solution of polypropylene in mixed xylenes at 380 K (225°F). The arrays were agitated simultaneously, side by side, separated by approximately 2-1/2 cm (one inch). An oscillation frequency of 54 Hz and a peak-to-peak displacement of approximately 1/2 cm (1/4 inch) were used. A larger amplitude might have been desirable but could not be achieved within the power limits of the shaker head.

(2) After approximately 15 minutes of agitation, fresh concentrated polymer solution was added to replace precipitated material and agitation was resumed for another 15 minutes.

(3) The fiberization chamber was drained of solution and refilled with hot solvent. Low-frequency agitation was then conducted to remove nonfibrous precipitate.

(4) Arrays were extracted with acetone in a Soxhlet extractor and then dried.

(5) Solutions and solvents from steps (1) to (3) were recycled by cooling (to precipitate polymer) and filtering. By use of this process, up to six arrays could be generated per day.

Preparation of Graphite Fiber Arrays for ISF Processing

While the above scale-up and process development were being achieved, preparation of unidirectional arrays of graphite fiber tow was initiated. Analysis of the Table 5-1 test matrix indicated that a minimum of 117 ISF-processed graphite fiber plies were required to make 12 composite panels. Accordingly, a large number of glass/epoxy frames with 25 cm (10 inch) by 12 cm (5 inch) inside dimensions were prepared. Graphite fibers were then bonded to the frames, unidirectionally, at an angle of 0°, 45°, or 90° with respect to the long axis of the frame. Because of the short duration of the program, and the associated time limit for procurement, it was not possible to obtain sufficient graphite fiber of any one type to prepare all specimens. Instead, three fiber batches were used: Celion-3000 without sizing or twist; and Celion-3000 and Celion-6000, both with the conventional Celanese epoxy-compatible sizing and low twist. Of course, only one fiber type was used in frames for a given test panel.

ISF Processing

Fiberization of the above specimens was accomplished by use of the process described above. Arrays of all three configurations (0^{o}, 45^{o}, and 90^{o}) were fiberized. In general, it was found that the 90^{o} samples (graphite fibers vertical during agitation) were easiest to process and the 0^{o} samples most difficult. This was ascribed to a "banjo effect," whereby loosely strung horizontal fibers were "strummed" by the solution during agitation. Initially this resulted in splits in the fiberized arrays. However, improved techniques were developed for stringing the graphite more tautly and the problem was eliminated. Typical specimens ready for lamination are shown in Figures 5-17 through 5-19.

After agitation, solvent extraction was performed in a large Soxhlet extractor using acetone. At least three 4-hour solvent wash cycles were performed on approximately 15 to 20 specimens at a time.

5.3 PHASE II - LAMINATION AND IMPREGNATION

Prior to development of impregnation techniques, a basic decision was made concerning the type of control specimens to be fabricated. After considerable discussion, two criteria were selected as necessary for control fabrication:

(1) The same batches of materials (graphite fiber, resin, and catalyst) and the same cure schedule should be used in GR/EP/ISF specimens and GR/EP controls.

(2) Graphite fiber content should be the same in experimental samples and controls.

It was anticipated that meeting these conditions would require nonstandard processing procedures and would yield control specimens of relatively low quality compared to "standard" composites. More importantly, however, it was recognized that the objective of the program was to determine whether In Situ fibers would improve stress transfer between graphite fibers. This could only be accomplished by matching all facets of microscopic structure (except In Situ Fiberization) in experimental specimens and controls, regardless of whether commercial quality composites were fabricated. This, then, was the philosophy taken in the development of suitable lamination and impregnation processes.

Figure 5-17. Typical fiberized array, 90° oriented graphite fibers.

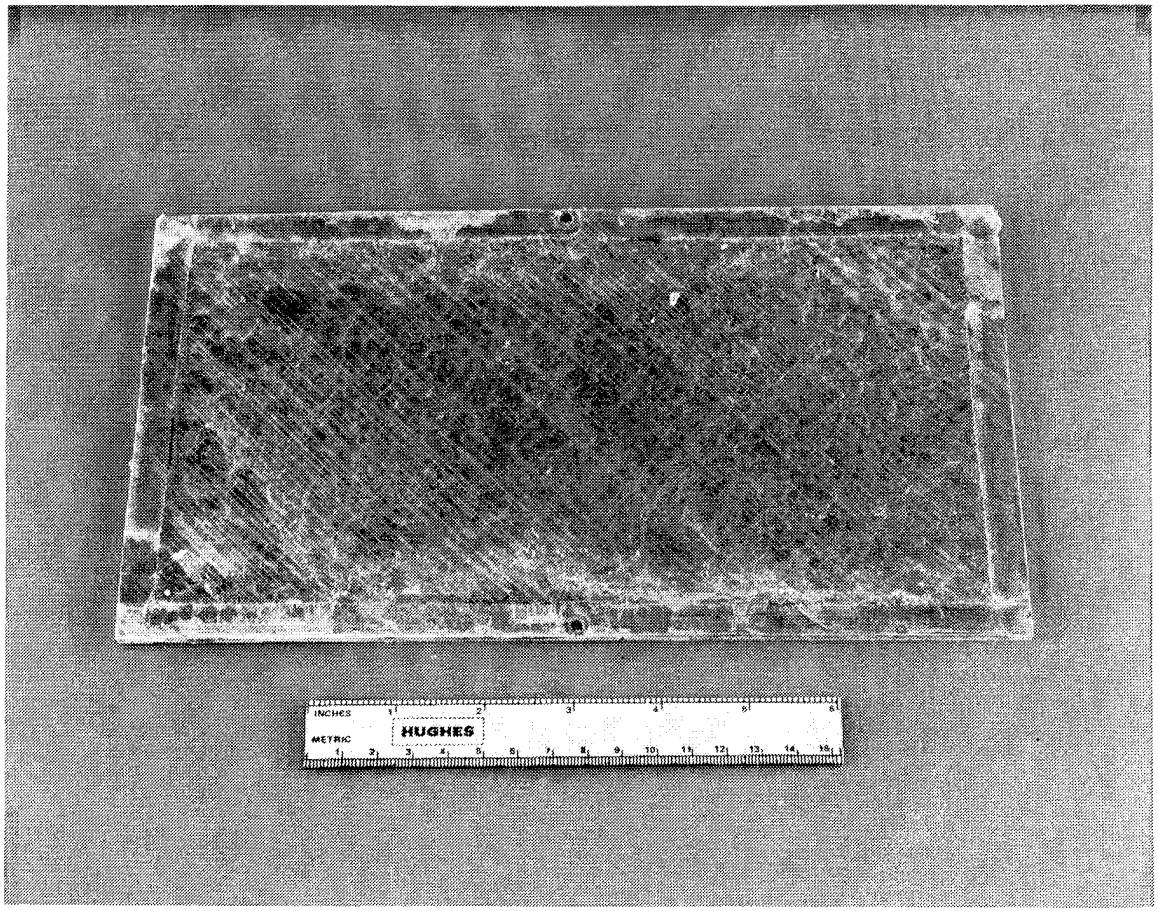

Figure 5-18. Typical fiberized array, 45° oriented graphite fibers.

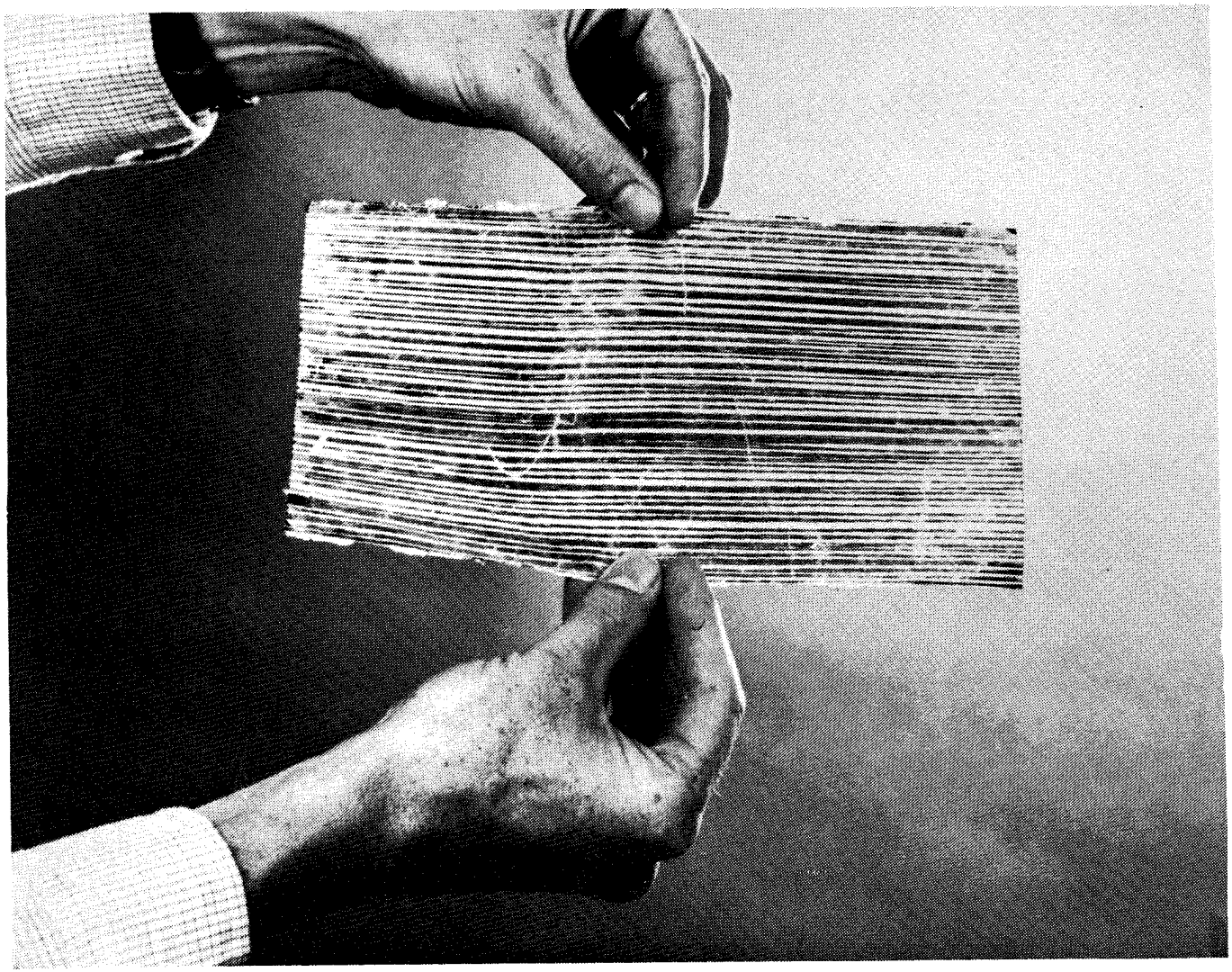

Figure 5-19. Typical fiberized array, 0º oriented graphite fibers, after removal from glass/epoxy frame.

Resin System Selection

At the beginning of Phase II, the decision was made to switch from Epon 828/HV to Epon 828/triethylene tetraamine (TETA). The HV catalyst was abandoned, despite Hughes' experience working with it in conjunction with polypropylene In Situ Fibers, primarily because of its sensitivity to vacuum processing techniques. Changing to TETA permitted conventional vacuum bag lamination procedures to be used, as opposed to the more time consuming and expensive compression molding process employed in preliminary sample fabrication. In addition, TETA was known to produce a less brittle, tougher epoxy system that is more generally applicable to composite laminate fabrication than is the HV catalyzed material.

GR/EP/ISF Specimen Fabrication

After selection of the new resin system, an experiment was performed to develop techniques for fabrication of GR/EP/ISF laminates of reasonable quality. Nine 0^{o} (graphite orientation on frame) fiber plies that had been subjected to early fiberization trials were used for this experiment. These initial GR/ISF plies were not of optimum quality but were judged adequate for development of a composite fabrication procedure. Of particular concern was the ability of the resin to adequately wet the fiberized polypropylene. The following impregnation and cure procedure was developed:

1. The nine fiberized plies were removed from the plastic frames by cutting the fibers just inside the frame periphery with a sharp knife.
2. The nine plies were stacked and the ends stitched together by use of a single Celion-3000 tow on each end. The stacked preform was weighed.
3. The preform was placed in a shallow pan inside a vacuum chamber and submerged in 828/TETA (100/8 parts by weight). A weight was placed on top of the submerged preform to prevent flotation. Vacuum (~25 in Hg, ~85 kn/m^2) was drawn and held 5 minutes.
4. The impregnated preform was removed from the resin batch and placed in an aluminum foil envelope which had been pretreated with mold release. In order to avoid inadvertent removal of polypropylene fibers, excess resin was not scraped from the preform surface.

5. The envelope preform was positioned between two aluminum caul plates in a heated-platen hydraulic press preheated to 325 K (125°F). Pressure was increased stepwise to 2.4 Mn/m^2(350 psig) over a 30 minute period and maintained 90 minutes. This rather high cure pressure was chosen to conform with the molding pressure used earlier to make the preliminary ISF composites with the 828/HV resin system. The part temperature increased, because of resin exotherm, to a maximum of 338 K (150°F).

6. The press temperature controller was turned off and the composite allowed to cool to room temperature under full pressure. The laminate was weighed.

The completed panel appeared to be of reasonable quality. Some small separations between the 0° graphite tows were visible, but these were believed to reflect the nonoptimum quality of the early fiberized plies. The panel appeared to be wetted by the resin, except in a few areas where the polypropylene fibers were heavily concentrated on the surface. These areas appeared white on the otherwise black panel.

Following apparently successful fabrication of the above test panel, thirteen more GR/EP/ISF panels were prepared - nine for testing in Phase III and four for Phase IV delivery to NASA for additional testing. The same basic process described above was used, though minor improvements were made as the program progressed. Specifically, modifications were incorporated to increase graphite fiber content in the panels and to minimize fiber spreading (bowing). These modifications were: (1) incorporation of bleeder plies against the layup to absorb excess resin, and (2) reduction of the cure pressure from 2.4 to 0.3 Mn/m^2 (350 to 50 psig). The cure cycles used were as follows: 1.5 hours at 325 ± 6 K (125° ± 10°F) for panels cured at 2.4 Mn/m^2; 6 hours at 325 ± 6 K (125° ± 10°F) for panels cured at 0.3 Mn/m^2. All panels were postcured 2 hours at 366 ± 6 K (200° ± 10°F) in an air-circulating oven.

It should be noted that standard prepregging techniques were not used in panel preparation. It was feared that the high viscosity of a B-staged resin, coupled with the very fine structure of ISF networks, might cause problems during lamination/squeeze out. Therefore, in order to avoid unnecessary complications, laminating was conducted while the resin was still uncured.

Figure 5-20 serves to summarize the three basic steps in GR/EP/ISF panel fabrication. Shown in this figure are, from left to right: (1) a 0° array of Celion-3000 graphite fibers mounted on a fiberglass/epoxy frame, (2) polypropylene fibers formed on a 90° array of Celion-3000 fibers, and (3) a 10-ply, $\pm 45^{\circ}$ fiberized panel after epoxy impregnation, lamination, and cure.

GR/EP Control Specimen Fabrication

As noted earlier, the primary consideration in fabrication of control specimens was to prepare GR/EP laminates which were as close to the GR/EP/ISF specimens in structure as possible. To this end, a rather unorthodox procedure was developed. First, graphite fibers were wrapped onto plastic frames. In order to facilitate sample preparation, the frames were somewhat larger than those used in the fiberization experiments. Next, frames were stacked, then impregnated with uncured resin, and finally laminated in a press. In an attempt to achieve sample thicknesses (and hence graphite contents) comparable to those of fiberized specimens, the press platens were closed to stops of appropriate heights. Initially, some difficulties were encountered as resin squeeze-out caused bowing and separation of the graphite tow. As experience was gained, this difficulty was reduced (though not eliminated) and better laminations were achieved. The cure schedules used were identical to those for GR/EP/ISF panel fabrications.

5.4 PHASE III - LAMINATE CHARACTERIZATION AND TESTING

Detailed descriptions of the fifteen panels fabricated for testing under the contract are shown in Table 5-3. All were 10-ply panels. Close-up photographs were taken of both sides of each of the nine GR/EP/ISF panels, and are shown in Appendix C. All GR/EP/ISF panels and GR/EP controls were then taken to the University of Wyoming for further characterization.

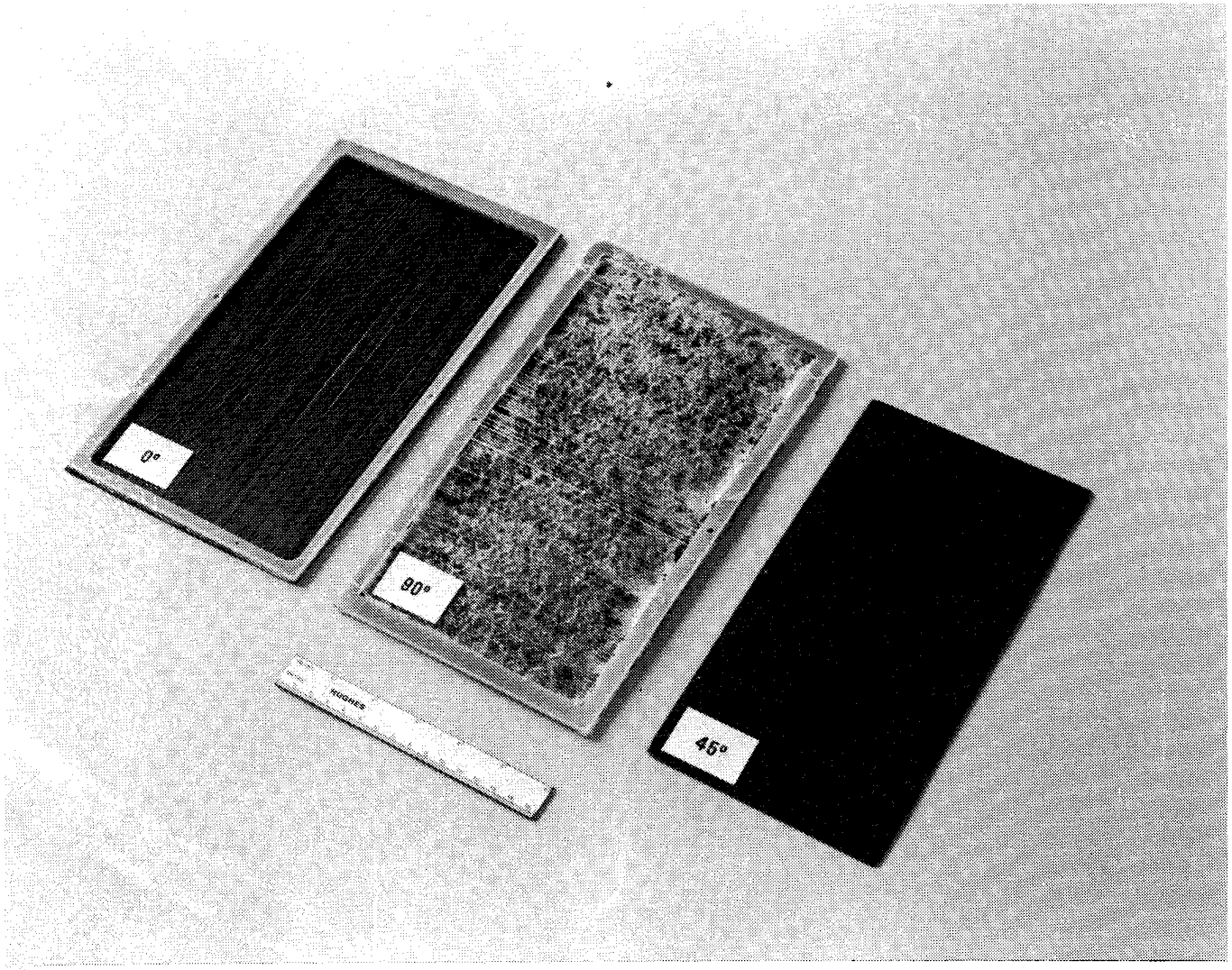

Figure 5-20. Summary of steps in GR/EP/ISF panel fabrication.

TABLE 5-3. LABORATORY FABRICATION RECORD FOR CONTRACT TEST PANELS

Panel No.	Fiberization	Carbon Fibers	Fiber Sizing	Ply Orientation in Panels	Cure Pressure, psig	Bleeder Plies Used	Dimension, cm		Thickness, cm Avg.	Weight, gm	Density, g/cm^3	Notes**
							L	W				
1	Yes	Celion-3000	Yes	$\pm 45^\circ$	50 ± 5	Yes	24.00	12.7	0.246	102.4	1.36	A, B
2	Yes	Celion-3000	Yes	$\pm 45^\circ$	50 ± 5	Yes	23.62	12.7	0.254	112.7	1.39	B, C
3	No	Celion-3000	Yes	$0^\circ - 90^\circ$	Stops	No	25.91	21.46	0.222	175.0	1.42	E
4	Yes	Celion-3000	No	$\pm 45^\circ$	350 ± 10	No	24.38	12.7	0.157	66.6	1.37	F
5	Yes	Celion-3000	No	$\pm 45^\circ$	50 ± 5	Yes	23.88	12.45	0.166	63.3	1.28	A, G
6	No	Celion-6000	No	$0^\circ - 90^\circ$	Stops	No	28.45	21.46	0.170	155.9	1.50	D, F
7	Yes	Celion-3000	Yes	0°	50 ± 5	Yes	23.75	12.7	0.226	96.0	1.41	H
8	No	Celion-3000	Yes	0°	Stops	No	25.02	15.24	0.235	125.5	1.40	
9	Yes	Celion-3000	No	0°	50 ± 5	Yes	23.19	13.41	0.302	129.5	1.38	D, H, I
10	No	Celion-6000	No	0°	Stops	No	24.89	15.11	0.284	146.4	1.37	
11	Yes	Celion-3000	No	90°	350 ± 10	No	24.13	12.7	0.183	78.8	1.40	F, J
12	Yes	Celion-3000	No	90°	50 ± 5	Yes	24.59	12.95	0.142	60.9	1.39	A, B, K
13	No	Celion-6000	No	0°	Stops	No	24.28	15.24	0.208	107.9	1.40	D, L
14	No	Celion-6000	No	0°	150 ± 10*	No	24.96	15.24	0.178	103.1	1.52	M
15	Yes	Celion-3000	Yes	90°	350 ± 10	No	26.16	12.57	0.198	97.3	1.49	N, O

*Stops positioned to match panel 12 thickness, but were not contacted at 150 psig press pressure.

**Notes:
A. Unwetted polypropylene fibers visible, particularly near panel periphery.
B. Localized surface roughness.
C. Carbon fiber waviness near one corner on bleeder side of panel.
D. Slight fiber bowing.
E. Slight fiber bowing and separations.
F. Minor surface pitting.
G. Low density.
H. Surface waviness on bleeder side.
I. Some scattered areas where unwetted polypropylene fibers are visible.
J. Surface waviness over approximately 5.1 cm x 5.1 cm area near panel center.
K. Local surface impression from stray fiber, near one end of panel.
L. Prominent separation of the carbon fibers approximately 2.5 cm from panel edge.
M. Slight fiber waviness.
N. Poor release from caul plate on one surface.
O. Pronounced fiber spreading.

A modified test matrix for sample characterization was developed which is shown in Table 5-4. Specific tests are described briefly in Table 5-5.

Prior to initiation of mechanical property testing, ultrasonic C-scan examinations were conducted on all panels. In general, the C-scans, which are shown in Appendix C, revealed a few voids and some graphite fiber spreading and bowing in both In Situ Fiberized and control specimens. More importantly, however, the fiberized panels showed large "white" areas which were interpreted as poor wetting, or delamination, at resin-fiber interfaces. The worst of the fiberized panels were therefore eliminated from further study.

Following C-scan analysis, test specimens were prepared from the best of the fiberized panels and from appropriate controls. Testing was then performed and two samples from each panel were analyzed by the acid digestion/burnout process employed earlier. Panel compositions are summarized in Table 5-6; several points are worth noting. First, the polypropylene content of fiberized specimens showed considerable variation, with an average of about 4 percent by volume. Second, the void contents of fiberized panels and unfiberized controls were similar - about 5 and 4 percent, respectively. Third, graphite fiber contents were relatively low, widely varied, and not generally well-matched between fiberized specimens and controls. The latter fact made it necessary to normalize strength and modulus data, as described below.

Final data for all tests are summarized in Tables 5-7 through 5-12 Both non-normalized and normalized data are shown. The latter were obtained from the former by multiplication by 50/X where "X" is the average percent graphite fiber of a given test panel (i. e., data were normalized to 50 percent graphite content).

TABLE 5-4. REVISED TEST MATRIX

Panel Type and Identification	Test Description	Test Temperature, (^{o}F)	No. Specimens Per Panel	Total No. of Specimens
Unidirectional:	0^{o} Tensile	RT	3	12
Panels 7 & 9 (fiberized)	0^{o} Compression	RT	3	12
Panels 8 & 10 (control)	90^{o} Tensile	RT	3	12
	0^{o} Iosipescu Shear	RT	3	12
	0^{o} Short Beam Shear	RT	3	12
	Acid Digestion	--	3	12
Unidirectional:	0^{o} Tensile	363 ±2.0(194^{o}±4^{o})	3	6
Panel 12 (fiberized)	0^{o} Compression	363 ±2.0(194^{o}±4^{o})	3	6
Panel 14 (control)	90^{o} Tensile	363 ±2.0(194^{o}±4^{o})	3	6
	0^{o} Iosipescu Shear	363 ±2.0(194^{o}±4^{o})	3	6
	0^{o} Short Beam Shear	363 ±2.0(194^{o}±4^{o})	3	6
	Acid Digestion	--	3	6
±45^{o}:	In-Plane Shear (±45^{o} Tensile)	RT	3	12
Panels 2 & 4 (fiberized)	±45^{o} Compression	RT	3	12
Panels 3 & 6 (control)	Acid Digestion	--	3	12

TABLE 5-5. DESCRIPTION OF MECHANICAL PROPERTY TESTS

Test	Reference	Specimen Dimensions, cm (10-Ply Laminates)
0° Tension	ASTM D3039	12.7 x 1.27
0° Compression	ASTM D3410 ("Celanese jig")	12.7 x 0.64
90° Tension	ASTM D3039	12.7 x 2.54
0° Iosipescu Shear	References A and B, below	5.08 x 1.27 double notched
0° Short Beam Shear	ASTM D2344	1.52 x 0.64
In-Plane Shear	ASTM D3518 ($\pm 45^{\circ}$ tensile)	12.7 x 2.54
$\pm 45^{\circ}$ Compression	(Straight coupon)	10.2 x 1.27

References:

A. Iosipescu, N., "New Accurate Procedure for Single Shear Testing of Metals," J. of Materials, vol. 2, no. 3, Sept. 1967, pp. 537-566.

B. Walrath, D. E., and Adams, D. F., "The Iosipescu Shear Test as Applied to Composite Materials," submitted for publication in Experimental Mechanics.

TABLE 5-6. COMPOSITION OF TEST PANELS

Panel No.	Fiberization	Specimen No.	Density, g/cm^3	Volumetric Percentage				
				Carbon Fiber	Epoxy Resin	Polypropylene Fiber	Voids	Total
2	Yes	1	1.45	49	44	3	4	100
		2	1.42	47	45	2	6	100
		Avg.	1.44	48	44	3	5	100
3	No	1	1.41	42	53	0	5	100
		2	1.39	38	57	0	5	100
		Avg.	1.40	40	55	0	5	100
4	Yes	1	1.34	36	50	7	7	100
		2	1.39	42	46	8	4	100
		Avg.	1.37	39	48	7	6	100
6	No	1	1.51	58	38	0	4	100
		2	1.48	54	43	0	3	100
		Avg.	1.50	56	41	0	3	100
7	Yes	1	1.48	55	39	2	4	100
		2	1.47	53	41	2	4	100
		Avg.	1.48	54	40	2	4	100
8	No	1	1.41	39	58	0	3	100
		2	1.40	38	59	0	3	100
		Avg.	1.41	39	58	0	3	100
9	Yes	1	1.41	44	48	2	6	100
		2	1.44	48	45	3	4	100
		Avg.	1.43	46	47	2	5	100
10	No	1	1.34	27	69	0	4	100
		2	1.32	25	71	0	4	100
		Avg.	1.33	26	70	0	4	100
12	Yes	1	1.40	41	46	10	3	100
		2	1.39	41	50	4	5	100
		Avg.	1.40	41	48	7	4	100
14	No	1	1.50	55	42	0	3	100
		2	1.48	51	46	0	3	100
		Avg.	1.49	53	44	0	3	100

Assumed specific gravities: Celion carbon fibers - 1.77, Epoxy resion - 1.25, Polypropylene fibers - 0.95.

TABLE 5-7. AVERAGED LONGITUDINAL AND TRANSVERSE TENSILE TEST RESULTS FOR UNIDIRECTIONAL PANELS

Panel No.	Orientation (Deg)	Fiberization	Test Temperature (K)	Strength (MPa)	Strength (ksi)	Modulus (GPa)	Modulus (Msi)	Poisson's Ratio**	Data Normalized to 50 Percent Carbon Fiber Content: Strength (MPa)	Strength (ksi)	Modulus (GPa)	Modulus (Msi)
7	0	Yes	RT	418	60.6	147	21.3	0.43	387	144	136	19.7
8	0	No	RT	973	141.1	117	16.9	0.41	1247	180.9	150	21.7
9	0	Yes	RT	514	74.6	99	14.4	0.70	559	81.1	108	15.7
10	0	No	RT	694	100.7	64	9.3	0.39	1335	193.7	123	17.9
12	0	Yes	363	568	82.4	76	11.0	1.07	693*	100.5*	93	13.4
14	0	No	363	1090*	158*	105*	15.2*	0.48	1177*	144*	99*	14.3*
7	90	Yes	RT	11	1.6	6.4	0.93	--	10	1.5	5.9	0.86
8	90	No	RT	30	4.3	6.8	0.99	--	38	5.5	8.7	1.27
9	90	Yes	RT	19	2.7	6.6	0.95	--	21	2.9	7.2	1.03
10	90	No	RT	21	3.1	5.7	0.82	--	40	6.0	11.0	1.58
12	90	Yes	363	11	1.6	2.3	0.34	--	13	2.0	2.8	0.41
14	90	No	363	21	3.0	5.4	0.78	--	20	2.8	5.1	0.74

*Only one value, not an average

**Poisson's ratio values appear to be extraordinarily high.

TABLE 5-8. AVERAGED LONGITUDINAL COMPRESSION TEST RESULTS FOR UNIDIRECTIONAL PANELS

Panel No.	Fiberization	Test Temperature (K)	Strength (MPa)	Strength (ksi)	Modulus (GPa)	Modulus (Msi)	Data Normalized to 50 Percent Carbon Fiber Content: Strength (MPa)	Strength (ksi)	Modulus (GPa)	Modulus (Msi)
7	Yes	RT	494	71.7	103	14.9	457	66.4	95.4	13.8
8	No	RT	683	99.1	50	7.2	876	127.1	64	9.2
9	Yes	RT	338	49.0	47	6.8	367	53.3	51	7.4
10	No	RT	705	102.3	33	4.8	1356	196.7	63	9.2
12	Yes	-	-	-	-	-	-	-	-	-
14	No	363	601	87.1	37	5.4	567	82.2	35	5.1

TABLE 5-9. AVERAGED TENSILE TEST RESULTS FOR ±45° PANELS

Panel No.	Fiberization	Test Temperature (K)	Axial Strength (MPa)	(ksi)	Axial Modulus (GPa)	(Msi)	Data Normalized to 50 Percent Carbon Fiber Content			
							Axial Strength (MPa)	(ksi)	Axial Modulus (GPa)	(Msi)
2	Yes	RT	61	8.9	12.7	1.84	64	9.3	13.2	1.92
3	No	RT	183	26.5	11.2	1.63	229	33.1	14.0	2.04
4	Yes	363	42	6.1	4.6	0.67	54	7.8	5.9	0.86
6	No	363	90	13.0	1.7	0.25	80	11.6	1.5	0.22

TABLE 5-10. AVERAGED COMPRESSION TEST RESULTS FOR ±45° PANELS

Panel No.	Fiberization	Test Temperature (K)	Axial Strength (MPa)	(ksi)	Axial Modulus (GPa)	(Msi)	Data Normalized to 50 Percent Carbon Fiber Content			
							Axial Strength (MPa)	(ksi)	Axial Modulus (GPa)	(Msi)
2	Yes	RT	70	10.2	7.9	1.14	73	10.6	8.2	1.19
3	No	RT	132	19.1	7.4	1.08	165	23.9	9.3	1.35
4	Yes	RT	79	11.5	8.2	1.19	101	14.7	10.5	1.53
4	Yes	363	54	7.9	7.3	1.07	69	10.1	9.4	1.37
6	No	363	79	11.5	5.2	0.75	71	10.3	4.6	0.67

TABLE 5-11. AVERAGED SHORT BEAM INTERLAMINAR SHEAR TEST RESULTS FOR UNIDIRECTIONAL PANELS

Panel No.	Fiberization	Test Temperature (K)	Strength (MPa)	Strength (ksi)	Data Normalized to 50 Percent Carbon Fiber Content: Strength (MPa)	Strength (ksi)
7	Yes	RT	39	5.6	36	5.2
8	No	RT	80	11.6	102	14.9
9	Yes	RT	28	4.0	30	4.3
10	No	RT	71	10.3	137	19.8
12	Yes	363	18	2.6	22	3.2
14	No	363	37	5.4	35	5.1

TABLE 5-12. AVERAGED IOSIPESCU SHEAR TEST RESULTS FOR UNIDIRECTIONAL PANELS

Panel No.	Fiberization	Test Temperature (K)	Shear Strength (MPa)	Shear Strength (ksi)	Shear Modulus (GPA)	Shear Modulus (Msi)	Data Normalized to 50 Percent Carbon Fiber Content: Shear Strength (MPa)	Shear Strength (ksi)	Shear Modulus (GPa)	Shear Modulus (Msi)
7	Yes	RT	34	5.0	3.7	0.54	31	4.6	3.4	0.50
8	No	RT	56	8.1	2.6	0.37	72	10.4	3.3	0.47
9	Yes	RT	55	8.0	3.0	0.43	60	8.7	3.3	0.47
10	No	RT	23	3.4	0.9	0.13	44	6.5	1.7	0.25
12	Yes	363	23	3.4	0.8	0.11	28	4.1	1.0	0.13
14	No	363	57	8.2	1.8	Q.26	54	7.7	1.7	0.25

5.5 DATA ANALYSIS AND DISCUSSION

After completion of testing, tabulated strength and modulus data, as well as raw stress-strain curves, were studied and compared. In addition, failed specimens were examined, both visually and microscopically, in order to elucidate failure mechanisms. The results of these efforts are described below.

Longitudinal Tension of Unidirectional Samples

Normalized tensile modulus results (Table 5-7) suggest that the fiberized specimens are less stiff than the controls at both ambient temperature and 363 K (194°F). The tabulated strength data indicate that the fiberized specimens are also substantially weaker. However, the latter results are subject to some question in view of the observed failure modes. At elevated temperature, all the fiberized samples and two of the three controls failed solely by shear of the adhesive bonds at the tabs. Hence, the In Situ Fibers were not tested. At ambient temperature, control failures were characterized by tensile fracture of graphite fibers, usually in the grips as shown in Figure 5-21. GR/EP/ISF specimen failures, on the other hand, were accompanied by modest tensile fracture of graphite fibers, accompanied by longitudinal shear fractures (Figure 5-22) or massive delaminations (Figure 5-23). Visual examination indicated substantial propylene at the latter fracture surfaces. This evidence of interlaminar weakness correlates with the C-scan results. As a final note, the measured values of Poisson's ratio were anomalously high, particularly for the GR/EP/ISF samples. The reason for this phenomenon is not understood but may correlate with the odd failure modes observed.

Overall the above results are interpreted as evidence that In Situ Fibers decrease transverse shear strength in GR/EP composites at ambient temperature and thereby prevent tensile failure. They may also marginally decrease the tensile modulus. At 363 K (194°F), the test results are inconclusive.

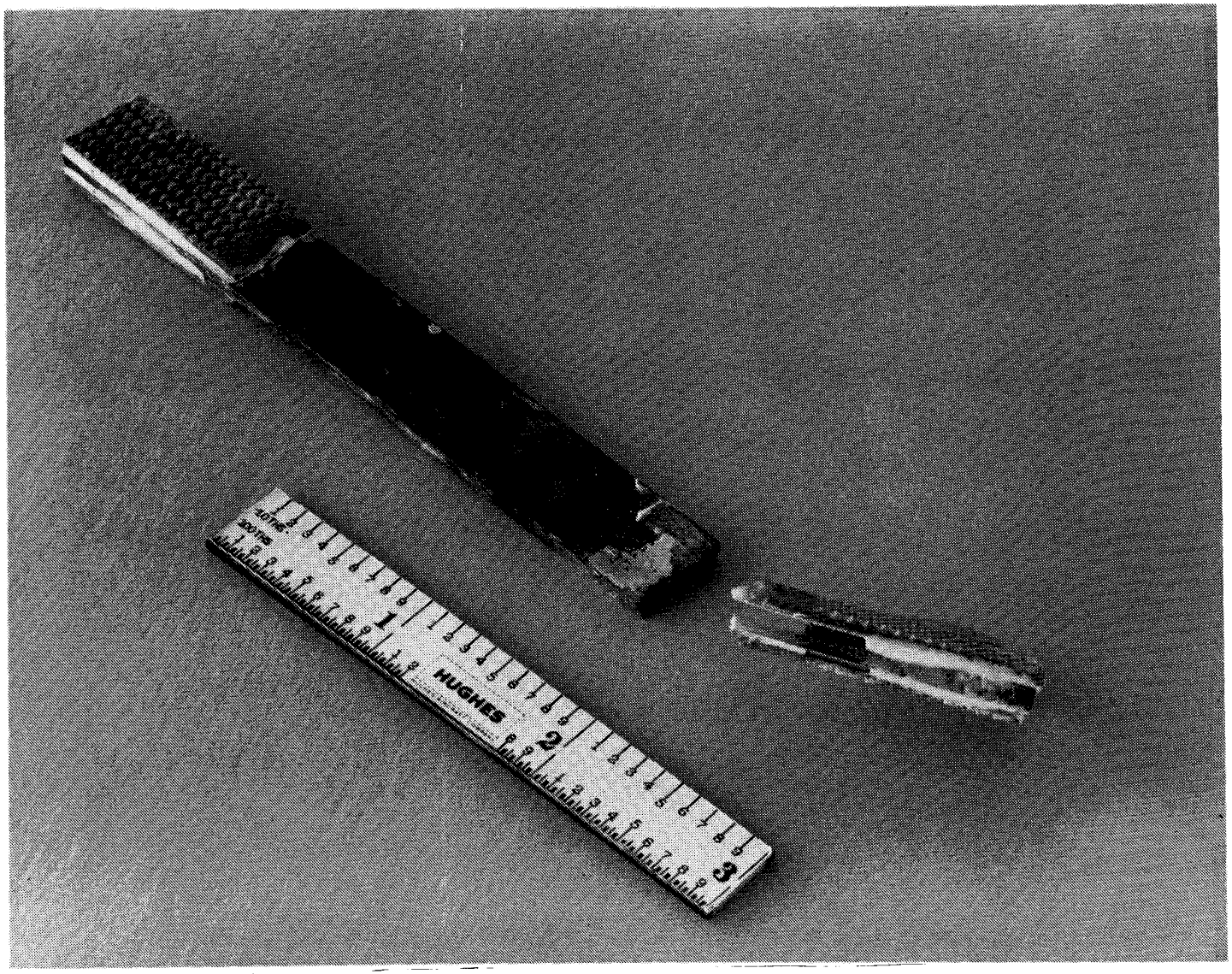

Figure 5-21. Unidirectional control specimen, after longitudinal tensile failure in the grip.

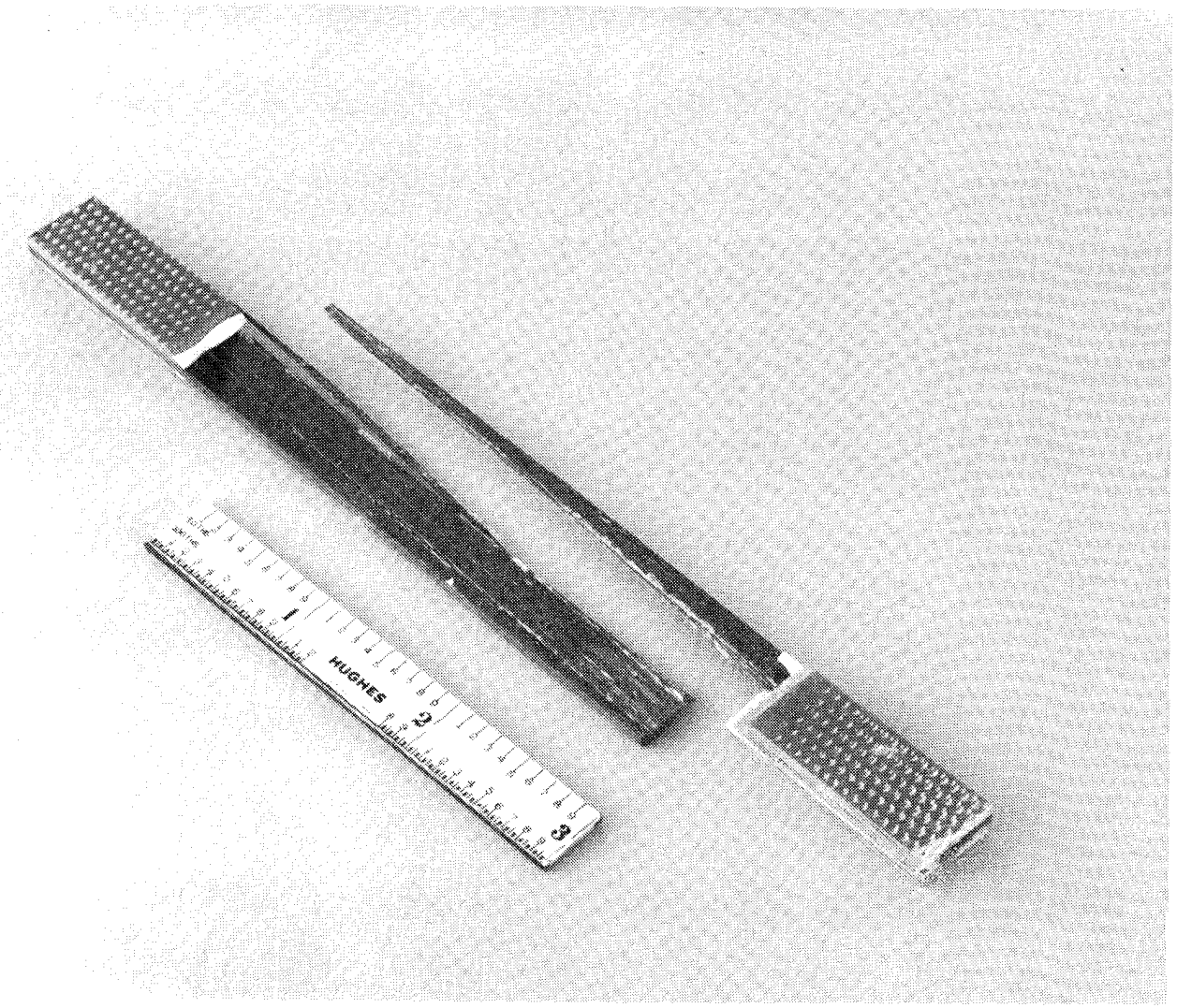

Figure 5-22. Unidirectional GR/EP/ISF specimen, after longitudinal tensile failure.

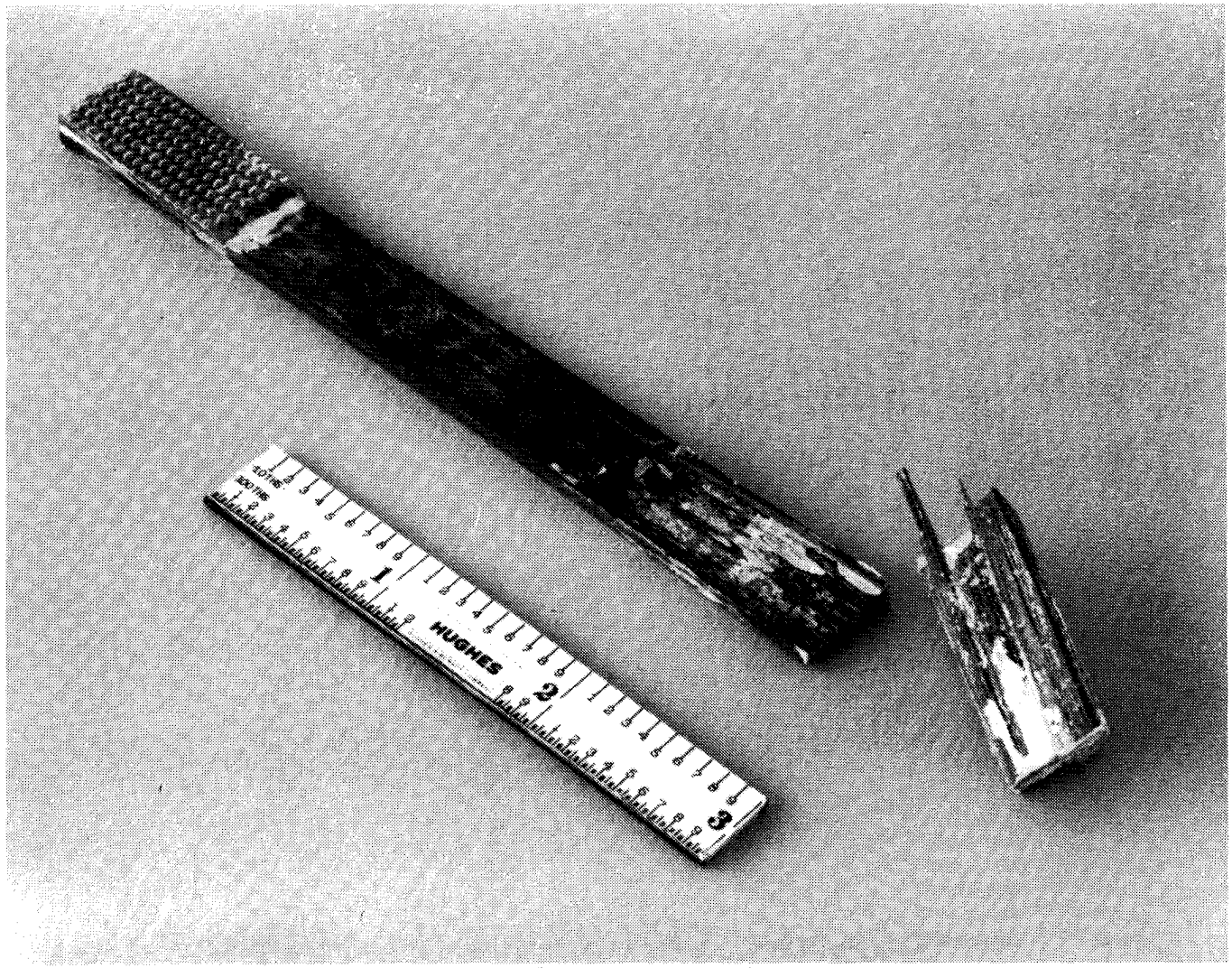

Figure 5-23. Unidirectional GR/EP/ISF specimen, after longitudinal tensile failure.

Transverse Tension of Unidirectional Samples

This test, which might be expected to be more sensitive to the presence of In Situ Fibers than is the longitudinal test, showed marked softening and weakening in the GR/EP/ISF specimens. Such was observed at both test temperatures. Examination of the stress-strain curves indicated somewhat higher strains at break for the controls at ambient temperature, but this can be readily explained by the lower graphite fiber contents of the controls. However, at the higher temperature, the fiberized specimens had markedly higher elongations than the controls: 3.0, 1.5, 1.6 versus 0.5, 0.5, 0.3 percent, respectively. This effect does not appear to be explained solely by the higher graphite content of the controls (53 vs 41 percent, see Table 5-6).

In sum, transverse tensile tests indicate that In Situ Fibers soften and substantially weaken composites at room temperature with little detectable effect on elongation. Toughness, or energy to failure, is therefore decreased. However, at 363 K (194^{o}F) weakening and softening appear to be accompanied by increased elongation. Toughness may therefore be little affected or it may actually increase.

Longitudinal Compression of Unidirectional Samples

Once again, ambient strengths of the fiberized samples were substantially lower than those of the controls. No fiberized specimens were run at elevated temperature. Interestingly, each of the control specimens was broken into two pieces, while all of the GR/EP/ISF samples, though fractured, were nevertheless still in one piece. The modulus data were greatly scattered for the fiberized specimens. These results may be related to the odd Poisson's ratio data discussed earlier, and both may reflect voids in the test samples.

Tension of ±45^{o} Samples

Strengths of fiberized specimens were again weaker than controls at both test temperatures. At room temperature, the controls were also slightly

stiffer. However, at 363 K (194°F) the fiberized specimens had substantially higher moduli. Finally, once again the ambient controls were broken into two pieces while all other specimens remained intact.

Compression of ±45° Samples

Fiberization caused a decrease in ambient strength and elongation but had little effect on ambient modulus. Conversely, at 363 K, the strength was not affected, but modulus was substantially higher in the fiberized specimens. All tested specimens looked similar.

Short Beam Shear

These tests showed poor strengths for the fiberized specimens at both temperatures.

Iosipescu Shear

These tests gave no clear results at ambient temperature but suggested that the In Situ fibers cause softening and weakening at 363 K.

Microscopic analysis of some failed specimens was performed, and in general, very small fibers were visible at the fracture surfaces of the GR/EP/ISF specimens. Shown in Figures 5-24 to 5-26, these fibers are presumably polypropylene and appear to be smooth and of smaller diameter than the originally deposited fibers, suggesting that they may have been drawn during sample deformation and/or fracture.

5.6 PHASE IV - SAMPLES FOR DELIVERY

Four GR/EP/ISF panels, and four GR/EP controls were prepared for delivery to NASA by use of the same techniques as are described above. The delivered panels are described in Tables 5-13 and 5-14.

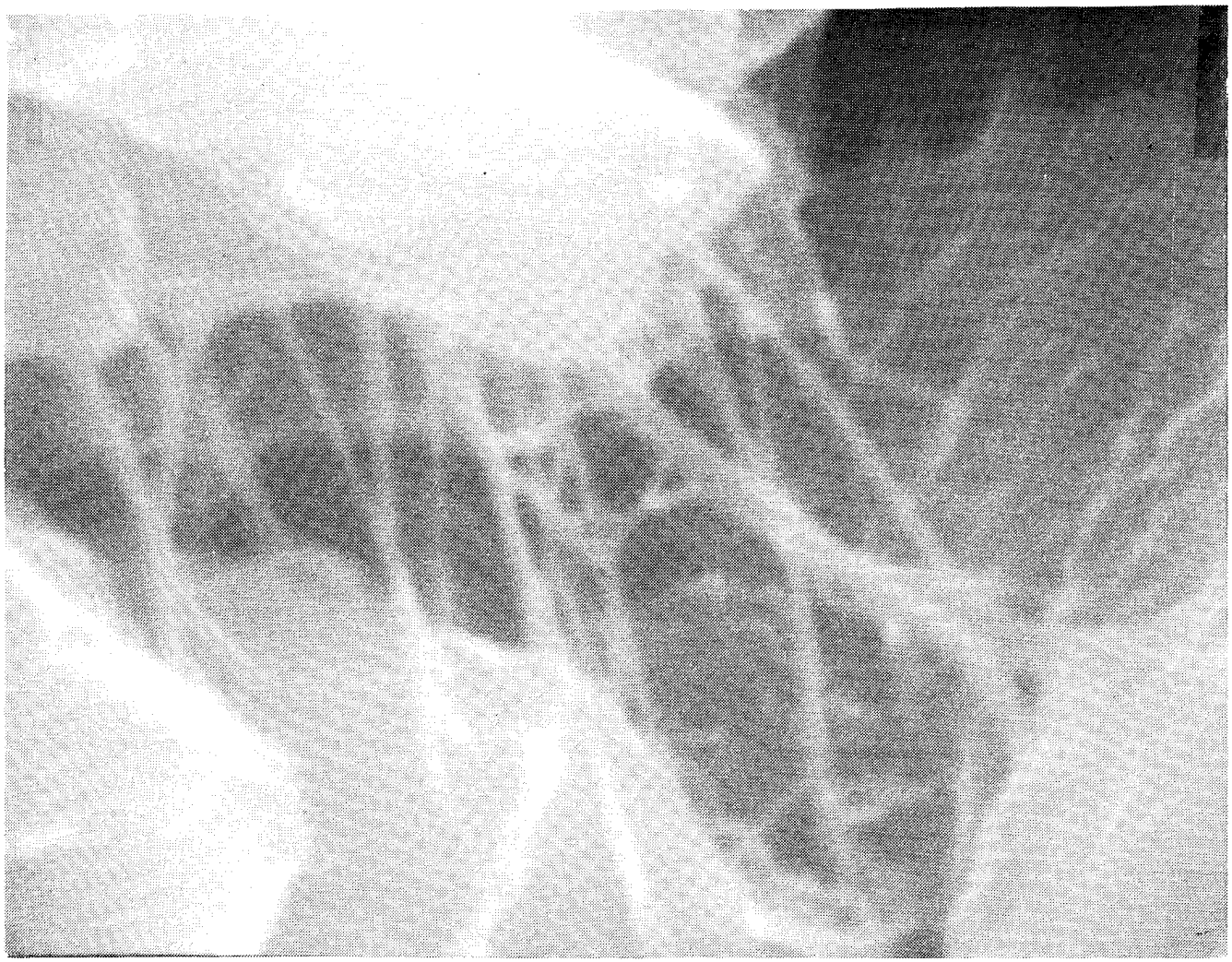

Figure 5-24. SEM of microfibers at fracture surface of unidirectional GR/EP/ISF specimen failed in transverse tension. Magnification ≈25,000X.

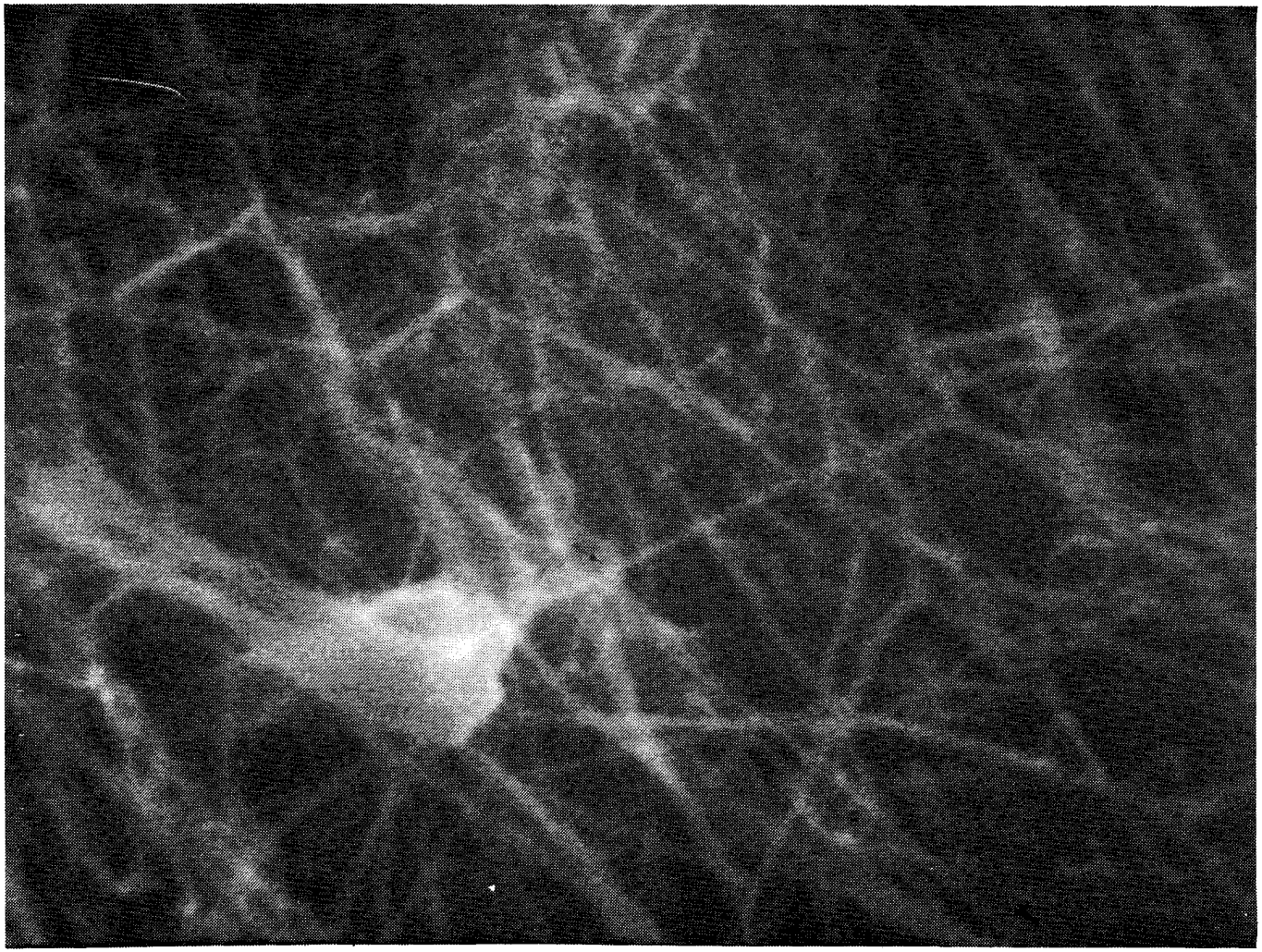

Figure 5-25. SEM of microfibers at fracture surface of ±45° GR/EP/ISF specimen failed in tension. Magnification ≈ 22,000X.

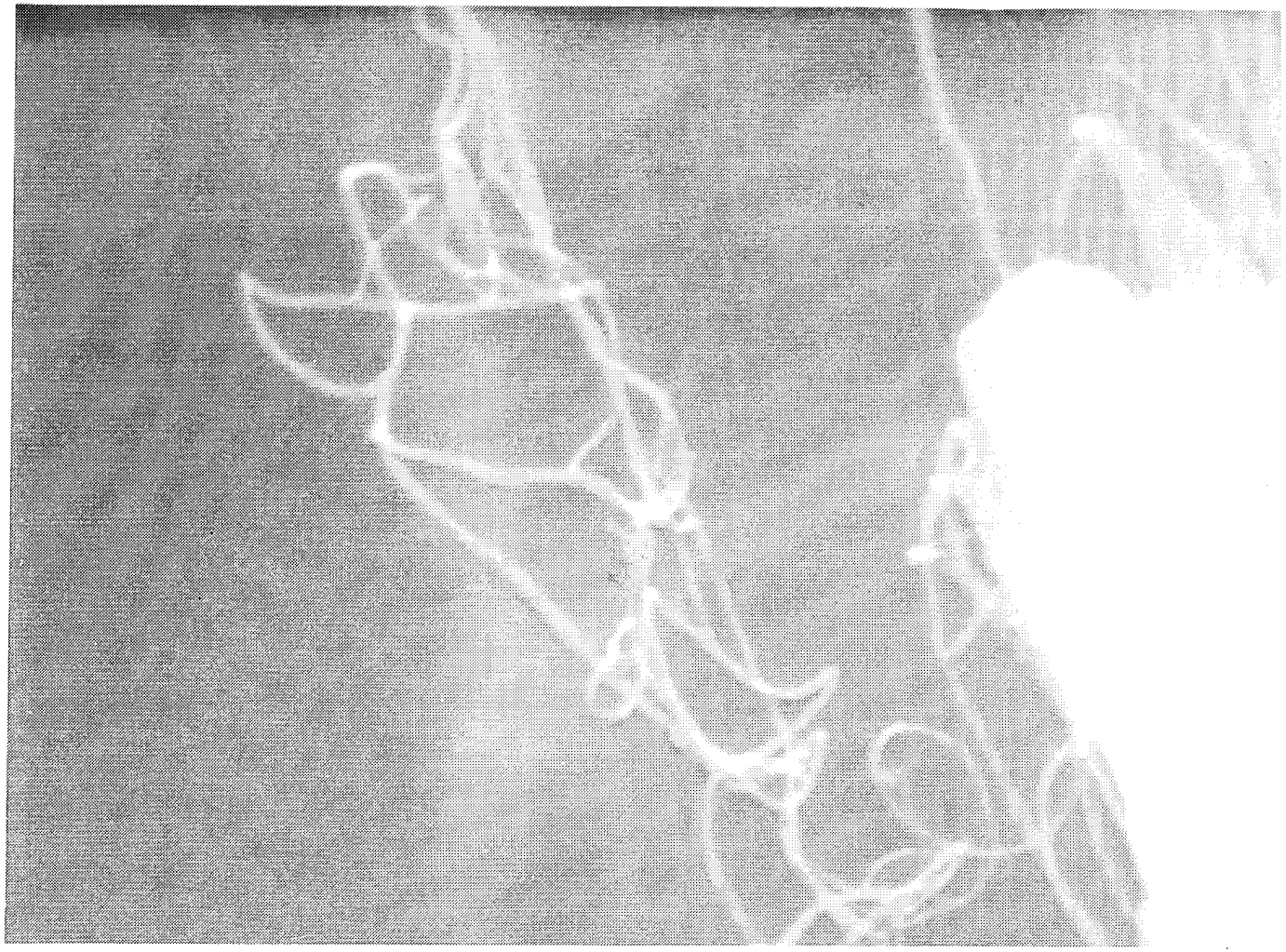

Figure 5-26. SEM of microfibers at fracture surface of ±45° GR/EP/ISF sample failed in compression. Magnification ≈18,000X.

TABLE 5-13. PANELS FOR CONTRACTUAL DELIVERY

Test	No. Specimens*		Specimen Size, cm*		No. Plies	Ply Orientation In Panels**	No. Panels 24.77 x 12.7 x 0.64 cm		Total Plies	
	Fiberized	Control	Test Direction	Transverse Direction			Fiberized	Control	Fiberized	Control
10° Off-Axis Tension	5	5	20.32	1.27	8	0°	2.54	2.54	8	8
Dynamic Modulus	5	5	5.1	1.27	3	90°	***2.54	***2.54	1	1
NRL Fracture Toughness	4	4	3.81	3.81	16	0, ±45°, 90°****	2.54	2.54	16	16
Impact Strength	3	3	10.16	10.16	8	0, ±45°, 90°****	2.54	2.54	8	8

*Complete panels, not machined, were provided.
**0° direction parallel to panel length (24.77 cm direction).
***Small panels, 7.62 cm length x 12.7 cm width, each made from one full-size ply cut into thirds.
****Ply stacking sequence symmetric about laminate mid-plane:

8-ply panels:

1. 0
2. +45
3. -45
4. 90
5. 90
6. -45
7. +45
8. 0

16-ply panels:

1.	0	9.	0
2.	+45	10.	+45
3.	-45	11.	-45
4.	90	12.	90
5.	90	13.	90
6.	-45	14.	-45
7.	+45	15.	+45
8.	0	16.	0

TABLE 5-14. LABORATORY FABRICATION RECORD, PANELS FOR CONTRACTUAL DELIVERY

Panel No.	Panel Code*	Carbon Fibers	Fiber Sizing	Fiber-ization	No. Plies	Ply Orientation	Cure Pressure, Psig	Bleeder Plies Used	Dimensions, cm		Thickness, cm			Weight, gm	Density gm/cm^3	Fiber Weight, gm**	Resin Content, wt. %	Completion Date	Notes***
									L	W	High	Low	Avg.						
D1	FS-2-90-3	Celion 3000	Yes	Yes	3	90°	50 ±5	Yes	13.08	8.38	0.076	0.074	0.0749	9.5	1.15	6	41	4-30-81	A, E, H
D2	S-2-90-3	Celion 3000	Yes	No	3	90°	Stops	No	13.21	8.26	0.079	0.074	0.076	11.0	1.32	-	-	5-04-81	D
D3	FS-2-0-8	Celion 3000	Yes	Yes	8	0°	50 ±5	Yes	24.26	13.46	0.188	0.157	0.173	74.5	1.32	50.5	32.6	4-30-81	A, D, F, G
D4	S-2-0-8	Celion 3000	Yes	No	8	0°	Stops	No	24.64	15.24	0.180	0.173	0.178	99.5	1.49	-	-	5-04-81	--
D5	FS-1-QI-8	Celion 3000	Yes	Yes	8	0°, ±45°, 90°	50 ±5	Yes	24.51	13.34	0.236	0.208	0.222	95.5	1.31	60	37.1	5-12-81	B, D, F, G
D6	S-1-QI-8	Celion 3000	Yes	No	8	0°, ±45°, 90°	Stops	No	24.13	15.24	0.2197	0.203	0.211	109.9	1.42	-	-	6-03-81	A, D
D7	FS-1-QI-16	Celion 3000	Yes	Yes	16	0°, ±45°, 90°	50 ±5	Yes	24.77	13.46	0.391	0.371	0.381	170.6	1.34	108.5	36.3	5-12-81	C, D, F, G
D8	S-1-QI-16	Celion 3000	Yes	No	16	0°, ±45°, 90°	Stops	No	23.11	15.24	0.386	0.384	0.385	194.2	1.43	-	-	6-03-81	B, E

*Description of Panel Code WW-X-YY-Z:
W: F = fiberized, S = sizing on carbon fibers
X: Fabrication number
Y: Fiber orientation (QI = quasi-isotropic)
Z: Number of plies

**Includes weight of ISF

***Notes:
A. Some fiber bowing
B. Pronounced fiber bowing
C. Slight fiber waviness
D. Some fiber separations
E. Pronounced fiber separations
F. Unwetted polypropylene visible, particularly near panel periphery
G. Surface waviness on bleeder side
H. One local indentation, approximately 0.32 cm dia.

6.0 CONCLUSIONS AND SPECULATIONS

6.1 SIP STUDY

The successful fiberization of PCTFE was considered to be a major step forward in the development of the In Situ Fiberization process for higher temperature applications. However, the inability to fiberize any of the aromatic backbone polymers was discouraging. Until such a step is taken, the fabrication of Strain Isolation Pads with 533 - 643 K (500-700^{o}F) capability by ISF techniques must be postponed. Nevertheless, it may still be feasible. The authors believe that such molecules as PPO and PPS may be fiberizable. To accomplish this, the authors believe two things will be necessary. First, higher molecular weight samples should be synthesized or obtained by other techniques such as fractionation of existing material. And second, an agitation system which is more powerful than that currently in use should be employed. This would allow high velocity gradients to be achieved during lower frequency agitation. The use of lower frequencies would in turn provide more time for these presumably slower crystallizing molecules to interact in their flow-deformed configurations.

SIP fabrication using ISF techniques may also be possible with other polyamic acids such as those which have been reported recently by NASA[10] and which are known to yield crystalline polyimides on heating. Agitating these polymers in a refluxing solvent offers a reasonable chance of In Situ Fiberization, particularly if more powerful agitation can be achieved.

Alternatively, it may be possible to fiberize a higher temperature material for SIP use by Hughes' "seeding" technique, utilizing polypropylene (see Section 3.1). PPO/PP would be a likely mixture for such processing since both polymers are soluble in mixed xylenes. If this mixture could be

fiberized, then the PPO would provide relatively high temperature capability, 533 K (500°F), while the PP would be essentially sacrificial.

Finally, it appears that the actual temperatures encountered by Strain Isolation Pads in the Shuttle's maiden flight were far less than 533 K, and indeed substantially less than even the melting point of polypropylene fibers, 443 K (340°F). Therefore, it may be worthwhile to consider ISF fabrication of SIP from readily processible polypropylene or from higher melting PCTFE, 493 K, (430°F). The difficulties of processing aromatic backbone polymers would then be avoided completely.

6.2 GR/EP/ISF STUDY

Clearly, this study did not demonstrate the improvement of GR/EP composite fracture toughness by the use of In Situ Fibers. However, it did provide at least one tantalizing result - the fiberized specimens' increased transverse tensile elongation at 363 K (194°F). Their increased modulus in ±45° tensile and compressive tests at the same temperature and the fact that control specimens separated into two pieces in several tests while the fiberized samples remained in one piece was also intriguing. However, it is not clear what the reasons are for the latter results - fiber reinforcement or just poor controls. The question remains open.

In addition, the work served to identify the causes of the structural weaknesses of the GR/EP/ISF composites. First, there is the apparent problem of poor ISF/resin wetting and bonding. Second, the In Situ Fibers tended to concentrate between, rather than among, the layers of graphite. Third, they appeared to prevent "nesting" of the graphite fibers, and thereby reduced total fiber volume. Fourth, the In Situ Fibers may not have been stiff enough to reinforce the epoxy; this hypothesis is suggested by the consistently low ambient temperature moduli of the GR/EP/ISF specimens compared to the controls.

This combination of effects may appear to be difficult to overcome, but in actuality all the above problems are potentially solvable. Independent experiments recently conducted at Hughes have shown that the first problem, that of poor wetting, can be eliminated. Good wetting has been achieved in polypropylene In Situ Fiber/epoxy composites without apparent

damage to the fibers, by use of prepregging techniques. Hughes also plans to conduct studies aimed at improving adhesion to In Situ Fibers. Techniques such as coating and etching will be investigated.

The other three above-mentioned problems are also potentially solvable if an improved lamination/cure process can be developed. Essentially what must be done is to achieve relative lateral motion of neighboring graphite fibers. This could potentially solve all three problems. As initially adjacent graphite fibers are displaced, graphite from other layers could move into the vacated area. Hence, the distinctive layering observed above may be eliminated. Also, the displacement, if successful, would result in a drawing of the In Situ Fibers which connect the moving graphite. The resultant drawn fibers would probably be similar to those observed at fracture surfaces (Figures 5-26 to 5-28). Such drawing would accomplish two things. First, the drawn fibers would be of much smaller diameter than the original In Situ Fibers and should thus have much less detrimental effect on graphite fiber nesting. Second, the drawn fibers would probably also have substantially increased modulus. This hypothesis is based on the currently held model of In Situ Fiber morphology - segments of extended chain polymer alternating with more randomly oriented regions. Presumably, the drawing process only deforms the latter, converting it into additional extended chain material, and thereby providing substantially increased fiber modulus. If so, then the final problem discussed above would be solved.

The above discussion is, of course, very speculative. However, it is not implausible, if a lamination process can be developed which allows separation of initially adjacent graphite fibers. Such a lamination process would necessarily involve careful manipulation of cure temperature, pressure, and time, but might not differ significantly from cycles commonly used commercially. If successful, it might very well yield GR/EP/ISF composites with the desired improved properties.

APPENDIX A

CALCULATED ESTIMATE OF VELOCITY GRADIENTS DURING IN SITU FIBERIZATIONS

A simple idealized agitation experiment is examined here - sinusoidal, vertical oscillation of a vertically oriented, flat plate in a polymer solution of infinite extent. Any departure from such a simple geometry should only serve to increase velocity gradients, and therefore the following analysis should give a lower limit on experimentally achieved velocity gradients.

The amplitude of vertical motion of the shear wave originating at the oscillating surface, and propagating in the "x" direction, can be described by[7]

$$y(x, t) = y_o\left[\sin(2\pi\nu t - 2\pi x/\lambda)\right]e^{-x/x_o} \qquad (1)$$

where t is time, ν is the frequency of oscillation, λ is the shear wavelength, and x_o is the distance over which the amplitude falls off by 1/e. Differentiation with respect to time yields the velocity, v,

$$v = \left(\frac{\partial y}{\partial t}\right)_x = 2\pi\nu y_o\left[\cos(2\pi\nu t - 2\pi x/\lambda)\right]e^{-x/x_o} \qquad (2)$$

Subsequent differentiation with respect to distance, x, then yields the velocity gradient

$$\left(\frac{\partial v}{\partial x}\right)_t = \frac{(2\pi)^2\nu y_o}{\lambda}\left[\sin(2\pi\nu t - 2\pi x/\lambda)\right]e^{-x/x_o} - \frac{2\pi\nu y_o}{x_o}\left[\cos(2\pi\nu t - 2\pi x/\lambda)\right]e^{-x/x_o} \qquad (3)$$

At the surface of the plate, $x = 0$, the velocity gradient is thus

$$\left(\frac{\partial v}{\partial x}\right)_{x=o} = \frac{(2\pi)^2 \nu y_o}{\lambda} \sin 2\pi\nu t - \frac{\omega y_o}{x_o} \cos 2\pi\nu t \qquad (4)$$

The maximum velocity gradient at the surface, obtained at $t = n/4$ (with $n = 1, 3, 5\ldots$), is then

$$\left(\frac{\partial v}{\partial x}\right)_{\substack{max, \\ x=o}} = \frac{(2\pi)^2 \nu y_o}{\lambda} \qquad (5)$$

The shear wavelength can be calculated from the expression[7]

$$G' = \rho' (\nu\lambda)^2 (1-r^2)/(1+r^2)^2 \qquad (6)$$

$$G'' = 2\rho (\nu\lambda)^2 r/(1+r^2)^2 \qquad (7)$$

where G', G'', and ρ are the solution dynamic storage modulus, dynamic loss modulus, and density, respectively, and

$$r \equiv \frac{\lambda}{2\pi x_o} \qquad (8)$$

Squaring and then adding equations 6 and 7 yields

$$G'^2 + G''^2 = \rho^2 (\nu\lambda)^4/(1+r^2)^2 \qquad (9)$$

Solving equation 9 for λ yields

$$\lambda = \frac{\sqrt{G'^2 + G''^2}}{\rho\nu^2} (1+r^2)^{1/2} \qquad (10)$$

For dilute polymer solutions

$$\sqrt{G'^2 + G''^2} \approx 2\pi\nu\eta \tag{11}$$

where η is the solution voscosity. Furthermore,

$$1 + r^2 \approx 1 \tag{12}$$

Combination of equation 10, 11, and 12 then yields:

$$\lambda \approx \frac{1}{\nu}\left(\frac{2\pi\nu\eta}{\rho}\right)^{1/2} \tag{13}$$

Finally, substitution of equation 13 into equation 5 yields

$$\left(\frac{\partial v}{\partial x}\right)_{\substack{\max, \\ x=o}} = \frac{(2\pi\nu)^2 y_o^{1/2}}{(2\pi\nu\eta)^{1/2}} = (2\pi\nu)^{3/2} \left(\frac{\rho}{\eta}\right)^{1/2} y_o \tag{14}$$

For a typical fiberization experiment,

$$\nu \approx 50 \text{ sec}^{-1}, \quad \rho \approx 1 \text{ g/cm}^3, \quad \eta \approx 0.01 \frac{3}{\text{cm sec}}, \quad y_o \approx 0.5 \text{ cm}$$

Therefore,

$$\left(\frac{\partial v}{\partial x}\right)_{\substack{\max, \\ x=o}} \approx 28,000 \text{ sec}^{-1}$$

This number is <u>substantially</u> larger than $1/\tau$ for typical agitation experiments in which $\tau \approx 2 \times 10^{-4}$ sec. Therefore, despite the simplicity of the model, the calculation clearly demonstrates that velocity gradients greater than $1/\tau$ are obtained in fiberization experiments.

APPENDIX B

ACID DIGESTION/BURNOUT TEST PROCEDURE

1. Weigh approximately 1-3 gram representative sample of the composite panel in air and in water.
2. Measure sample dimensions; calculate bulk density.
3. Place sample into 400 ml glass beaker filled with 200 ml of nitric acid. Heat to 366 K (200°F) on hot plate.
4. After 4 to 8 hours have elapsed, check to see if resin is digesting properly. If it has, pour acid-fiber mixture through filter (181 glass cloth), to retain all carbon and polypropylene fibers.
5. Replace solution with clean acid for second phase of digestion process, and repeat step 3.
6. After 4 to 8 hours have elapsed, pour acid through filter to retain all fibers.
7. Place fibers in beaker, and fill beaker with approximately 300 ml of D.I. water. Boil samples for 1 hour.
8. Pour water through filter as before (181 glass cloth). Retain all fibers.
9. Rinse samples 2 times with D.I. water at room temperature. Pour through filter and retain all fibers.
10. After second rinse, place beaker containing the fiber into oven at 339 K (150°F) for 12 hours minimum to dry fibers.
11. When fibers are dry, weigh them and complete calculations for resin, fiber, and void contents.
12. To determine polypropylene content, place beaker with sample in oven. Raise temperature to 533 K (500°F) for 1 hour to burn off the polypropylene and reweigh.

The following additional factors were determined and used in calculating the composite compositions:

1. Weight loss of Celion carbon fibers during acid digestion = 1.4 percent.

2. Weight loss of polypropylene fibers during acid digestion = 0.29 percent.

3. Weight loss of carbon fibers during 533 K (500°F) burnout = 0.0 percent.

The following specific gravities were assumed:

Celion carbon fibers - 1.77

Epoxy resin - 1.25

ISF polypropylene - 0.95

APPENDIX C
PHOTOGRAPHS AND C-SCANS OF PANELS

Close-up photographs were taken of both sides of each of the nine GR/EP/ISF contract test panels. These photographs are shown on the following pages. C-scans of panels are also shown.

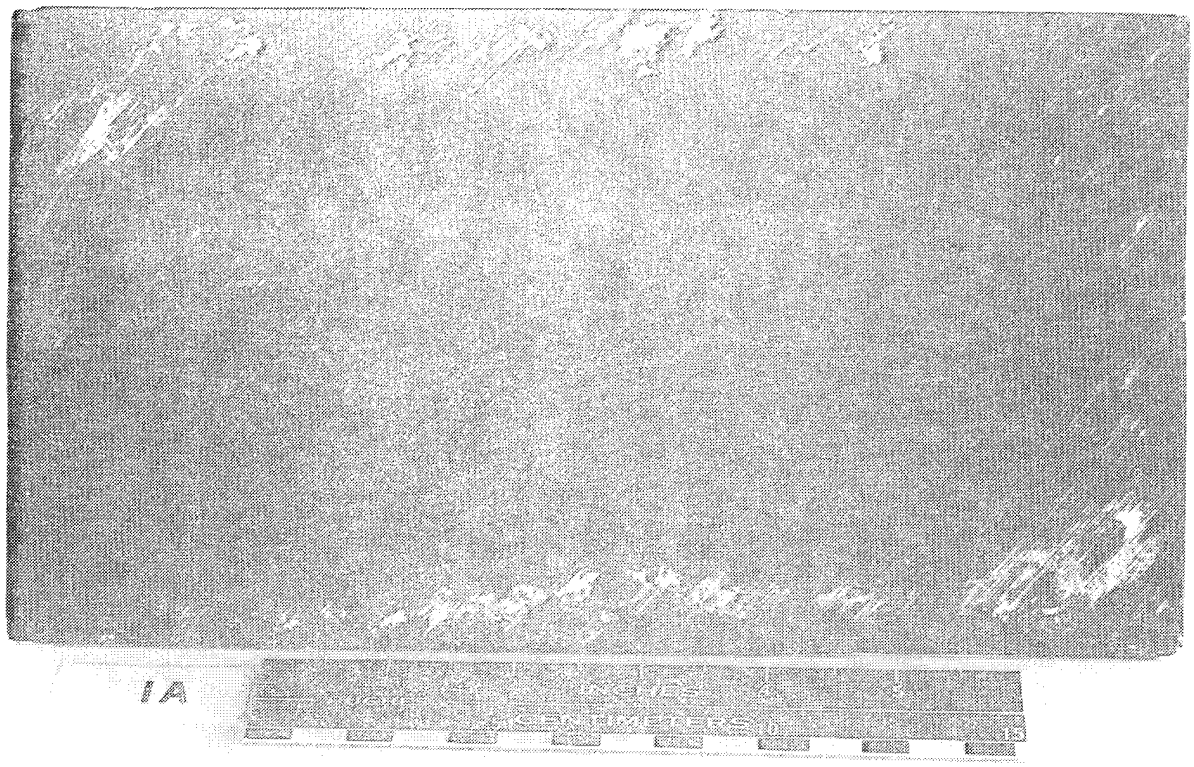

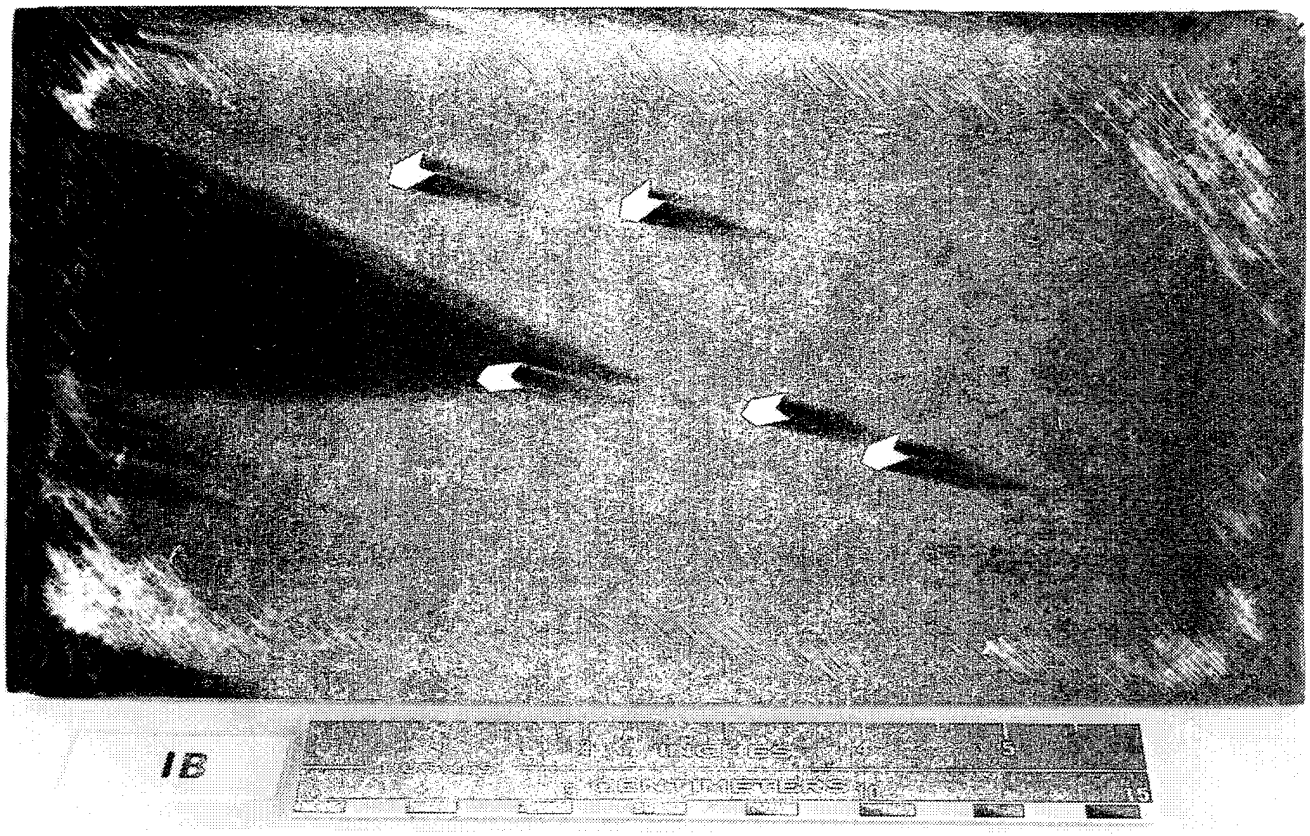

Figure C-1. Photographs of both sides of panel 1.

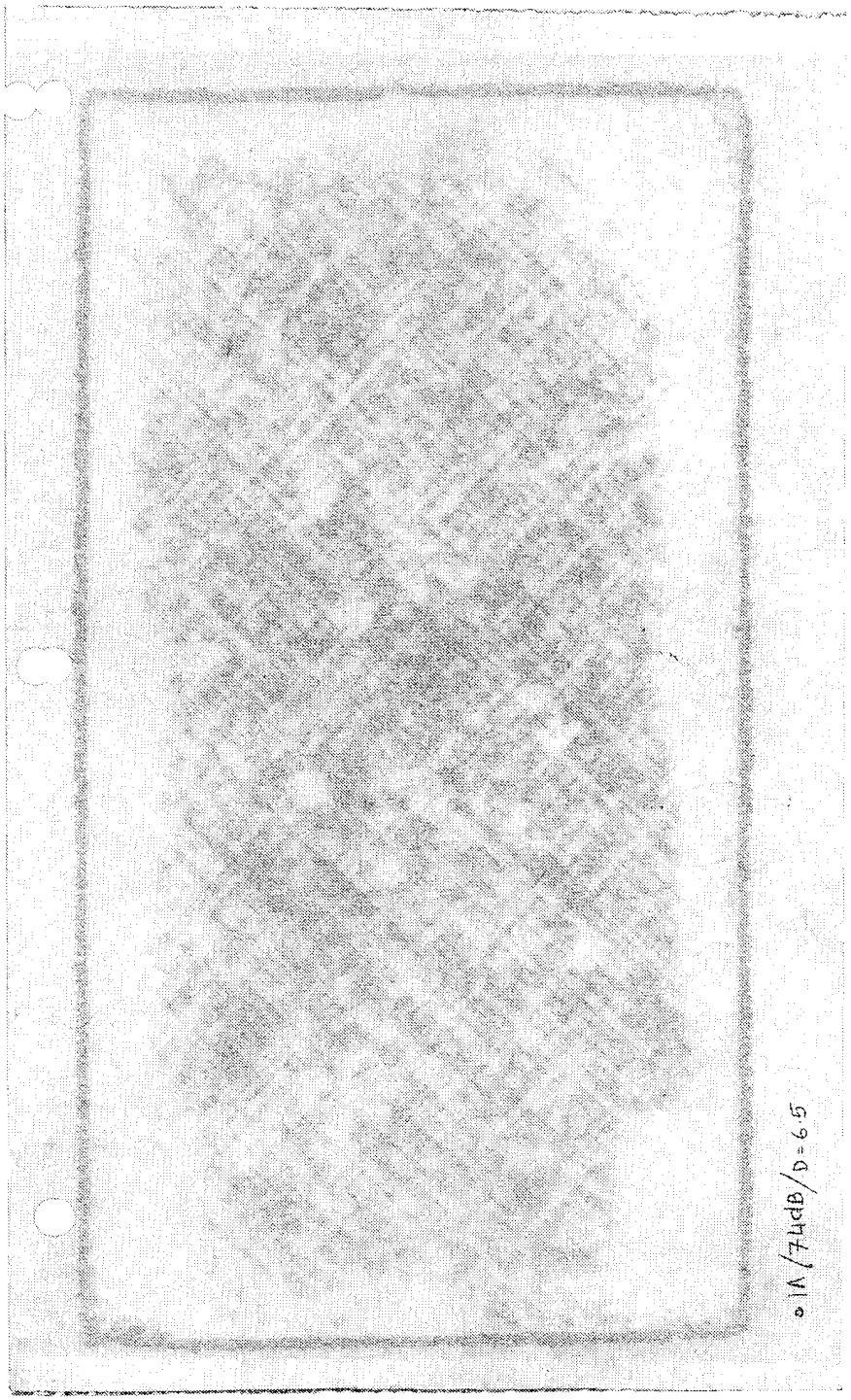

Figure C-1A. Ultrasonic C-scan of panel 1.

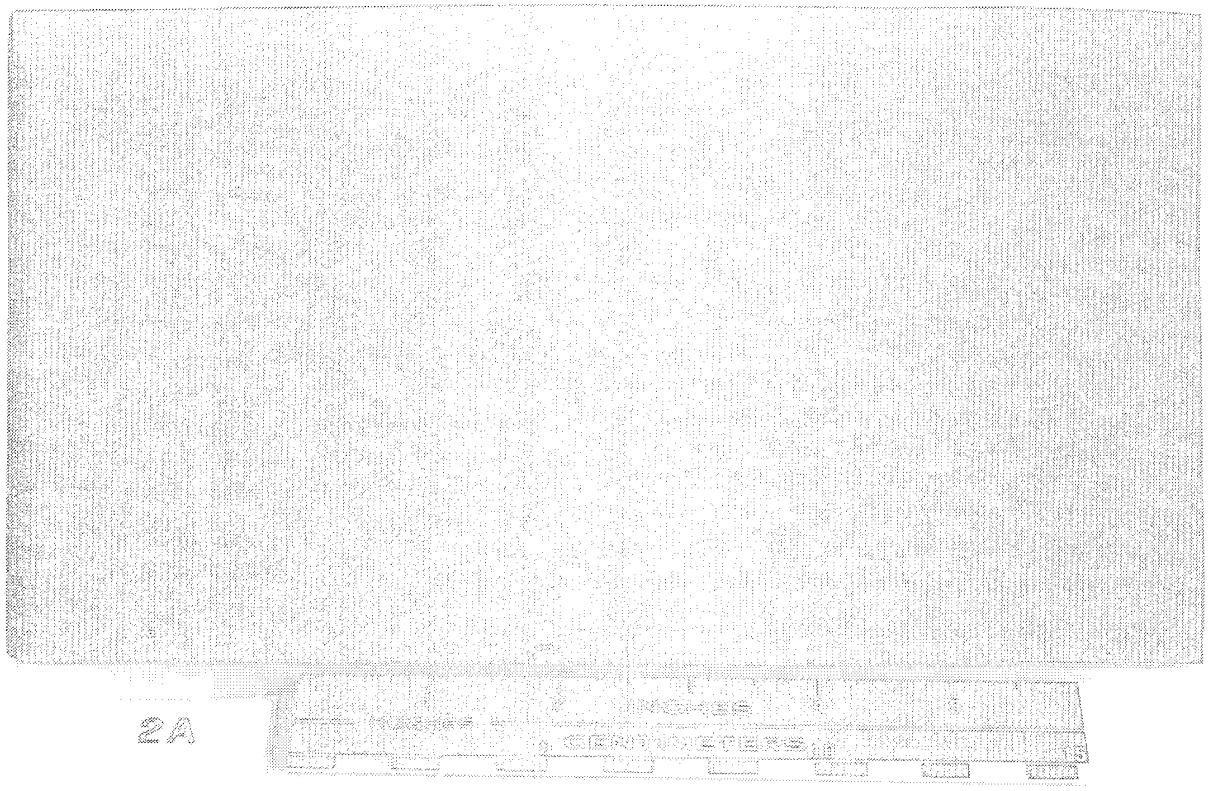

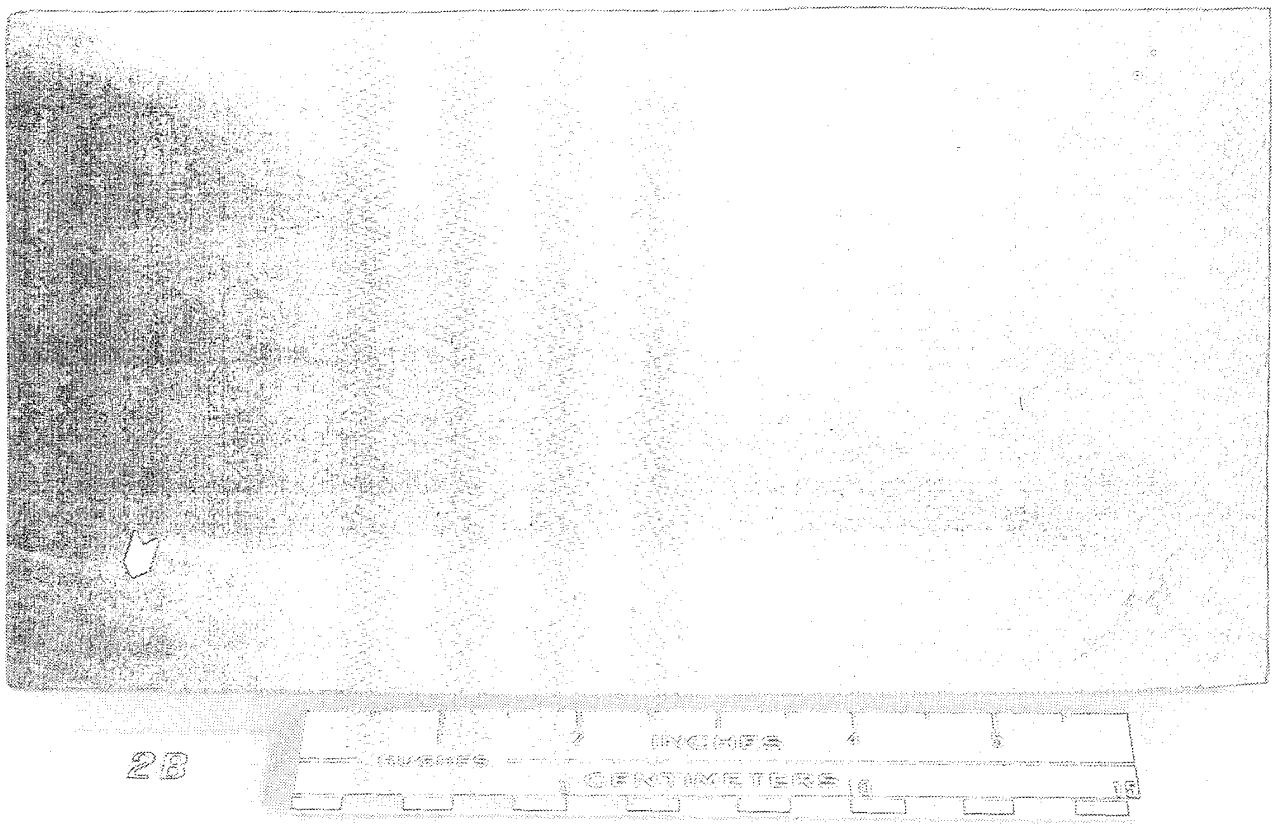

Figure C-2. Photographs of both sides of panel 2.

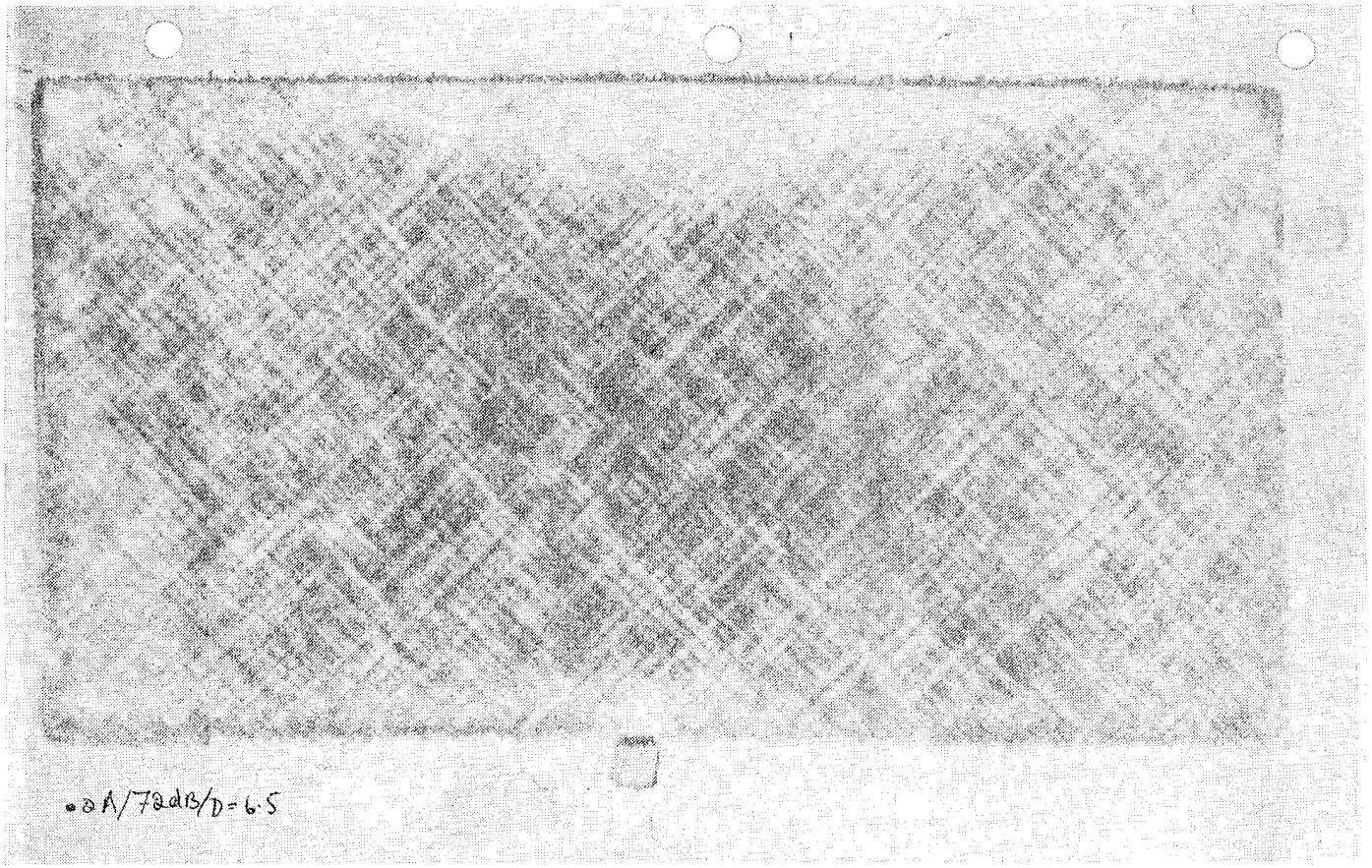

Figure C-2A. Ultrasonic C-scan of panel 2.

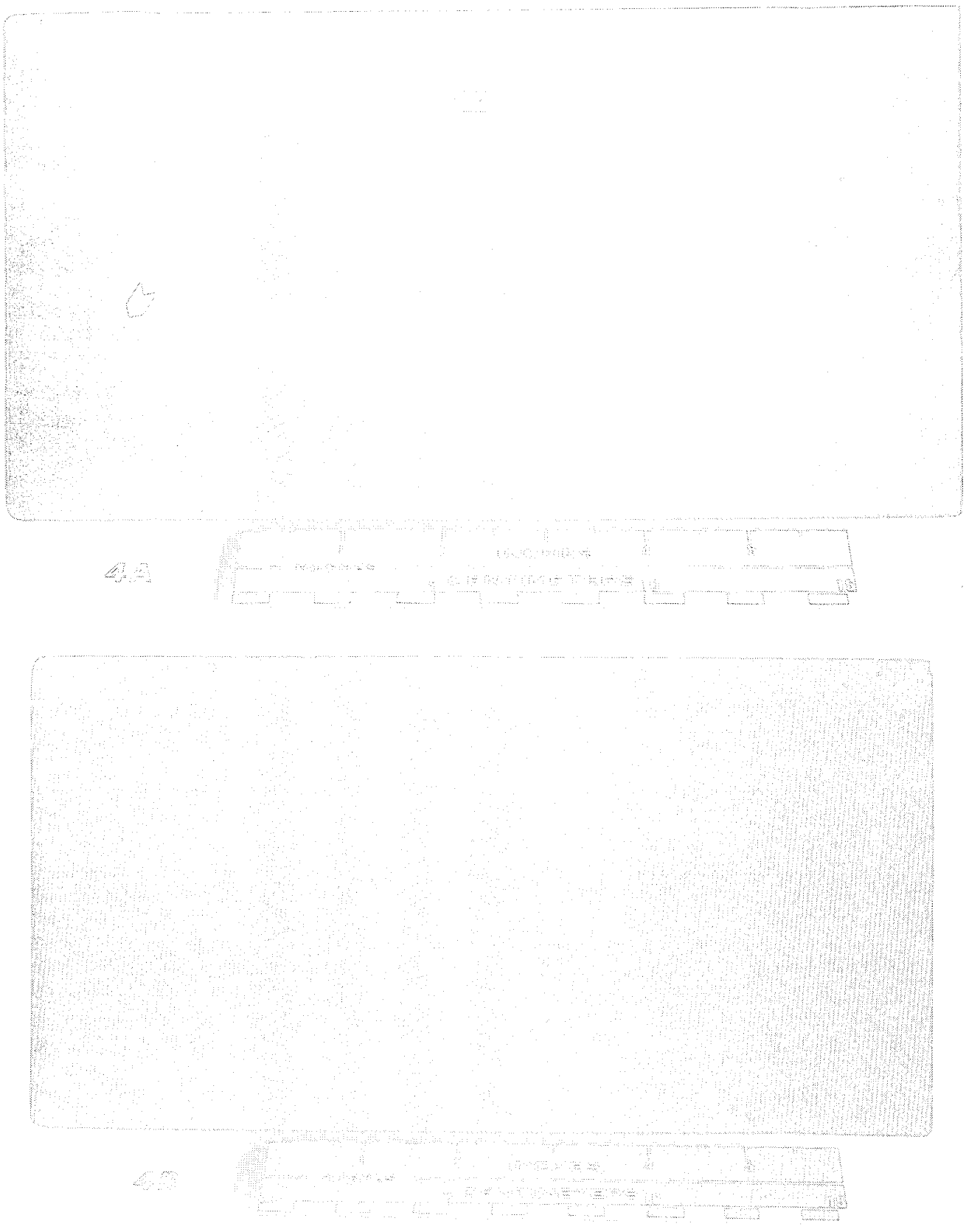

Figure C-3. Photographs of both sides of panel 4.

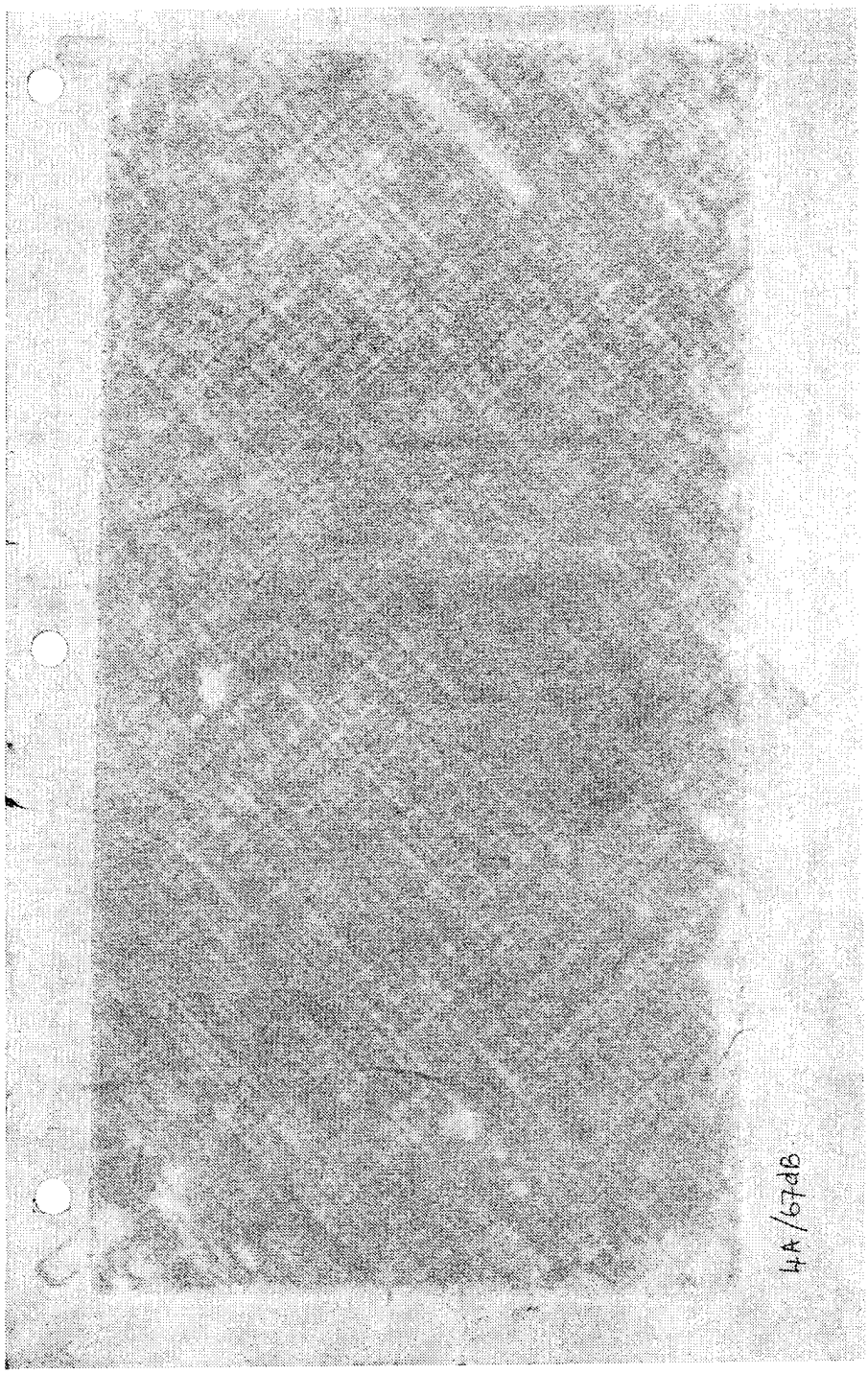

Figure C-3A. Ultrasonic C-scan of panel 4.

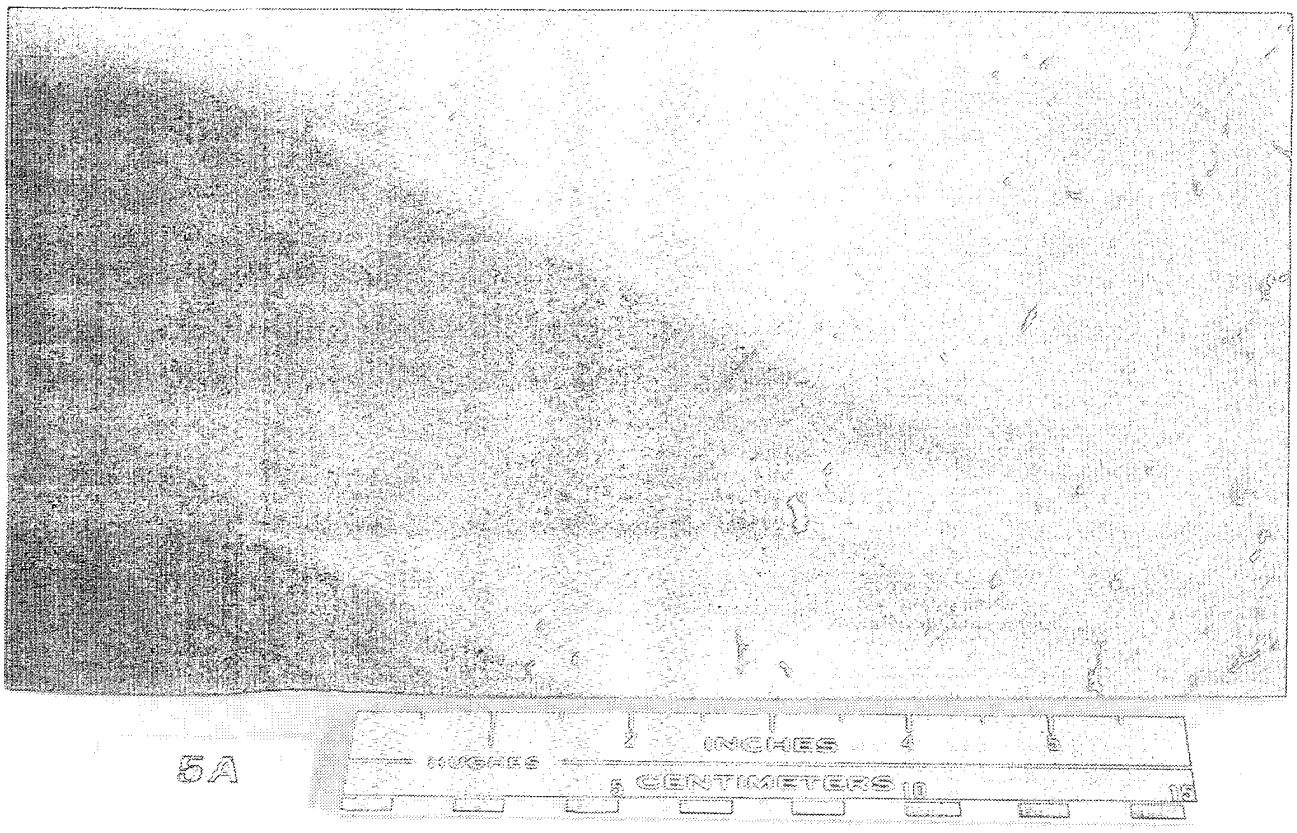

Figure C-4. Photographs of both sides of panel 5.

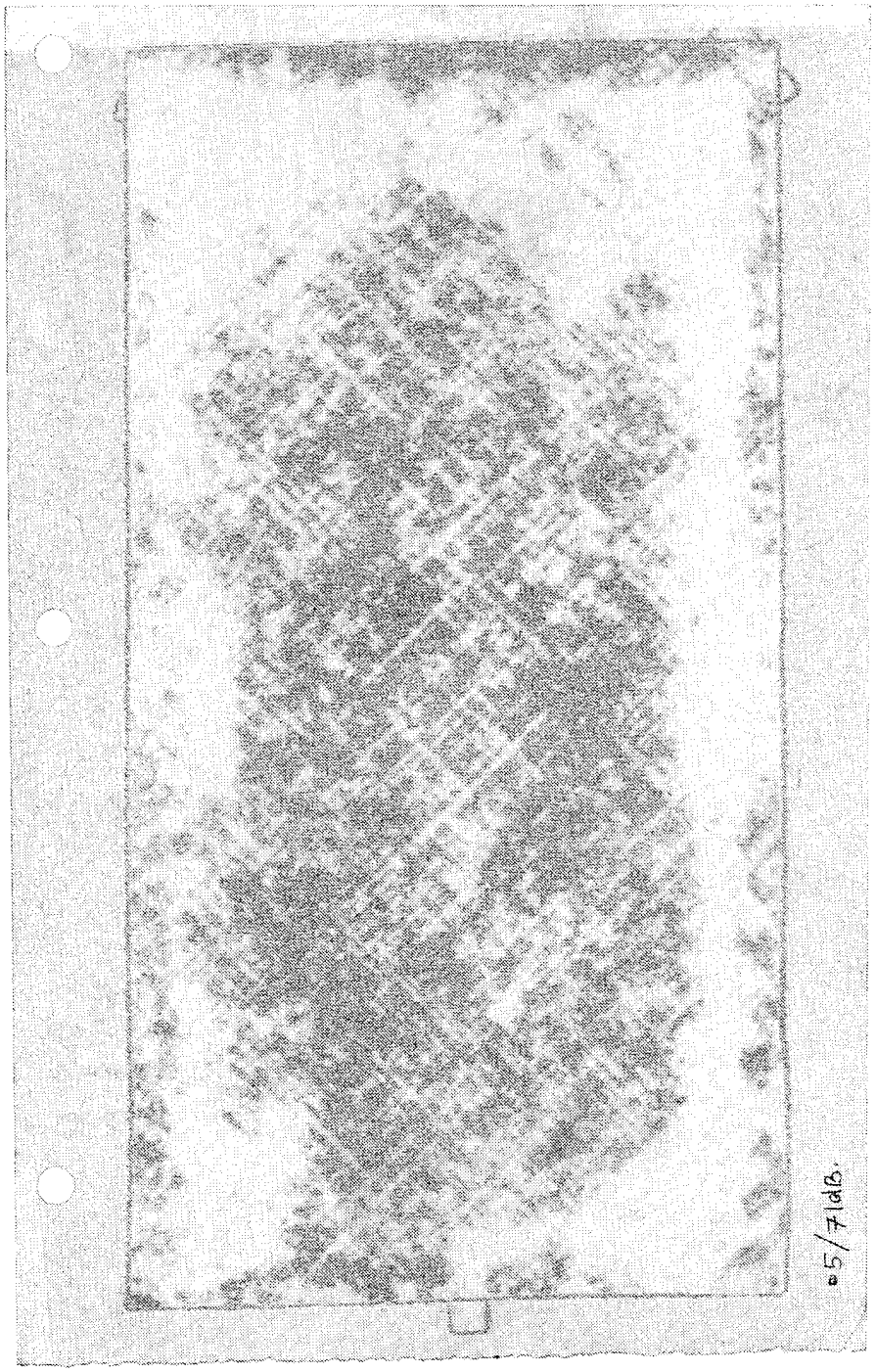

Figure 4-A. Ultrasonic C-scan of panel 5.

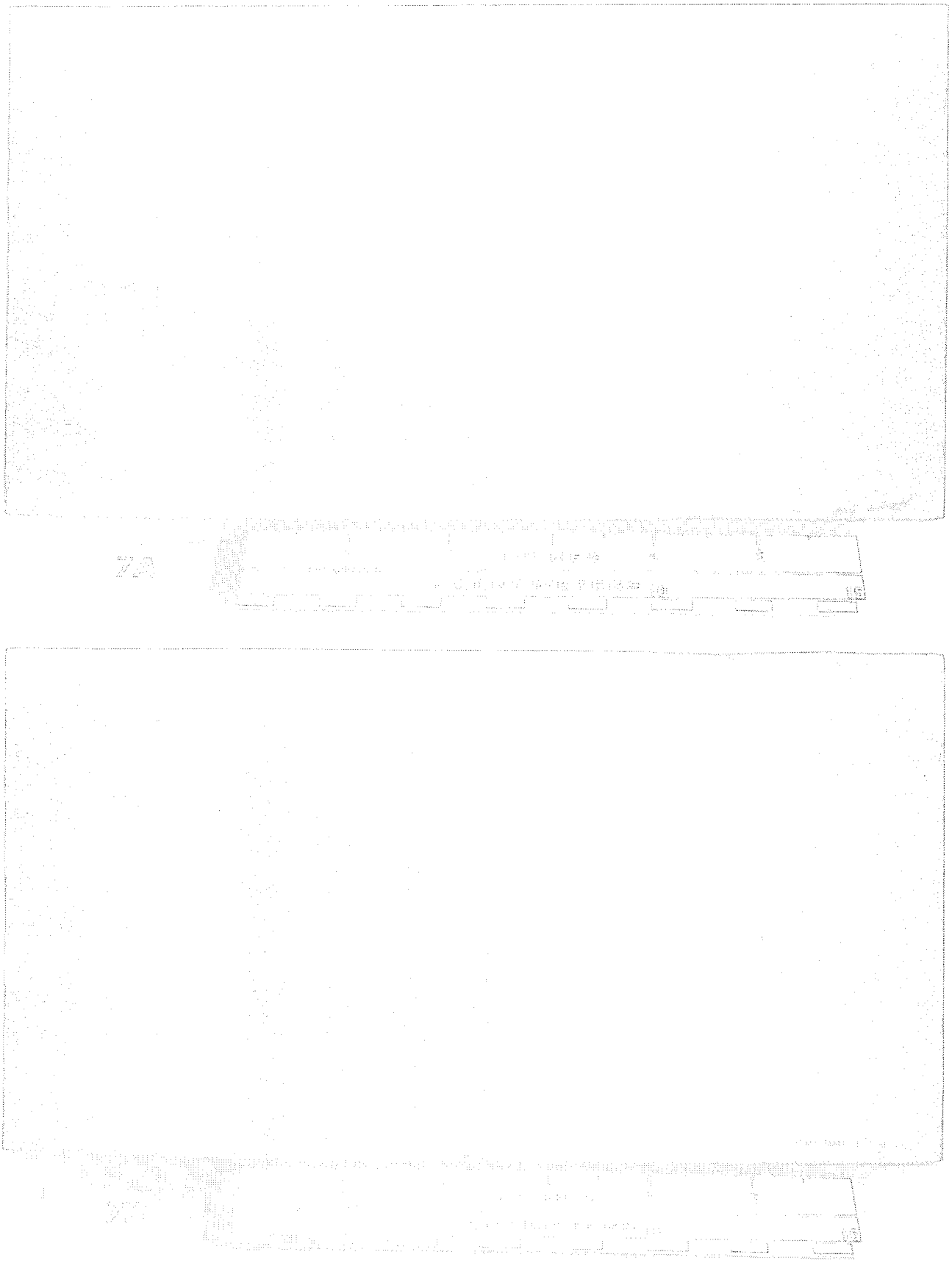

Figure C-3. Photographs of both sides of panel 7.

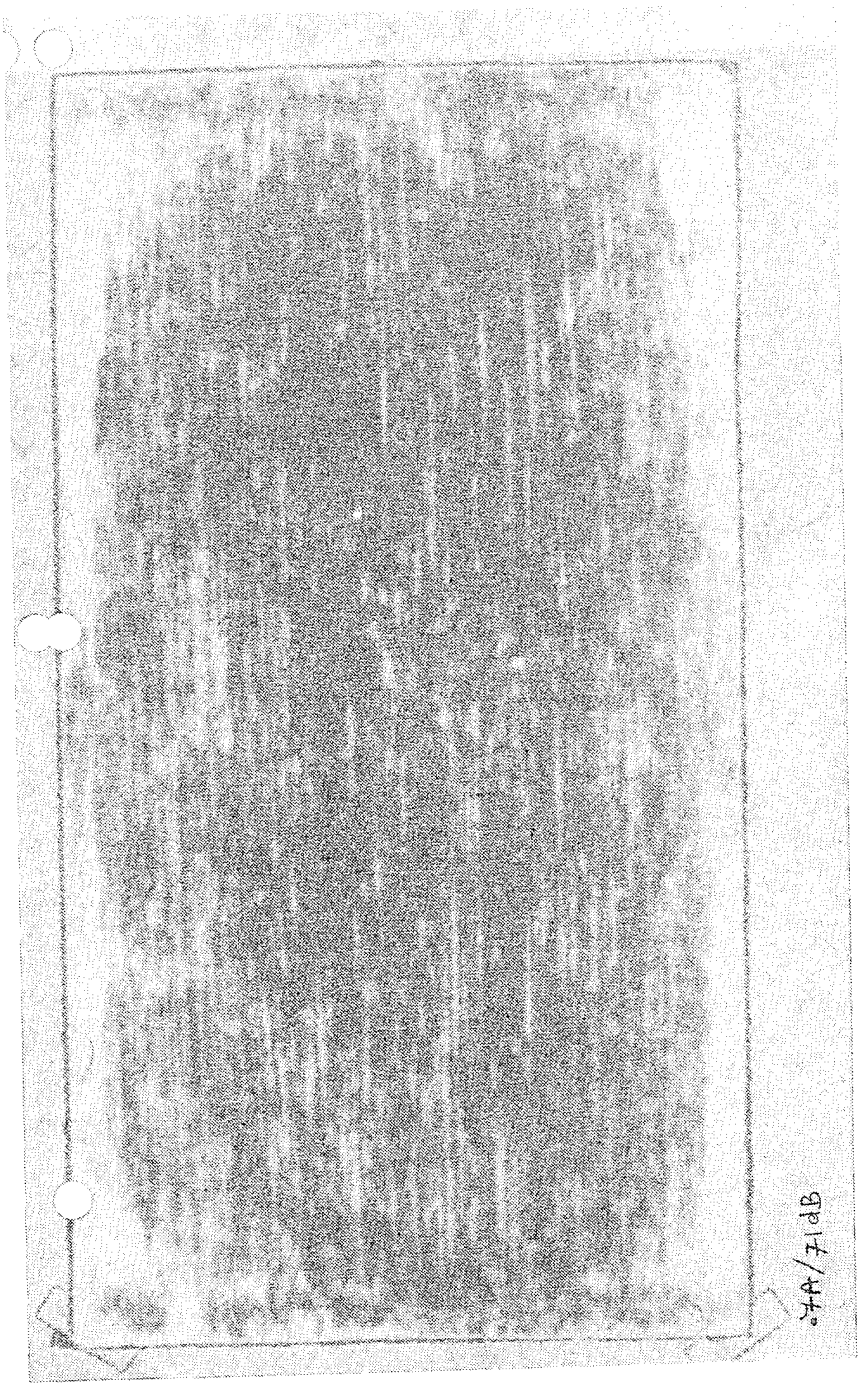

Figure C-5A. Ultrasonic C-scan of panel 7.

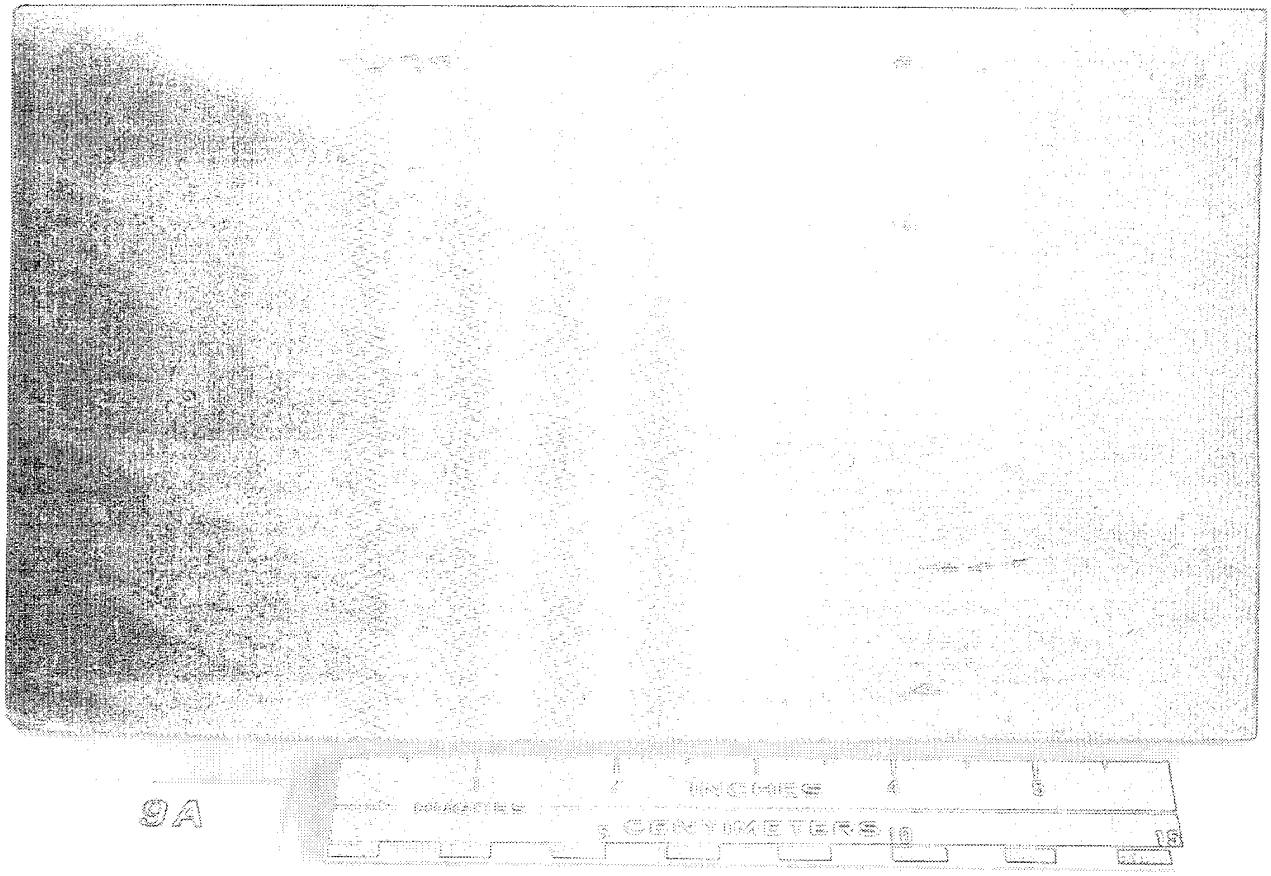

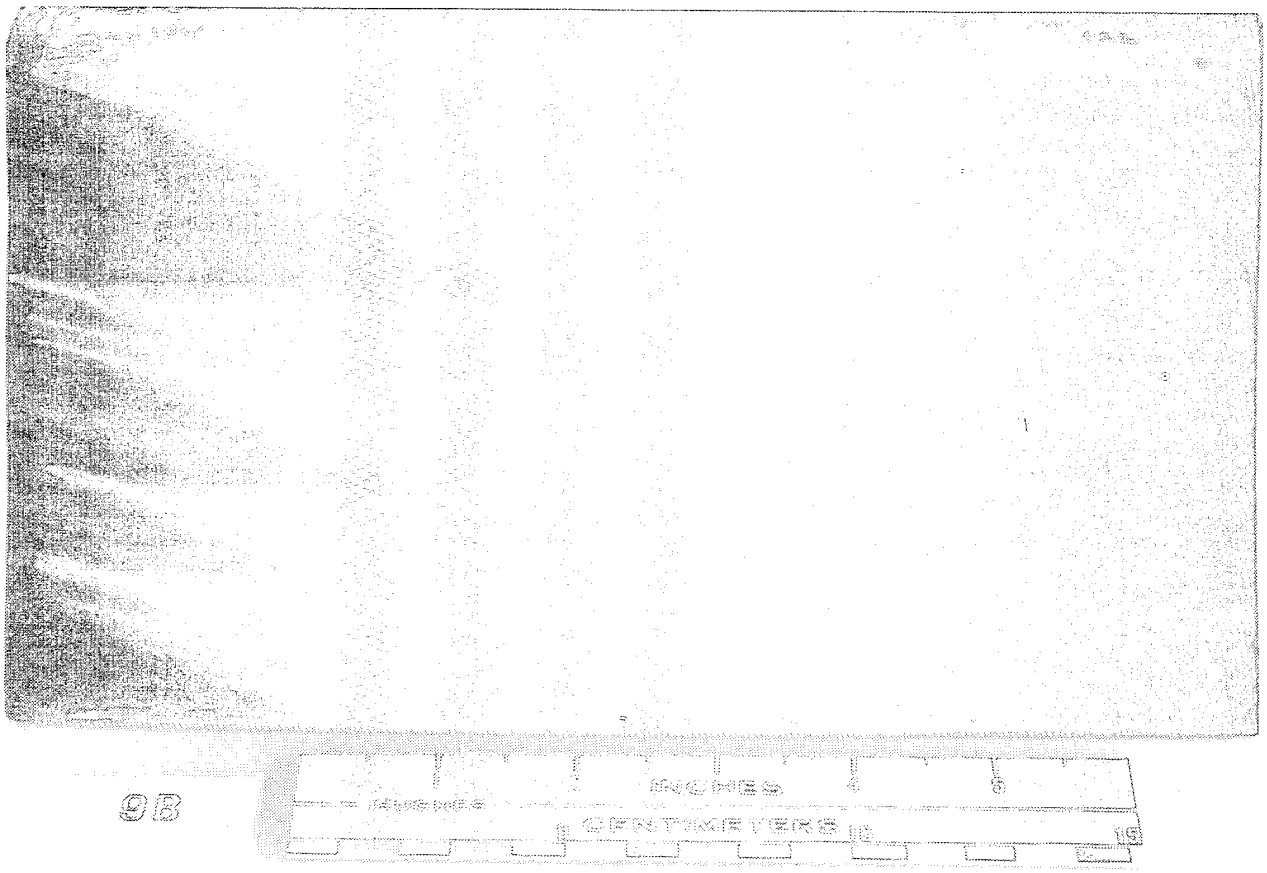

Figure C-6. Photographs of both sides of panel 9.

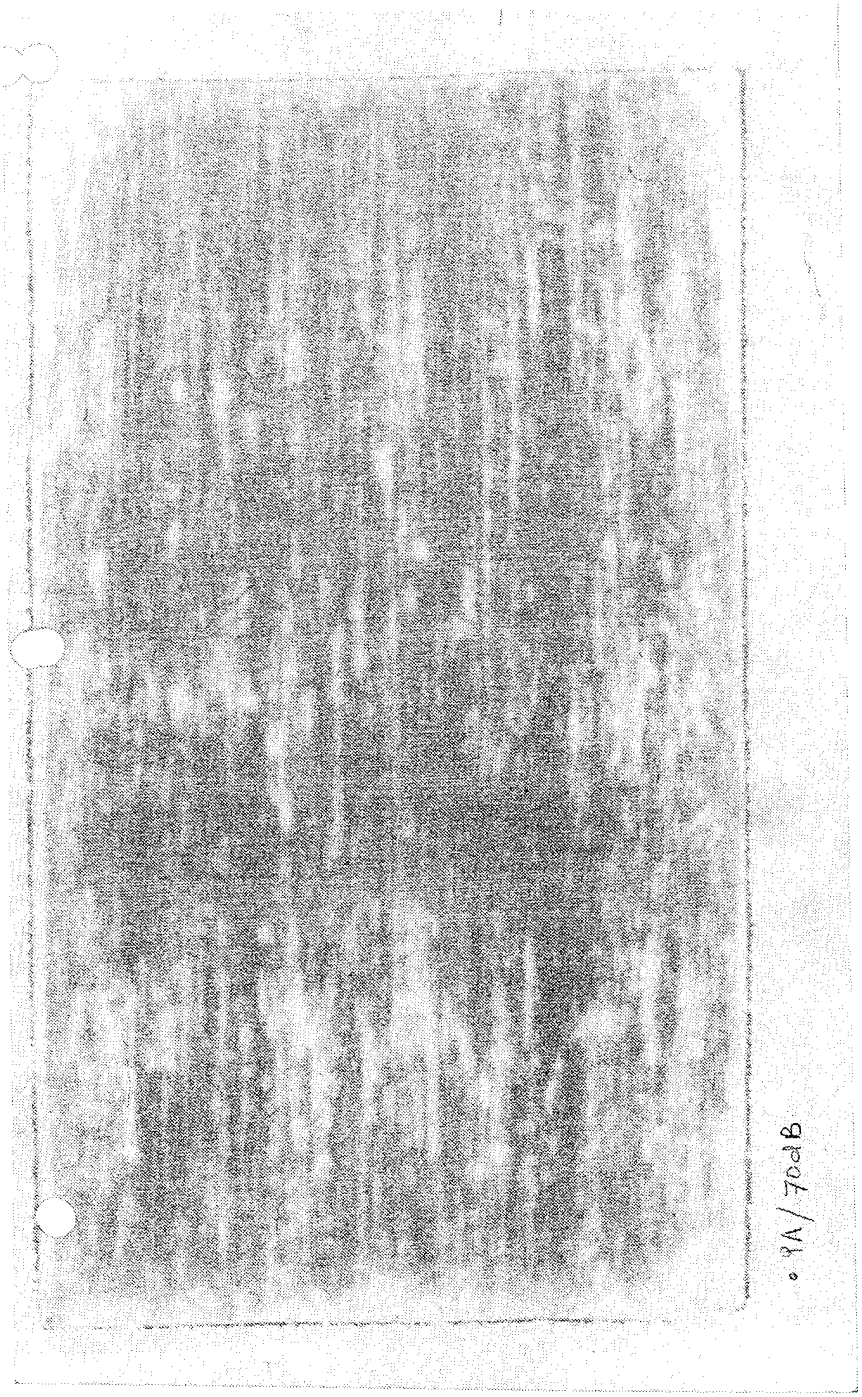

Figure C-6A. Ultrasonic C-scan of panel 9.

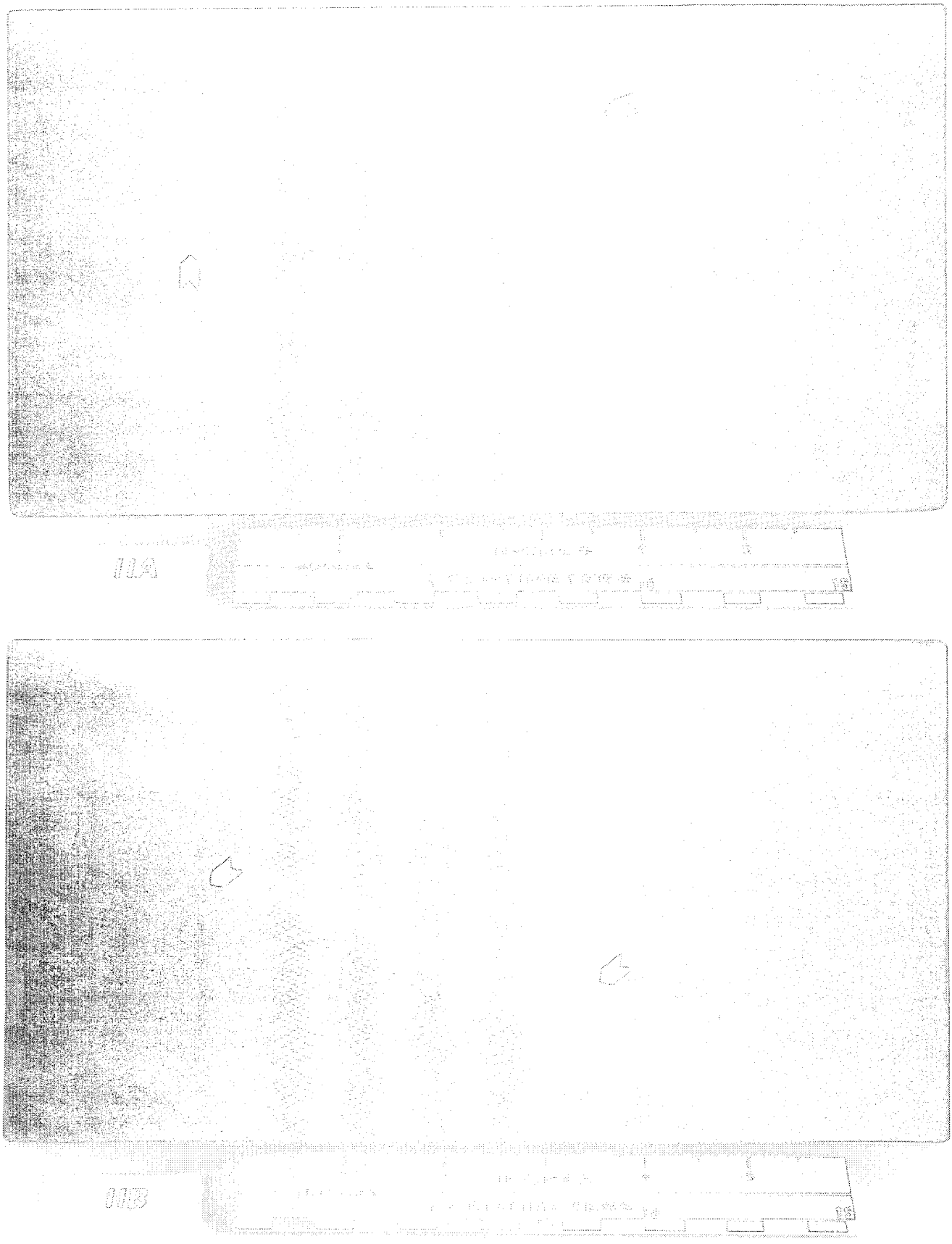

Figure C-7. Photographs of both sides of panel 11.

Figure C-7A. Ultrasonic C-scan of panel 11.

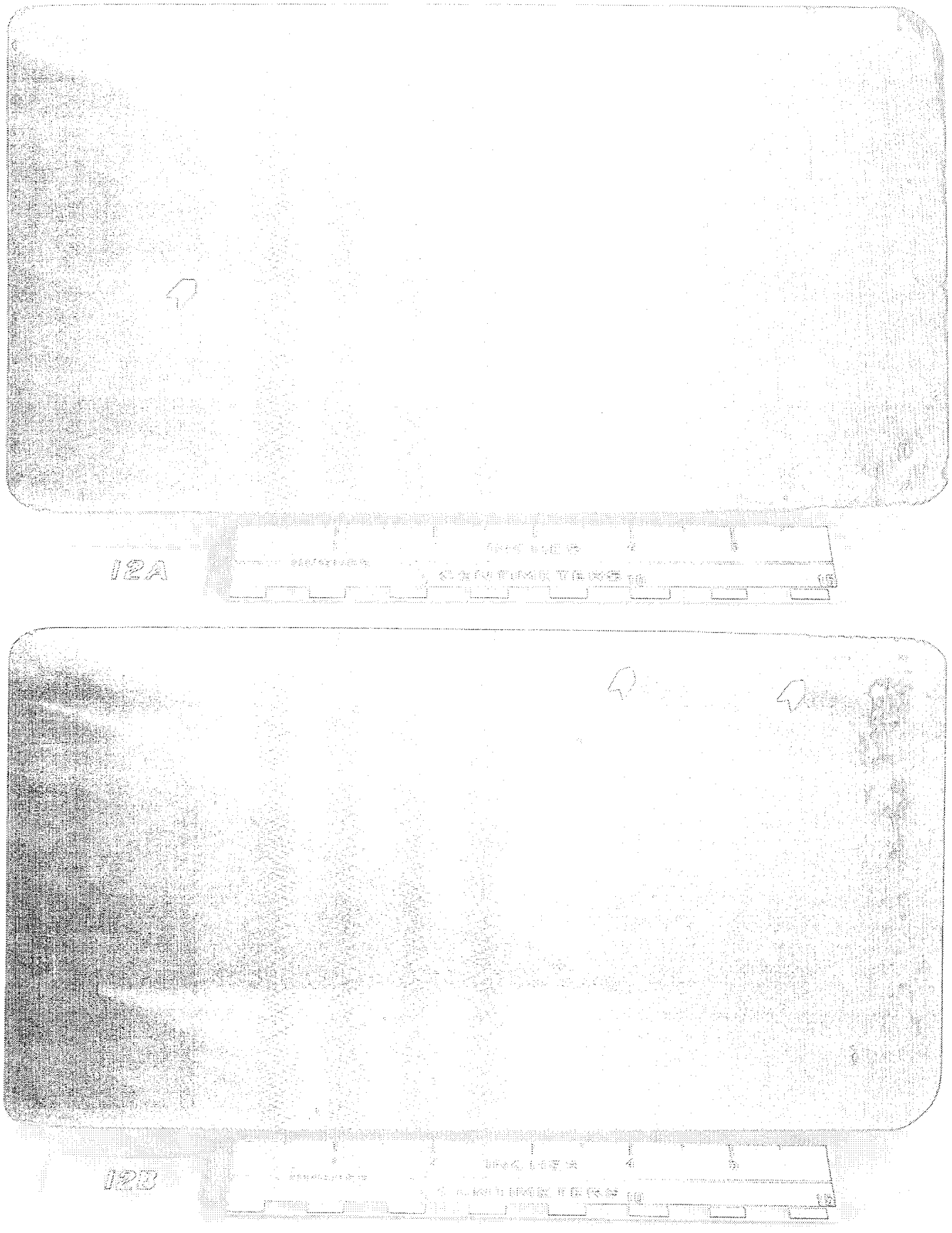

Figure C-8. Photographs of both sides of panel 12.

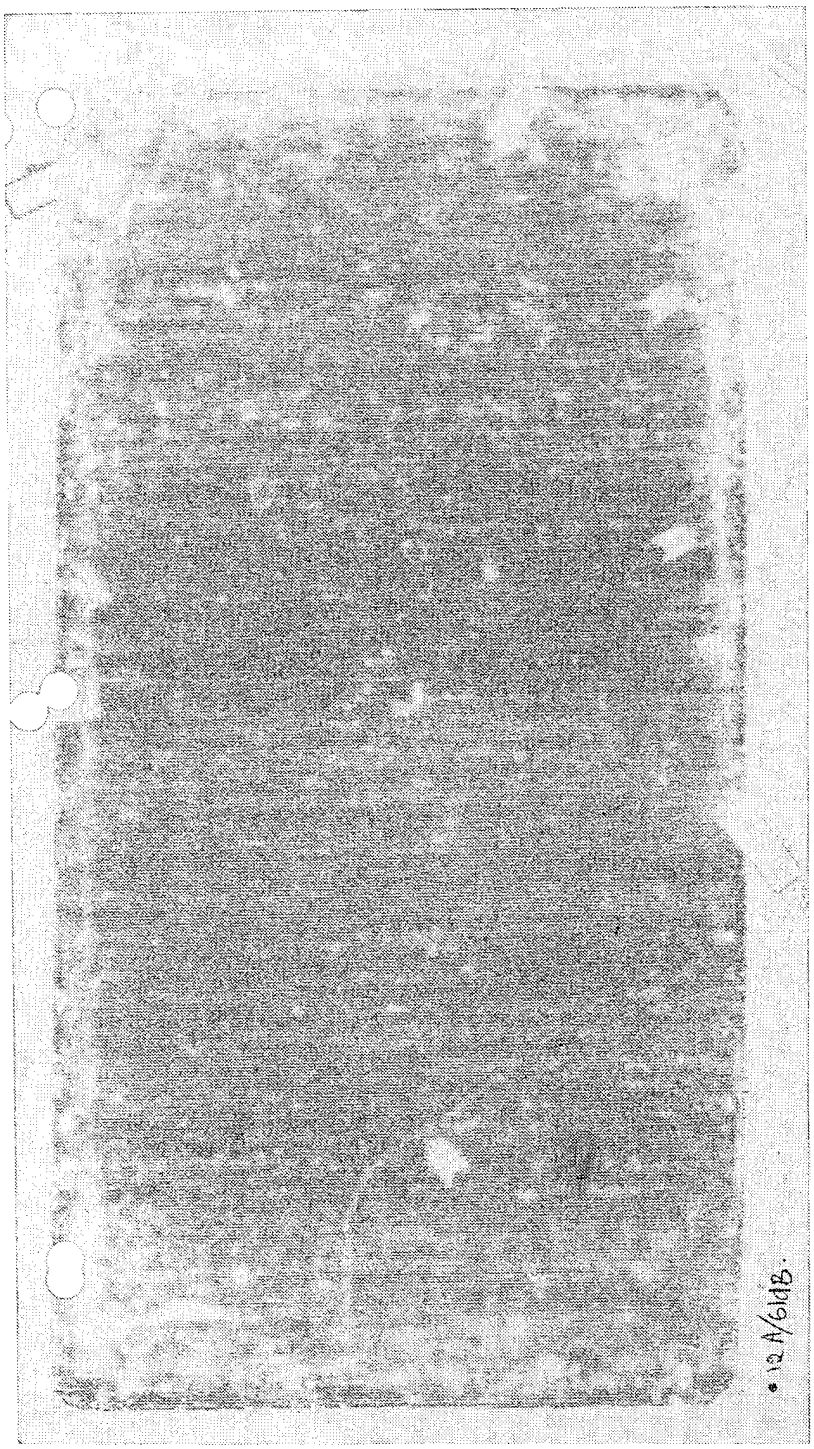

Figure C-8A. Ultrasonic C-scan of panel 12.

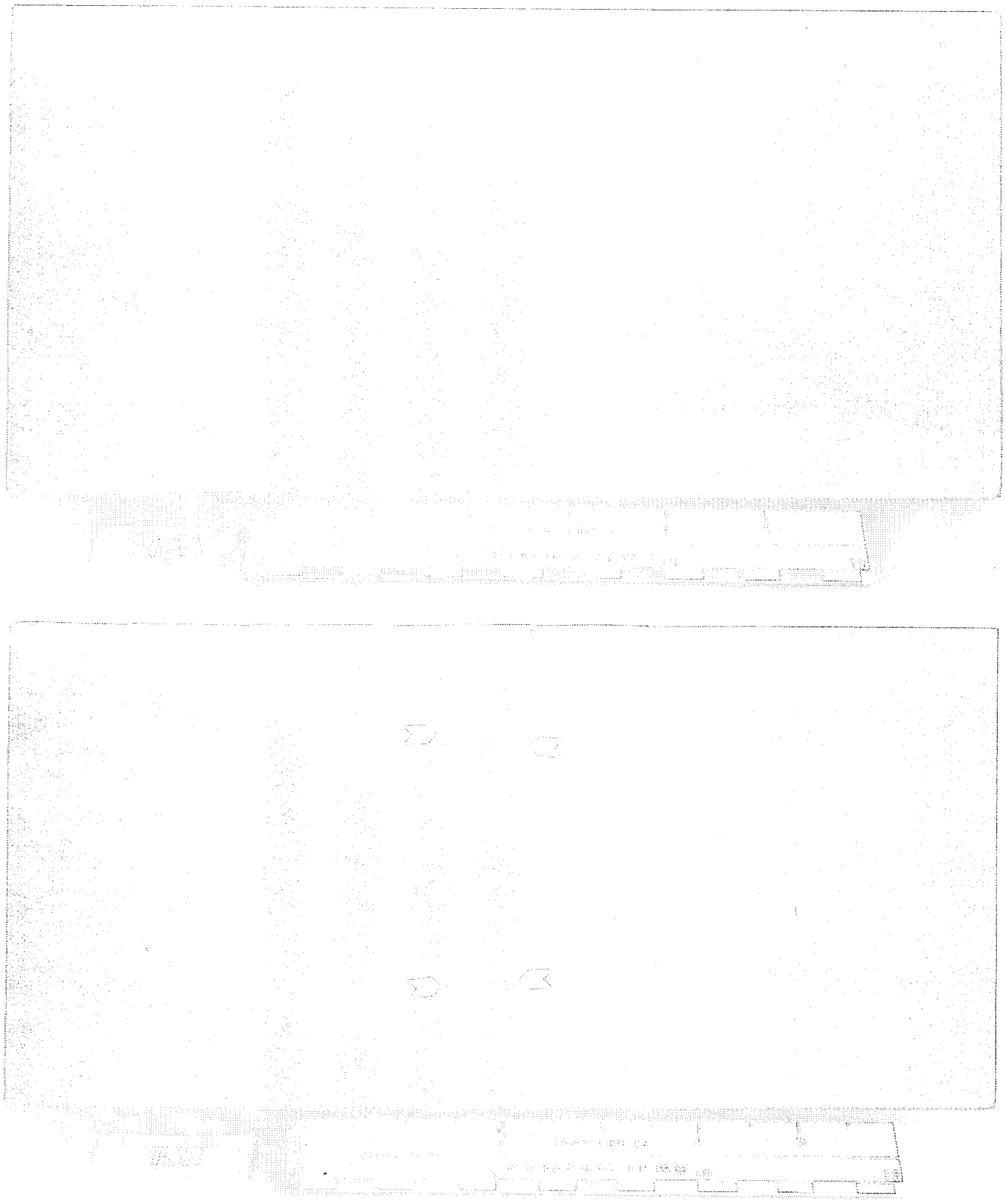

Figure C-9. Photographs of both sides of panel 15.

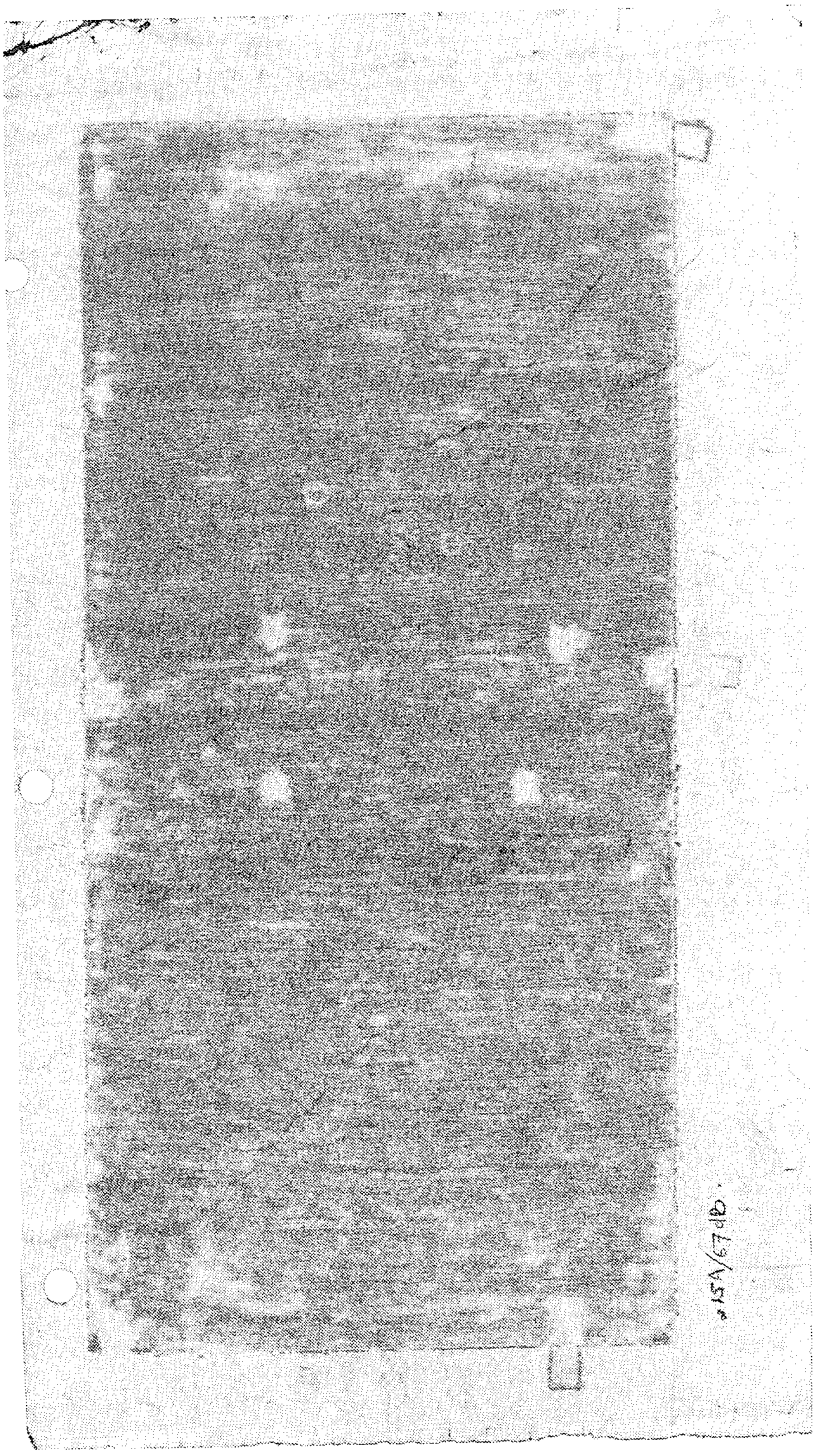

Figure C-9A. Ultrasonic C-scan of panel 15.

REFERENCES

1. L. B. Keller; et al, U.S. Patent Nos. 4, 127, 624, dated Nov. 28, 1978, 4, 037, 010, dated July 19, 1977 and 4, 198, 461 dated Apr. 15, 1980.

2. L. B. Keller; and R. K. Jenkins: Interconnected Fibre Masses Precipitated From Solutions of Polymers. Nature, V. 278, No. 5703, 439-441, Mar. 29, 1979.

3. A. Keller: Current Account of Chain Extension Fibrous Crystallization and Fiber Formation. Journal of Polymer Science - Polymer Symposia, 58, University Bristol HH Wills Phys. Lab. Bristol B58, Avon, England, 395-422, 1977.

4. A. Zwijnenburg; and A. J. Pennings: Longitudinal Growth of Polymer Crystals From Flowing Solutions. 4. Mechanical-Properties of Fibrillar Polyethylene Crystals. Journal of Polymer Science Polymer Letters Edition, 14, State Univ. Groningen, Dept. Polymer Chem., Groningen, Netherlands, 339-346, 1976.

5. J. Smook; J. C. Torfs; P. F. Van Hutten; and A. J. Pennings: Ultrahigh Strength Polyethylene by Hot Drawing of Surface Growth Fibers. Polymer Bulletin, 2, State Univ. Groningen, Dept. Polymer Chem., Groningen, Netherlands, 293-300, 1980.

6. A. J. Pennings: Bundle-Like Nucleation and Longitudinal Growth of Fibrillar Polymer Crystals From Flowing Solutions. A Review. Journal of Polymer Science - Polymer Symposia, 59, State Univ. Groningen, Dept. Polymer Chem., Groningen, Netherlands, 55-86, 1977.

7. J. D. Ferry: Viscoelastic Properties of Polymers, Second ed., John Wiley & Sons, New York, N.Y., 1970.

8. R. A. Orwoll; T. L. St. Clair; and K. D. Dobbs: Phase-Behavior of Some Polyamic Acid Plus Ether Systems. Journal of Polymer Science, Polymer Physics Edition, 19, College of William & Mary, Dept. Chem., Williamsburg, Virginia, 1385-1393, 1981.

9. Polymer Handbook, J. Brandrup, E. H. Immerget, Eds., John Wiley & Sons, New York, N.Y., pIV-23, 1975.

10. T. L. St. Clair; and A. K. St. Clair: Crystalline Polyimides Containing 4,4-Bis (3,4-Dicarboxyphenoxy)-Diphenyl Sulfide Dianhydride. Journal of Polymer Science - Polymer Chemistry Edition, 15, NASA Langley Research Center, Hampton, Virginia, 1529-1533, 1977.

1. Report No.	2. Government Accession No.	3. Recipient's Catalog No.
NASA CR-3616		

4. Title and Subtitle	5. Report Date
APPLICATION OF IN SITU FIBERIZATION FOR FABRICATION OF IMPROVED STRAIN ISOLATION PADS AND GRAPHITE-EPOXY COMPOSITES	September 1982
	6. Performing Organization Code: 76-21-13
7. Author(s): R. W. Rosser, R. W. Seibold, and D. I. Basiulis	8. Performing Organization Report No.: FR-81-76-945
	10. Work Unit No.
9. Performing Organization Name and Address: Hughes Aircraft Company, Centinela & Teale Sts., Culver City, CA 90230	11. Contract or Grant No.: NAS1-16437
	13. Type of Report and Period Covered: Contractor Report
12. Sponsoring Agency Name and Address: National Aeronautics and Space Administration, Washington, D.C. 20546	14. Sponsoring Agency Code

15. Supplementary Notes

Langley technical monitor: Norman Johnston
Final Report

16. Abstract

An accelerated study has been performed to determine the feasibility of applying Hughes Aircraft Company's patented In Situ Fiberization (ISF) process to the fabrication of: (1) improved Strain Isolation Pads (SIPs) for the Space Shuttle, and (2) improved graphite/epoxy (GR/EP) composites. The ISF process involves the formation of interconnected polymer fiber networks by agitation of dilute polymer solutions under controlled conditions. Most previous work was performed using aliphatic hydrocarbon polymers which have limited high temperature capabilities.

In Task 1 of the program, attempts were made to advance ISF technology by fiberization of high temperature polymers which would be suitable for SIP use. Progress was made toward that objective with the successful fiberization of polychlorotrifluoroethylene, a relatively high melting polymer. Attempts to In Situ Fiberize polymers with even greater thermal stability were not successful. The latter difficulty is presumed to derive from poor solubility, low molecular weight, and/or high chain stiffness, all caused by the presence of aromaticity in the backbone of such materials.

During Task 2, two dimensional arrays of graphite fiber were interconnected with polypropylene In Situ Fibers. Following epoxy resin impregnation and lamination of the arrays into panels, mechanical property tests were performed to gauge the effectiveness of the In Situ Fibers for improvement in intralaminar shear strength, and hence fracture toughness. Test results were generally, though not universally, unpromising. Poor performance is believed to reflect incomplete In Situ fiber/resin wetting, poor graphite fiber packing, and perhaps low In Situ Fiber moduli.

17. Key Words (Suggested by Author(s))	18. Distribution Statement
In Situ Fiberization Polypropylene Fibers Strain Isolation Pads Graphite-Epoxy Composites	Unclassified-Unlimited Subject Category - 24

19. Security Classif. (of this report)	20. Security Classif. (of this page)	21. No. of Pages	22. Price
Unclassified	Unclassified	126	A07

For sale by the National Technical Information Service, Springfield, Virginia 22161

NASA-Langley, 1982